การสังเคราะห์ฟิล์มบางคาร์บอนคล้ายเพชรบนแผ่นรองรับอลูมินาโดยเทคนิค
การตกสะสมไอเชิงเคมีเสริมด้วยไมโครเวฟพลาสมา

นางสาวโชติวรรณ รัตนเสถียร
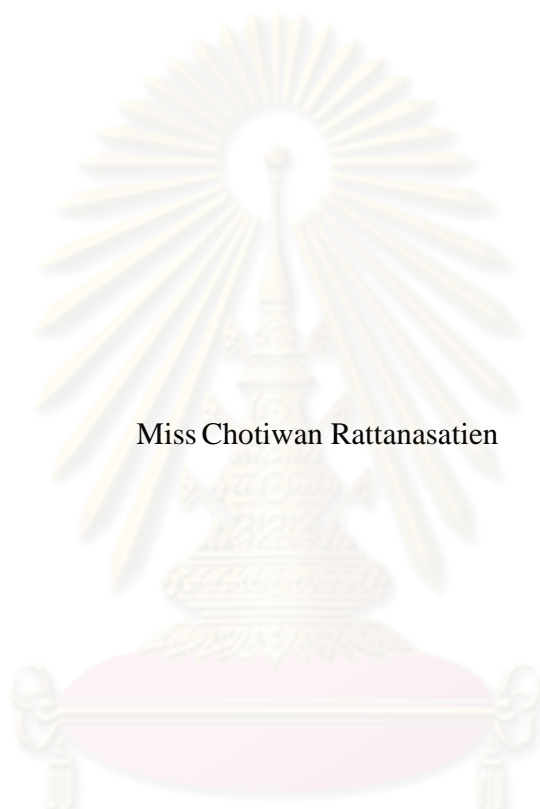
SYNTHESIS OF DIAMOND-LIKE CARBON THIN FILM ON ALUMINA
SUBSTRATE BY MICROWAVE PLASMA ENHANCED
CHEMICAL VAPOR DEPOSITION TECHNIQUE

Miss Chotiwan Rattanasatien

A Thesis Submitted in Partial Fulfillment of the Requirements
for the Degree of Master of Engineering Program in Chemical Engineering
Department of Chemical Engineering
Faculty of Engineering
Chulalongkorn University
Academic Year 2010

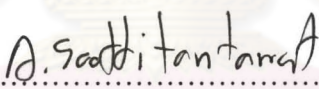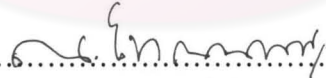| Thesis Title	SYNTHESIS OF DIAMOND-LIKE CARBON THIN FILM ON ALUMINA SUBSTRATE BY MICROWAVE PLASMA ENHANCED CHEMICAL VAPOR DEPOSITION TECHNIQUE
By	Ms. Chotiwan Rattanasatien
Field of Study	Chemical Engineering
Thesis Advisor	Assistant Professor Nattaporn Tonanon, Ph.D.
Thesis Co-advisor	Assistant Professor Boonchoat Paosawatyanyong, Ph.D.

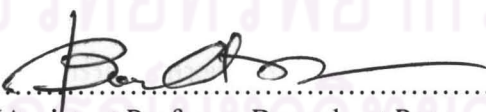Accepted by the Faculty of Engineering, Chulalongkorn University in Partial Fulfillment of the Requirements for the Master's Degree

............................Dean of the Faculty of Engineering

(Associate Professor Boonsom Lerdhirunwong, Dr. Ing.)
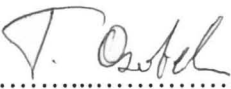
THESIS COMMITTEE

.... Chairman

(Apinan Soottitantawat, Ph. D.)

.... Thesis Advisor

(Assistant Professor Nattaporn Tonanon, Ph. D.)

.... Thesis Co-advisor

(Assistant Professor Boonchoat Paosawatyanyong, Ph.D.)

.... Examiner

(Assistant Professor Varong Pavarajarn, Ph.D.)

.... External Examiner

(Assistant Professor Tanakorn Osotchan, Ph.D.)

โชติวรรณ รัตนเสถียร : การสังเคราะห์ฟิล์มบางคาร์บอนคล้ายเพชรบนแผ่นรองรับอลูมินา โดยเทคนิคการตกสะสมไอเชิงเคมีเสริมด้วยไมโครเวฟพลาสมา. (SYNTHESIS OF DIAMOND-LIKE CARBON THIN FILM ON ALUMINA SUBSTRATE BY MICROWAVE PLASMA ENHANCED CHEMICAL VAPOR DEPOSITION TECHNIQUE) อ.ที่ปรึกษาวิทยานิพนธ์หลัก: ผศ.ดร. ณัฐพร โทณานนท์, อ.ที่ปรึกษา วิทยานิพนธ์ร่วม: ผศ.ดร. บุญโชติ เผ่าสวัสดิ์ยรรยง, 106 หน้า

งานวิจัยนี้ได้ศึกษาผลของปัจจัยหลักที่ใช้ในการสังเคราะห์ฟิล์มบางคาร์บอนคล้ายเพชรบน แผ่นรองรับอลูมินาโดยเทคนิคการตกสะสมไอเชิงเคมีเสริมด้วยพลาสมาที่คลื่นไมโครเวฟด้วยแก๊ส ผสมระหว่างมีเทน และไฮโดรเจน โดยเงื่อนไขที่ใช้ในการสังเคราะห์ได้แก่ ความเข้มข้นของแก๊ส มีเทน 0.5-5 เปอร์เซ็นต์ ความดัน 10-50 ทอร์ และระยะเวลาที่ใช้ในการสังเคราะห์ 5-30 ชั่วโมง ผล การวิเคราะห์ด้วยรามานสเปกโทรสโกปีพบว่าฟิล์มที่สังเคราะห์ในทุกๆตัวอย่างแสดงพีคที่เลขคลื่น บริเวณ 1332 ต่อเซนติเมตร และบริเวณ 1550 ต่อเซนติเมตร ซึ่งแสดงถึงลักษณะเฉพาะของเพชร และคาร์บอนเฟสที่เป็นแกรไฟต์หรืออสัณฐาน ตามลำดับ จากการคำนวณค่าความกว้างที่ความสูง ครึ่งหนึ่งของพีคที่เลขคลื่น 1332 ต่อเซนติเมตร พบว่ามีค่าลดลงเมื่อความดันและระยะเวลาที่ใช้ใน การสังเคราะห์เพิ่มขึ้น สอดคล้องกับค่าความแข็งและความขรุขระของฟิล์มที่มีค่าเพิ่มขึ้น นอกจากนี้ ยังพบว่าความหนาแน่นของนิวคลีไอร์ และอัตราการโตของเกรนมีค่าเพิ่มขึ้นเมื่อความดันและ ระยะเวลาที่ใช้ในการสังเคราะห์เพิ่มขึ้นอีกด้วย แต่ในทางตรงกันข้ามเมื่อความเข้มข้นของแก๊ส มีเทนเพิ่มขึ้น จะทำให้เกิดผลของการแตกตัวซ้ำของนิวคลีไอร์ที่ได้ ส่งผลให้ขนาดเกรนและความ ขรุขระมีค่าลดลง และผลจากการวัดค่าความแข็งของฟิล์มมีค่าลดลงด้วย ผลจากการวิเคราะห์ด้วย กล้องจุลทรรศน์อิเล็กตรอนแบบส่องกวาดแสดงให้เห็นว่าฟิล์มที่ได้มีการจัดเรียงตัวกันอย่าง หนาแน่นและต่อเนื่องบนแผ่นรองรับอลูมินา จึงน่าจะสรุปได้ว่าปัจจัยหลักที่ใช้ในการสังเคราะห์ ฟิล์มบางคาร์บอนคล้ายเพชรมีผลอย่างมากต่อคุณลักษณะของฟิล์มที่ได้ พบว่าความแข็งของอลูมินา ก่อนการเคลือบด้วยฟิล์มบางคาร์บอนคล้ายเพชรมีค่า 7.3±2.0 จิกะพาสคัล และเมื่อทำการ สังเคราะห์ฟิล์มที่ความเข้มข้นของแก๊สมีเทน 1 เปอร์เซ็นต์ ความดัน 30 ทอร์ เป็นเวลา 30 ชั่วโมงนั้น สามารถทำให้ฟิล์มมีค่าความแข็งสูงถึง 52.2±2.1 จิกะพาสคัล

ภาควิชา......วิศวกรรมเคมี..........ลายมือชื่อนิสิต โชติวรรณ รัตนเสถียร

สาขาวิชา......วิศวกรรมเคมี..........ลายมือชื่ออ.ที่ปรึกษาวิทยานิพนธ์หลัก.................

ปีการศึกษา............2553..........ลายมือชื่ออ.ที่ปรึกษาวิทยานิพนธ์ร่วม.................

5070259121 : MAJOR   CHEMICAL ENGINEERING

KEYWORDS : DIAMOND-LIKE CARBON FILM / CHEMICAL VAPOR DEPOSITION / ALUMINA / MICROWAVE PLASMA

CHOTIWAN RATTANASATIEN: SYNTHESIS OF DIAMOND-LIKE CARBON THIN FILM ON ALUMINA SUBSTRATE BY MICROWAVE PLASMA ENHANCED CHEMICAL VAPOR DEPOSITION TECHNIQUE THESIS ADVISOR: ASSISTANT PROFESSOR NATTAPORN TONANON, Ph.D., THESIS CO-ADVISOR: ASSISTANT PROFESSOR BOONCHOAT PAOSAWATYANYONG, Ph.D., 106 pp.

We have studied the influence of the main process parameters on the formation of the diamond-like carbon films on alumina substrates deposited by microwave plasma enhanced chemical vapor deposition (MW-PECVD) technique. Process parameters include methane (CH_4) concentration (0.5-5%), deposition pressure (10-50 torr), and deposition time (5-30 hr). Raman analysis showed peak at around 1332 cm^{-1} and 1500-1600 cm^{-1}, corresponding to diamond and graphite or amorphous carbon phase. The FWHM of the diamond peak decreased significantly with increasing deposition pressure and time, resulting in an increase of hardness and surface roughness of the films as well as nucleation density and growth rate. In contrast, an increase in CH_4 concentration could lead to more secondary nucleation effect, resulting in a decreasing of grain size and surface roughness. Surface analysis by scanning electron microscopy (SEM) revealed a dense continuous film on the alumina substrate. It could be concluded that the main process parameters has significantly affected the characteristics of DLC films. The hardness of alumina found to increase from 7.3±2.0 GPa in uncoated to the maximum film hardness of 52.2±2.1 GPa, after coated with DLC film with CH_4 concentration of 1%, deposition pressure of 30 torr, and deposition time of 30 hr.

Department : ……..Chemical Engineering….Student's Signature : Chotiwan Rattanasatien

Field of Study : ...Chemical Engineering... Advisor's Signature : …

Academic Year : …………2010…………..Co-advisor's Signature :

ACKNOWLEDGEMENTS

CONTENTS

LIST OF TABLES

LIST OF FIGURES

Figure   Page

Figure   Page

Figure   Page

CHAPTER I

INTRODUCTION

1.1   Research motivation

Diamond has extreme physical and chemical properties, for example extreme hardness, high wear resistance, high corrosion resistance, high thermal conductivity, variable electrical resistivity, and high optical transparency and other properties [1, 2]. Combined with these properties, diamond is far more effective and efficient than other materials used for hard coating, cutting and grinding tools and as electronic devices [3-6]. However, the high cost of material production has limited the commercial use of diamond thin films to only few very specialized applications. A large number of deposition techniques have been employed for successful deposition of diamond from vapor phase. Deposition techniques are mainly divided into two major categories, namely chemical vapor deposition (CVD) and physical vapor deposition (PVD). In CVD techniques, the source of carbon is an activated gas phase. PVD techniques rely on excitation of the target that is usually solid to produce the necessary material for film formation. In addition to the basic difference in the way that material transfer from the vapor phase to the solid phase is achieved [7, 8]. In CVD of diamond, the driving cost factors include low reagent utilization, low deposition rate, high energy consumption, large thermal management loads at the substrate and capital equipment costs [9]. A variety of CVD techniques have been proposed for diamond growth such as microwave plasma CVD (MW-CVD) [10-12], hot filament CVD (HF-CVD) [13-14], radio frequency plasma CVD (RF-CVD) [15-16], DC plasma [17-19], etc. Diamond formed by sp^3 hybridized carbon atoms is a unique structure in nature. Its unique properties make it suitable for a variety of commercial application. Not only be prominently as a gemstone, but also a very useful industrial material. The diamond coated cutting tools, abrasive wheels are a few products used routinely in industry [8].

Currently, ceramic materials are important in many industries, especially grinding technology with ball-mill, in which incorporate the uses of alumina grinding ball. However, wear could occur in the grinding ball after the long use. Thus, this

proposed work is focused on the properties improvement of alumina surface coated with synthesize diamond-like carbon (DLC) thin films using microwave plasma enhanced chemical vapor deposition (MW-PECVD) technique. This technique can increase hardness and wear resistance, resulting to an increase in life time span of the alumina usage.

There are many researches of diamond film deposited on alumina substrate that has been applied in several applications. For example Linjun Wang *et al.* [20] studied the growth of polycrystalline diamond films on alumina substrates by microwave plasma CVD using gaseous mixture of methane and hydrogen. They controlled the process pressure in the range of 1.5-5 kPa (11.4-38 torr) and the substrate temperature in the range of 700-900 °C by adjusting the microwave power level. They found that decreasing the gas pressure in nucleation process was an efficient method to enhance diamond nucleation density on alumina substrates. The optimum substrate temperature for a good-quality diamond films on alumina substrate was in the range of 800-860 °C. Based on Mo *et al.* [21], their research studied a nucleation mechanism for diamond film deposited on alumina by microwave plasma CVD using methane and hydrogen gaseous mixture. They showed that by using suitable pretreatment such as polishing the substrate with diamond particles and pre-depositing a nondiamond carbon layer under high methane gas concentration, could enhance the nucleation of the diamond. Ternyak *et al.* [13] reported about evolution and properties of adherent diamond films grown on alumina by hot-filament chemical vapor deposition (HF-CVD) technique. The substrates were ultrasonically abraded with mixed poly-disperse slurry that allows well adherents diamond films and high nucleation density. They described that the reason for well adherents between alumina substrate and diamond film was high carbon diffusivity onto alumina grain boundaries, which prevented the delamination of diamond film.

The main aim of this research is to investigate the influences of methane concentration, deposition pressure and deposition time. The properties of DLC thin films were characterized using Scanning Electron Microscopy (SEM), Raman spectroscopy, Atomic Force Microscopy (AFM) and nanoindentation testing. The expectation of the diamond films properties will increase in hardness.

1.2 Research objective

The objective of this research is to investigate the effects of the CVD diamond growth conditions on DLC thin films deposited on alumina substrates using MW-PECVD technique in order to obtain the optimum conditions, which can lead to an increase in hardness of the films and examine the influences of the conditions to the surface morphology, structure of carbon, surface roughness and hardness on CVD diamond films.

1.3 Research scopes

1.3.1 Synthesis of DLC thin films on alumina substrates by MW-PECVD technique under various conditions, for instance:

1.3.1.1 $CH_4:H_2$ %: 0.5, 1, 2, 3 and 5 %

1.3.1.2 Deposition pressure: 10, 20, 30 and 50 torr

1.3.1.3 Deposition time: 5, 10, 20 and 30 hr

1.3.2 Characterization of DLC thin films with the following techniques :

1.3.2.1 Scanning Electron Microscopic (SEM) technique is used to investigate surface morphologies on grown DLC thin films deposited on alumina substrates.

1.3.2.2 Raman spectroscopy technique is used to analyze the bonding structure of the films.

1.3.2.3 Atomic force microscopy technique is used to investigate the surface roughness of the films.

1.3.2.4 Nanoindentation test is used to examine the hardness of the films.

1.4 Benefits

The expected benefit from this research is to increase in hardness of DLC thin films deposited on alumina substrates using MW-PECVD technique.

1.5   Thesis organizations

This thesis can be divided into five chapters. Chapter I provide the general introduction to lead the objective and scope of this research. Chapter II knowledge and open literature dealing with diamond growth for CVD technique were presented. The experimental procedure as well as the instrument and techniques used for characterizing the resulting DLC films were also described in Chapter III.

In Chapter IV, the results on diamond-like carbon thin film deposition using MW-PECVD technique were presented. The influences of the ratio of methane to hydrogen gas, deposition pressure and deposition time were investigated. The characterization of the films using Scanning Electron Microscopy (SEM), Raman spectroscopy, Atomic Force Microscopy (AFM) and nanoindentation testing were described.

Finally, conclusion of this work and recommendations for future research work were provided in Chapter V.

CHAPTER II

THEORY BACKGROUND

2.1 Alumina

Aluminium oxide (Al_2O_3) is commonly known as alumina in the ceramic community. Alumina has been considered as one of the most promising advance materials used for varieties of application such as media ball, wear-resistance material, cutting tool and orthopaedic implant due to its distinctive chemical, mechanical and thermal properties [22].

2.1.1 Crystal structure

The most common form of crystalline alumina (Fig. 2.1) is known as corundum (α-aluminium oxide). Al_2O_3 has an internal structure where oxygen ions are positioned in the closely-packed hexagonal (cph) arrangement and stacked with Al^{+3} ions, occupying two-thirds of octahedral interstices. The lattice parameter of the hexagonal crystallographic cell is a = 0.475 nm and c = 1.297 nm, which differ entirely from the diamond structure. As a result, the diamond nuclei cannot grow from an α- Al_2O_3 directly. The details on adhesion of diamond film on alumina are described in 2.1.4 [7, 22].
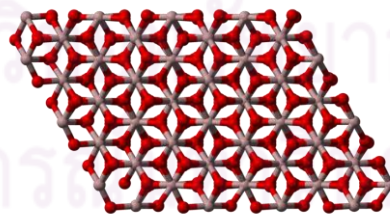
Figure 2.1   Crystal structure of α-aluminium oxide [22].

2.1.2 Processing method

Alumina is the most widely used as inorganic chemical for ceramics and is produced from the mineral bauxite using the Bayer process. Bauxite is a mixture of hydrated aluminium oxide with iron oxide (FeO_2), silica (SiO_2), and titania (TiO_2) impurities. The Bayer process produces a nominal 99.5% Al_2O_3 product. The alumina can be prepared in a range of grades to suit specific applications, where the grades differ by the size and shape of the crystals and the impurity content [7, 22].

The steps in the Bayer process are as follow [7]:

Digestion: The roughly bauxite is treated with a sodium hydroxide (NaOH) solution. Most of the hydrated alumina goes into solution as sodium aluminate:

$$Al(OH)_3(s) \ + \ NaOH(aq) \ \longrightarrow \ Na^+(aq) \ + \ Al(OH)_4^-(aq)$$
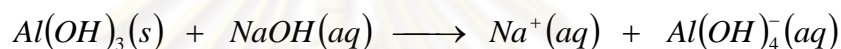
Filtration: The solid impurities, mainly SiO_2, TiO_2, and FeO_2, remain undissolved and are separated by filtration.

Precipitation: After cooling, the filtered sodium aluminate solution is seeded with very fine and at a lower temperature that the aluminium hydroxide reforms as the stable phase. Having reduced the pH by bubbling CO_2 through the solution encouraged the precipitation.

Washing: The precipitation is filtered and washed to reduce the sodium content.

Calcination: The powder is calcined at temperature ranging between 1100-1200 ºC to convert the hydroxide to the oxide:

$$2Al(OH)_3(s) \ \longrightarrow \ Al_2O_3(s) \ + \ H_2O(g)$$
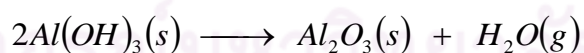
At this stage the alumina is in the form of agglomerates of small grains.

Milling: The powder is then milled to give the desired particle size and particle size distribution. The alumina produced in this way contains ≥99.5% of Al_2O_3.

2.1.3 Forming techniques

There are numbers of techniques used to shape ceramics. The selection of shaping operation for a particular product is very dependent on the size and dimensional tolerances of the product, the levels of required reproducibility, economic considerations, and most importantly, the required shape. Each of the techniques can be described as followed [7, 23]:

2.1.3.1 Dry pressing

Dry pressing is ideally suited to the formation of simple solid shapes and it consists of three basic steps: filling the die, compacting the contents and ejecting the pressed solid. Because the dry pressing process is simple and involves low capital equipment costs; it is the most widely and commonly used as high-volume forming process for ceramics. Production rates depend on the size and shape of the part and the type of press used.

2.1.3.2 Hot pressing

Pressing can also be performed at high temperatures in which a process is known as hot pressing. The die assembly used for hot pressing is very similar to dry pressing. The main difference is that the die assembly is contained within a high-temperature furnace in hot pressing. During hot pressing, the ceramic powders may sinter together to form a high-density component. Hot pressing, like dry pressing, is limited to simple solid shapes, such as flat plates, blocks, and cylinders. More complex or large shapes are difficult and often impossible to be produced by hot pressing.

Isostatic pressing involves the application of hydrostatic pressure to a powder in a flexible container. The advantage of applying pressure in all directions is that there is more uniform compaction of the powder and more complex shapes can be produced than with uniaxial pressing. Isostatic pressing can be performed either with or without applying heat.

2.1.3.3   Cold isostatic pressing

Powder is weighted and put into a rubber bag then a metal mandrel is inserted to seal the mouth of the rubber bag. The sealed bag is placed inside a high-pressure chamber filled with a fluid and it is hydrostatically pressed. Once pressuring is completed, the pressure is released slowly until the mold is removed from the pressure chamber and the pressed component is removed from the mold.

2.1.3.4   Hot isostatic pressing

The hot isostatic press (HIP) requires heat and pressure simultaneously. A furnace is constructed within a high-pressure vessel and the pressed objects are placed inside. Fig. 2.2 shows a typical HIP arrangement. Temperature can be up to 2000 ℃ and pressures are typically in the range of 30-100 MPa in which a gas is used as the medium pressure. Argon is a gas most commonly used for HIPing, but oxidizing and reactive gaseous can be also used. Now HIPing is used for a wide variety of ceramic components, such as alumina-based tool bits and the silicon nitride nozzles used in flue-gas desulphurization plants by the utility industry. The advantages of the HIPing process are becoming more important as the interest in structural ceramics.
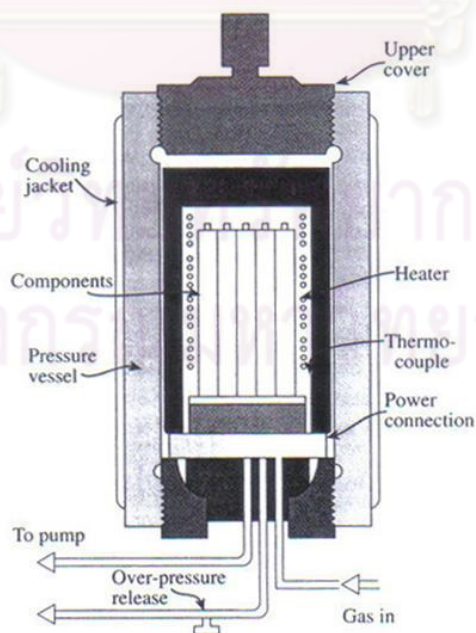
Figure 2.2   Schematic of a hot isostatic pressing apparatus [23].

2.1.3.5 Injection molding

Injection molding can be applied to shape and form ceramic components if the ceramic powder is added to a thermoplastic polymer. The ceramic powder is added to the binder and is usually mixed with several other organic materials to provide a mass that has the desired rheological properties. Firstly, the plastic mass is heated in order to indentify thermoplastic polymer, which becomes soft then it is forced into a mold cavity. The heated mixture becomes a fluid and is not self-supporting. The mixture is allowed to cool in the mold when the thermoplastic polymer hardens. Because of the large volume fraction of organic material used in the mixture, there is a high degree of shrinkage of injection-molded components during sintering. However, complex shapes are retained with very little distortion during sintering.

2.1.4 Properties and applications of alumina

Alumina is the most cost effective and widely used material in the ceramic community. The raw materials from which this high performance technical grade ceramic is made are readily available at reasonably priced, resulting to a reasonable cost of fabricated alumina shapes. With an excellent combination of properties and an attractive price, it is widely used in ranges of applications [7, 24]. Alumina properties and applications are given in Table 2.1.

Table 2.1 Typical properties and applications of alumina [25].

Properties	Applications
Hard (7-9 GPa), wear-resistant and high strength (2100 MPa)	Grinding media, cutting tool and mechanical parts
Resists strong acid and alkali attack	Laboratory instrument tubes and sample holders
Good thermal conductivity (18 W/m•K) and thermal expansion coefficient ($8.1 \times 10^{-6} K^{-1}$)	Furnace liner tubes and Thermometry sensors

However, alumina could wear after a certain period of time. Hence, this work aims to improve an alumina surface by diamond coating and as a result, its hardness of alumina increase.

2.1.5 Adhesion of diamond film on alumina

The alumina structure is very different from the diamond structure, therefore the diamond nuclei cannot grow from an α- Al_2O_3 directly. It is easy to form a non-diamond carbon on the alumina surface, and the diamond nuclei can be formed preferentially on the surface with a diamond-like or amorphous carbon phase. In process of diamond deposition on the alumina substrate, the initial deposited positions are porosity, grain boundaries and vacancies on the surface of the substrate, in which encourage high carbon diffusion into the substrate during the process [13]. This process can be described in three parts: (1) non-diamond carbon deposited on the substrate at the grain boundaries and vacancies of the surface, (2) diamond nuclei formed on the non-diamond surface and (3) diamond nuclei grew up and formed stable nuclei [21, 26]. However, alumina substrates without surface pre-treatment have coarse morphologies, large number of grain boundaries and a hole existed in the surface. Therefore, surface pre-treatment can induce a number of small diamond particles, reduce the roughness of the alumina surface, but generate a large number of scratches with small size in the surface. Diamond films can grow directly on the diamond particles reserved on the surface. Moreover, scratches will increase the surface energy of the substrate and reduce the contact angle and the barrier potential of nucleation [13, 21].

2.2 Carbon Atom and Diamond Structure

Diamond and graphite are crystal forms of carbon. The ideal structure of graphite is a close-packed hexagonal crystal with the carbon in sp^2 hybridization as shown in Fig. 2.3, representing the infinite layers of carbon atom. The carbon atoms form three σ bonds due to the overlap of three sp^2 superimposed orbital, and a π bond form the interaction of p orbital. The in-plane C-C distance is 0.14 nm and the inter-plane C-C distance is 0.34 nm. The carbon atoms form strong covalent bonds in plane and weak Van der Waals bond between the planes. Carbon atoms have four free

electrons, where one carbon atom is linked to three carbons so only three free electrons are paired and it is left with one free electron. Thus carbon atoms in graphite only utilize three of the four valence electrons for the covalent bonds formation. The fourth electron is free to move from one carbon to another, hence it can conduct heat and electricity [27].
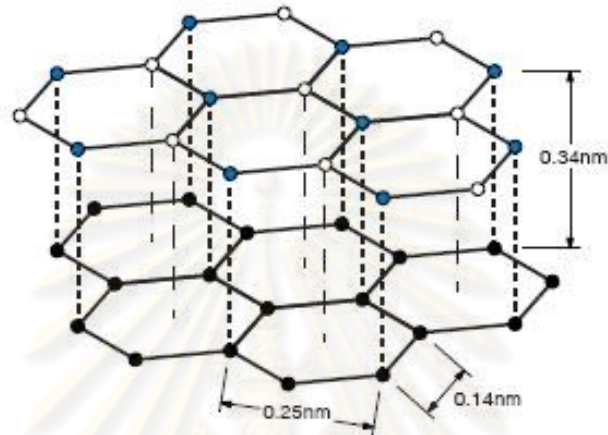
Figure 2.3 Crystal structure of graphite [28].

The diamond structure (Fig.2.4) shows a three-dimensional network of strong covalent bonds. The diamond structure is cubic with cube edge length of a_0 is 0.3567 nm. The diamond structure can be defined as two interpenetrating face-centered cubic (FCC) structure with interatomic distances of 0.154 nm. Each atom is covalently bonded to four other carbon atoms in a form of a tetrahedron. Although the structure is simple, there are lots of consequences for understanding the exceptional properties of diamond. The most common and most utilized implication of the structure is the fact that the carbon crystals are top ranked in hardness and exhibit exceptional tribological properties [8, 29].
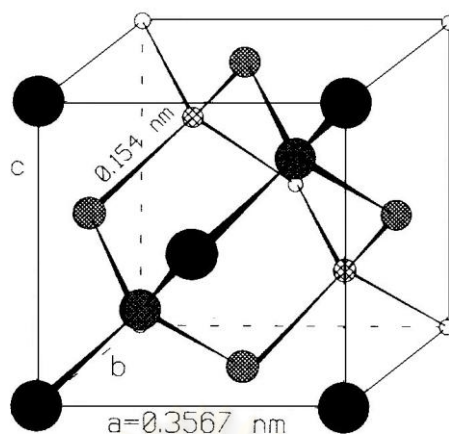
Figure 2.4 The cubic unit cell of diamond structure [29].

Many forms of solid carbon can be produced by CVD process because of the hybrid sp, sp^2 and sp^3 carbon orbitals that are readily available for bonding. A mechanism of diamond nucleation and growth process requires a structural knowledge of the competing crystalline and amorphous phases. Cubic diamond containing only sp^3 carbons and graphite containing only sp^2 carbons are most widely known as phases of crystalline carbon [29]. However, the structure of diamond formed by sp^3 hybridization carbon atoms is unique in nature. Its unique properties make it suitable for a variety of commercial applications. Table 2.2 represents the properties and applications of diamond.

Table 2.2 Properties and applications of diamond [8].

Properties		Applications
Hardness (GPa)	85-100	Drill bits, polishing materials, cutting tools, coating materials
Coefficient of friction	0.05-0.15	Wear resistance coating on lenses, bearings, tools or hard disk, sliding parts
Chemical inertness	Inert	Coating for reactor vessels, sample containers for analytical instruments
Thermal conductivity $(W \cdot m^{-1} \cdot K^{-1})$	2000	Insulating heat sinks for high power electronics
Thermal expansion coefficient $(\times 10^{-6} \cdot K^{-1})$	1.2	

2.3 Diamond-like carbon (DLC) film

Diamond-like carbon films are metastable amorphous materials, which may include a microcrystalline phase. Diamond-like carbon can also be known as an amorphous carbon material, which composed mainly of carbon and hydrogen and a simple random network of covalently bonded carbon as shown in Fig. 2.5. DLC films contain sp^3, sp^2, and even sp^1 in coordination with carbon atoms in a disordered network. DLC films are amorphous with a significant fraction of sp^3 hybridized carbon atoms, which can contain a significant amount of hydrogen. Depending on the deposition conditions, these films can be fully amorphous or contain diamond crystallites. The differences in both structures and chemical bonds between sp^2 and sp^3 hybridized carbon produce the variety of the DLC film properties [29-30]. The properties of DLC films, listed in Table 2.3, cover a wide range of values between those of diamond and graphite.

Table 2.3 Properties and applications of diamond-like carbon films [30].

Properties	Applications
transparency in visible and infrared	optical coatings, both antireflective and wear resistant
chemical inertness in acids, alkalis, and organic solvents	chemically passivating coating, corrosion-protective coatings of magnetic media
high hardness (5-80 GPa) and low friction coefficient (<0.01-0.7)	tribological and wear-resistant coatings
wide range of electrical resistivities (10^2-10^{16} Ω/cm)	insulating coatings

The term 'diamond-like carbon' is used mainly for these materials because their properties are most similar to those diamonds. High hardness and the chemical resistance of DLC films make them good candidates for the use as wear-resistant coatings on metals and on optical and electronic components [29].
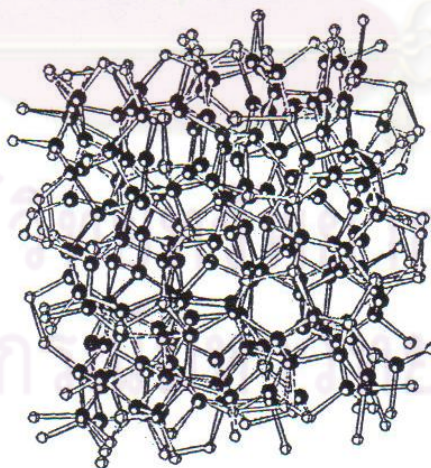
Figure 2.5 Schematic representation of DLC structure [31].

2.4 Plasma

Plasma is a kind of ionized gas. When a solid is heated so sufficiently that the thermal motion of the atoms breaks the crystal lattice structure apart, usually liquid is formed and when a liquid is heated enough for atoms to vaporize off the surface faster than they recondense, the gas is formed. When the gas is heated enough that the atoms collide with each other and knock their electrons off in the process, plasma is formed, known as 'fourth state of matter' (Fig. 2.6). In most materials the dynamics of motion are determined by forces between near-neighbor regions of the material. Typically in the laboratory, a small amount of gas is heated and ionized by driving through an electric current. The thermal capacity of the container is used to keep it from getting hot enough to melt, resulting alone ionize.

Generally, these means of plasma formation give energy to free electrons in the plasma directly, and then electron-atom collisions liberate more electrons and the process cascades until the desired degree of ionization is achieved [32]. Collision processes in the gas phase can be broadly divided into elastic and inelastic collisions, depending on whether the internal energies of the colliding particles are converted. Neutral particles usually have two types of energy, kinetic energy and potential energy, which may be a form of electronic excitation, ionization, dissociation, etc. An elastic collision is one in which there is an interchange of kinetic energy only; it is also called a collision of the first kind. An inelastic collision is one in which the internal energy changes. The simplest collisions are elastic, so the kinetic energy is conserved. But since the electron and any atom have greatly different masses, so the electron only changes its momentum without significantly changing its kinetic energy. When the electron is moving in an electric field, elastic collisions generally have the effect of restricting its velocity in the direction of the field. The charge particles collide incessantly with on another and with the neutral particles in the plasma. The distance traveled by a given particle between two successive collisions is called its free path. The magnitude and direction of free path are distributed at random. The mean free path is the average of the free paths traveled by charged particle collisions with neutral particles. Therefore, it is inversely proportional to the gas density and the gas pressure at a given gas temperature [33].

16
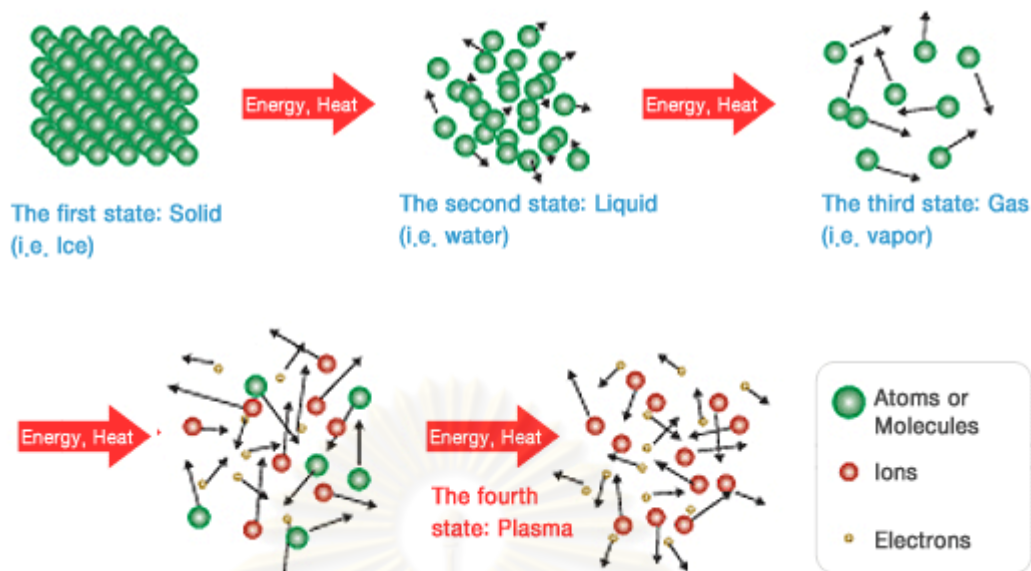
Figure 2.6 The four states of matter [34].

2.5 Chemical vapor deposition (CVD) technique

Chemical vapor deposition is the technique of modifying properties of material surface by depositing a compound layer through chemical reactions in the gaseous medium surrounding the material. CVD may be defined as a technique in which a mixture of gaseous interacts with the surface of a substrate at a relative high temperature, resulting in the decomposition of some constituents of the gas mixture and the formation of a solid coating film of a compound on the substrate [35].

The growth of diamonds from the vapor phase is basically a chemical reaction in which the formation of the diamond structure (carbon with sp^3 bond hybridization) and the graphitic structure (carbon with sp^2 bond hybridization) compete. This process occurs either in the solid-gas interface or at the vapor phase. The precursor gas is initially diluted with excess hydrogen. Energy is needed to activate the gas phase in order to produce diamond films. This gas phase contains a mixture of molecules, radicals, ions, and electrons that oscillate randomly in three dimensions. These energies could come from many variety of sources such as hot filament, electrical discharge (DC, RF or MW), or even from a combustion flame [8, 36].

The fundamental sequential steps that occur in every CVD process are sketched in Fig. 2.7 include [37]:

1. The total gas flows from gas inlet lines to the reaction zone
2. Chemical reactions in the gas phase will produce reactive radicals, atom ions and electrons
3. The initial reactants and reactive species are transported to the substrate surface
4. Adsorption (chemical and physical) and diffusion of reactive species on the substrate surface
5. The reactive species will react on and diffuse close to the substrate surface
6. Diamond nucleation forms on the substrate surface and starts to grow
7. The by-products of surface reactions will be desorbed back into the gas phase.
8. The reaction by-products will be transfer to main flow.

Main gas flow region

Gas phase reactions

Transfer of
by-product to mainflow

GAS

Transport to surface

Readsorption of
film precursor

Surface diffusion
& Surface reaction

Desorption of volatile surface
reaction products

Adsorption of film precursor

Nucleation & growth

Step growth

SOLID
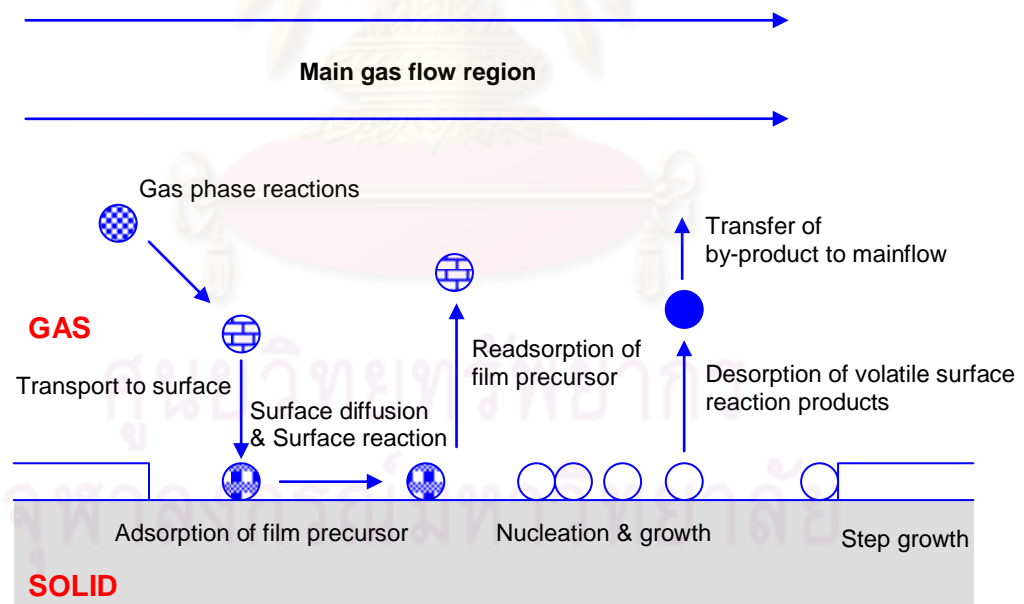
Figure 2.7   Sequence of gas transport and reaction processes contributing to CVD film growth [38].

The influence of diamond nucleation and growth processes requires knowledge of its complex deposition chemistry. This chemistry is complex in comparison to most deposition system because of the competition for deposition among sp^2 and sp^3 types of carbon and because of many possible chemical reactions resulting from the complexity of CVD systems. There are several reactions or important precursor species for deposition, of which importance depends on experimental parameters, such as pressure, temperature, composition, activation mode and reactor geometry. An understanding of the competitive molecular processes, resulting in carbon deposition is needed if the simultaneous deposition of diamond is controlled.

Fig. 2.8 schematically shows the complexity of the competitive processes occurred during diamond growth. The competitive rates of deposition of sp^2 and sp^3 carbon, the conversion of sp^2 and sp^3 carbon and the reverse, etching of the various forms of carbon, and other such processes determine the net deposition quality. It is known that these processes do not only increase gas phase processes which may alter concentrations of hydrocarbon precursors, but also site-specific chemical reactions occurred on surfaces [9, 29].
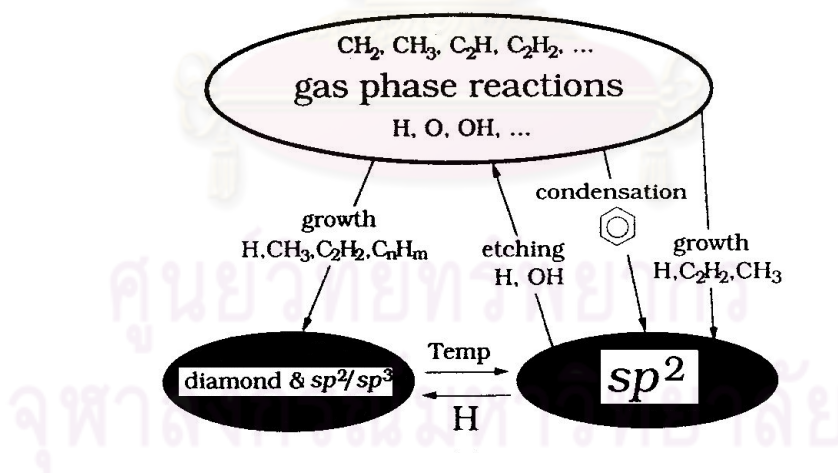
Figure 2.8   Schematic diagram of chemical species and reactions pathways leading to various forms of deposition carbon [29].

2.5.1 Microwave plasma enhanced chemical vapor deposition

In the plasma enhanced CVD (PECVD) technique, the heating of the gas mixture is attained by creating high energy plasma that activates the chemical reactions at considerably reduced temperature as compared to the conventional CVD [35]. A PECVD system is illustrated schematically in Fig. 2.9. A combination of gaseous is fed into the vacuum system and forms active species in the plasma, including precursors or monomers that are deposited in a thin film on the substrate. Different reactors are designed in order to get only the desired process. For this purpose, there are many operating parameters (external variables) such as pressure, substrate temperature, gas composition, gas flow rate, electrical power and frequency, and reactor geometry. The internal variables are electron and ion densities and fluxes, electron and ion temperature, neutral gas molecules and the free radicals produced in the reactor. The understanding and the control of the relationship between the external and internal variables are important due to the large number of above parameters involved and the complexity of any plasma medium have become important for advancement of plasma aided manufacturing [39-41].
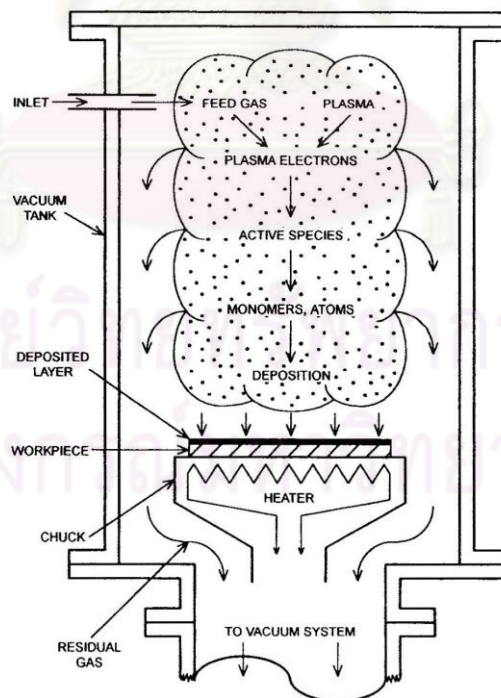
Figure 2.9 Schematic illustration of reactor for plasma enhanced chemical vapor deposition (PECVD) [39].

In a microwave plasma CVD (MWCVD) reactor, microwave power is coupled into the vacuum chamber via quartz window in order to create a discharge. The microwaves couple energy into gas phase electrons caused the electrons to move very quickly. When they collide with the molecules of gas inside the chamber, they dissociate the molecules of the gas into atoms. Further collisions between the electrons and the atoms result in ionization, forming ions and free radicals. Finally, diamond is deposited onto a substrate, which is immersed in the plasma [1, 41].

The two common types of MWCVD reactor are the NIRIM-type and the ASTEX-type reactor as shown in Fig. 2.10. In ASTEX-type reactor, microwaves are coupled into a cavity through a quartz window using an attenna. Microwave plasma CVD (MWCVD) techniques have been used much more extensively than any other techniques for the growth of diamond films. This technique has a number of advantages over the other techniques of film growth such as an electrodeless process avoiding contamination of the films due to electrode erosion. Furthermore, the microwave discharge at 2.45 GHz, being a high frequency process, produces high plasma density with high energy electrons. This could result in high concentration of atomic hydrogen and hydrocarbon radicals [9].

It is generally well known that the CH_4 molecules are decomposed into some hydrocarbon neutral radicals (CH, CH_2, CH_3), ionic radical (CH^+, CH_3^+, $C_2H_5^+$), and atomic or ionic hydrogen (H, H^+). The hydrocarbons etch into the substrate surface and create the dangling bonds on it, the neutral hydrocarbon radicals are adsorbed at the dangling bonds. At the same time, more of graphite-like sp^2 bonded phases are etched by atomic or ionic hydrogen and the diamond films are formed [29]. Therefore, the hydrocarbon and hydrogen ions density and the ion energy have great influence on the characteristics of DLC films.

(a)

(b)
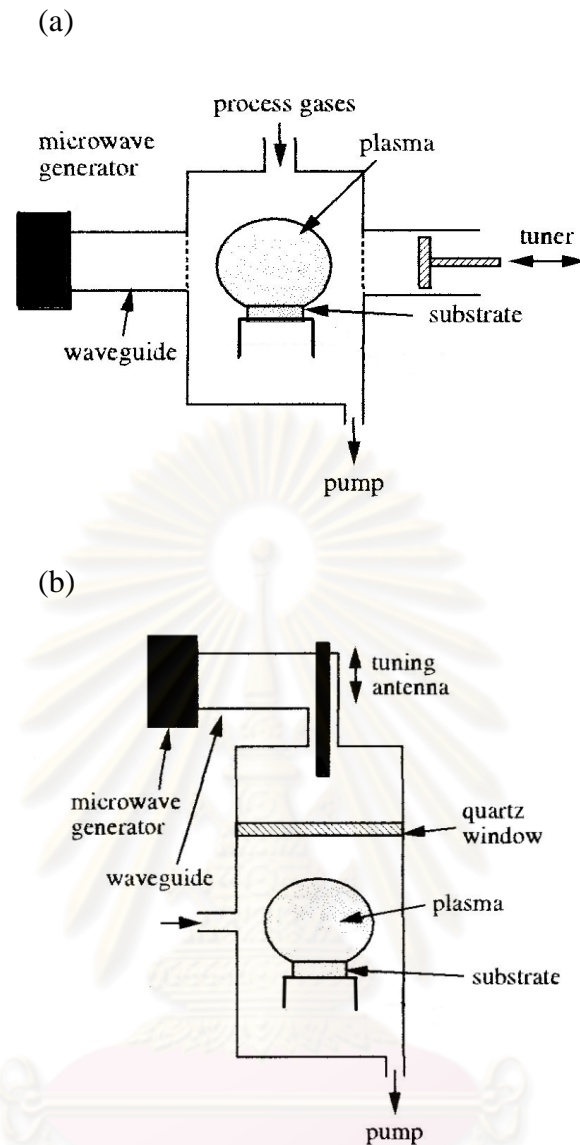
Figure 2.10 Example of the common types of microwave plasma reactor. (a) NIRIM-type and (b) ASTEX-type [1].

2.6 Nucleation growth of diamond film

Substrate pretreatment played an important role to control the nucleation, morphology, orientation and the surface roughness. Surface scratching with diamond powder [42-44] and substrate biasing [45-46] are the common techniques used to increase the nucleation density and decreasing incubation time. The most commonly used method of substrate pretreatment to increase the nucleation density is scratching with diamond powder. Ion implantation [47-48] and chemical etching [49-50] of substrate surfaces are one of the other treatments used to increase the nucleation

density and adhesion of the film to the substrate. Nucleation density and surface damage of the substrate strongly depend on the size of the diamond particles used for the pretreatment method. In the substrate pretreatment process, small fragments of diamond particles are embedded in the substrate materials and directly acted as the nucleation center of diamond growth. Scratching the substrate causes serious surface damage and hence the application of the coating for optical and electronic materials needs alternative nucleation techniques [8, 9].

According to Linjun Wang *et al.* [20], the research showed that the surface pretreatment of the substrate was commonly needed to obtain a continuous film. Based on their experiment, alumina substrates were ultrasonically cleaned with diamond powder suspended in acetone. Then, the microwave plasma CVD technique using a gaseous of methane and hydrogen was applied to deposit diamond films on substrate. It is proven by SEM, XRD and Raman measurements that diamond films were in good quality.

Wang *et al.* [45] studied the nucleation growth of diamond on molybdenum using hot filament CVD technique. The process was performed with negative bias of -300V in order to remove any contaminants on the surface and to activate the surface. They found that the negatively biased pretreatment greatly enhanced the nucleation density of diamond films on molybdenum, which were investigated by scanning electron microscopy.

Based on Chattopadhyay *et al.* [49], they studied the synthesis of diamond on cemented carbide substrate by hot filament CVD technique. The experiment showed that the substrate was etched with $HCl+HNO_3+H_2O$ (1:1:1) solution for 15 minutes at room temperature. From the SEM results, the etching pretreatment also increased the surface roughness of the substrate surface, in which it helped to hold the diamond coating to the substrate.

2.7 The CVD diamond growth conditions

In the CVD process, the optimization of diamond growth parameter space is very large and complex. The influences of the important parameter, controlling the films quality, including the substrate material, substrate temperature, concentration of gas methane, and deposition pressure are described as below.

2.7.1 Substrate materials

The influences of substrate materials are found to affect the growth properties of diamond films. The thermal expansion of substrate material should be comparable with diamond. This is because the high growth temperature in currently processes, a substrate will be expanded and thus the diamond coating will be grown upon and bonded directly to an expanded substrate. For this reason, the diamond film will have significant compressive stresses from the shrinking of the substrate and causes bowing of the sample, cracking and flaking or delamination of the film. The based substrate for vapor phase of growth diamond film is various, such as Mo, WC, Co, Pt, Cu, Fe, Ti, Ti alloy, TiC, Si, SiC, Si_3N_4, Al_2O_3, etc. [8].

Ristic *et al.* [50] studied that diamond films grown on different substrates (Cu, Si, WC-Co, Mo) by hot filament CVD technique. In all their experiment, the working gaseous mixture was 1% methane in hydrogen. The total gas pressure was 30 mbar. The position time was around 30 hr. The surface morphology of growth diamond films are given in SEM micrographs. They found that a well-faceted diamond crystals continuous coating were deposited on Cu, WC-Co and Mo substrates, whereas the morphology of diamond films grown on Si substrates were obtained a fine-grained. From the results on XRD and Raman measurements presented crystalline phase and high-quality diamond films on these substrates.

In this work, the DLC thin films are grown on alumina substrate. Deposition of diamond coating is utilized the ability of the material to increase hardness and wear resistance. However, the properties of diamond growth films are also upon to other parameters such as substrate temperature, methane gas concentration and deposition pressure.

2.7.2 Substrate temperature

The influences of substrate temperature are found to affect on the growth diamond films. In various CVD methods, diamond growth takes place at substrate temperature between 300 and 1200 °C. At low temperature, the formation of active sites is slow because it is limited by the low rate of reaction. With the increase of temperature, this rate is increased. However, at high temperature (>1200 °C), the number density of active species decreases due to their thermal decomposition and subsequent graphitization. The sp^2 carbon formed at these high temperatures is rapidly etched away by hydrogen atom. These phenomena explain the maximum in diamond growth rate with substrate temperature. At higher temperature than this maximum, the increasing density of surface radical enhanced sp^2 formation; while at lower substrate temperature, the condensation of aromatics can lead to a possibly amorphous sp^2 and sp^3 carbonaceous network [29]. Therefore, the substrate temperature of diamond growth in this work was kept in the range of 300-350 °C. In this experimental set up, he substrate is heated predominantly by heat transfer from the plasma gas rather than by direct microwave absorption [36].

Kulisch *et al.* [42] studied the influence of substrate temperature on the growth of nanocrystalline diamond films on silicon substrate in the range of 520-770 °C. They found that the growth process was thermally activated, leading to increasing growth rates with increasing temperature and the properties of crystalline (e.g. the grain size) of the films were almost not affected by the temperature in the range.

Study by Tyagi *et al.* [51] showed that the crystalline nature of the films deposited on molybdenum substrate change from polycrystalline to single crystal as they increase substrate temperature and for a certain set of parameters the growth of the diamond single crystals can be seen. The films were polycrystalline in the range of substrate temperature 850–900 °C, as the substrate temperature increasing.

Yan *et al.* [19] studied the effect of substrate temperature ranging from 750 to 950 °C on microstructure and the quality of diamond films deposited by DC arc plasma jet CVD technique. The results indicated that the covered crystalline planes on film surfaces changed from {220} to {111} planes as the temperature increased from 750 °C to 930 °C. For the diamond film deposited at 870 °C, there were still a few

interspaces, but for the films deposited at 930 °C and 935 °C, the films were very dense. It indicated that the temperature had a significant effect on the film density. In addition, the purity of the film increased with increasing temperature in the range of 750-900 °C, and when the temperature exceed 900 °C, the purity decreased.

2.7.3 Methane gas concentration

Diamond films have been grown from a variety of carbon-containing species mixed in certain concentrations with other reactive and inert gaseous. A large variety of carbon-containing species have been employed to synthesize diamond using CVD technique. These include methane, propane, butane, ethylene acethylene and carbon monoxide. In addition to carbon-containing carrier, the gas phase must usually contain nondiamond carbon etchings and diamond phase stabilizing agents, such as hydrogen, oxygen, chlorine, and fluorine atoms [8, 36]. The main factor affecting to the deposition characteristics with the increase in the initial hydrocarbon concentration are higher concentrations of growth species and therefore it is a larger deposition rate; increased formation of graphitic, which reduced film quality; and lower hydrogen atom concentrations [29]. The growth of diamond thin films normally requires the methane gas diluted in the hydrogen gas. In this work, methane gas concentration is varied between 0.5-5% in order to examine the film quality.

Askari *et al.* [43] reported that a low value of methane concentration is chosen in order to obtain a well-faceted good polycrystalline diamond films grown on titanium substrate, whereas a high value of methane concentration was preferred to achieve a smooth and fine-grained nanocrystalline diamond films with a surface roughness.

Buhlmann *et al.* [44] studied the influence of the methane/hydrogen gas ratio between 1-12.5%. They found that at low methane concentrations, faceted diamond deposits were formed on silicon substrate, whereas at higher methane contents, ballas or cauliflower-like morphology was observed. The methane content necessary for the faceted-to-ballas or cauliflower-like transition decreased with increasing temperature.

Regarding to Li *et al.* [18], the research was based on the effect of methane gas concentration on diamond films deposited on molybdenum substrate by DC-plasma

jet CVD technique. It was reported that at the beginning of diamond nucleation, diamond crystallites orientation was random, and the influence of CH_4 concentration was negligible. At a low CH_4 concentration (1%) and the substrate temperature of 850 °C, a high quality diamond film was prepared. The film structure was polycrystalline and (111) face was observed. When increasing CH_4 concentration, diamond film has more local clusters, amorphous graphite. Thus, higher CH_4 concentration had negative influence on preparing high quality diamond film. In addition, CH_4 concentration had significant affects on film uniformity, growth rate and crystal sizes.

2.7.4 Deposition pressure

The total pressure of hydrogen-hydrocarbon gaseous mixture determines the recombination length, the lifetime, and the drift distance of atomic hydrogen. In the condition of low pressure, the electrons and molecules are not in thermal equilibrium. Due to the difference in mass between electrons and ions, the electrons accelerate rapidly in an electric field, while the ions move slowly. However, there is no redistribution of energy between electrons and molecules and the gas temperature remains relatively cool due to the large electron mean free path. Thus, atomic hydrogen and neutral carbon-containing radicals, needed for the growth of diamond, are primarily generated by the high energy electrons of which concentration is relatively small. In addition, the growth rate in low pressure plasma is expected to be small. In the condition of high pressure, it causes the electron mean free path is small which could result to the redistribution of energy between electrons and molecules. So, the gas temperature is as near as the temperature of the electron, and both temperature can cause the generation of atomic hydrogen and neutral carbon-containing radicals. Consequently, the expectation of the growth rate in the high-pressure will increase [29]. Thus, the deposition pressure in this work is varied between 10-50 torr in order to investigate the influence of pressure on the formation of DLC thin films.

Liang *et al.* [14] studied the effect of pressure on the deposition of nanocrystalline diamond (NCD) films on silicon substrate in a hot filament chemical vapor deposition (HFCVD) system was investigated employing a 1% CH_4 in H_2 gas mixture. They found that diamond films as the growth pressure decreasing from 5.0 to

0.125 kPa, showed a gradual reduction of the diamond grain sizes from sub-micrometer to nanometer scale. In addition, the surface roughness of the deposited diamond films also decreased with the reduction of the growth pressure.

2.8   Film characterizing technique

The DLC films quality have been investigated by a variety of techniques. The characterizations of surface morphology are examined by scanning electron microscopy (SEM). Raman spectroscopy is the most widely used techniques to characterize carbon bonding in DLC thin films. Finally, the investigations of mechanical properties are evaluated by nanoindentation testing.

2.8.1   Scanning electron microscopy (SEM)

Scanning electron microscopy (SEM) is one of the most widely used techniques to characterize thin film surface morphology. It operates by scanning a focused electron beam over a surface and sensing the secondary electrons emitted from the surface. The electron beam can be focused on a very small and the beam size is the detrimental factor of the microscopy resolution. It is often necessary to coat a diamond film surface with a thin layer of gold or carbon for avoiding charging effects. Working at low electron voltage is always useful for avoiding the charging effect while working with insulating films. It has been recognized that diamond films produced on nondiamond substrates are comprised of different surface morphologies depending on the deposition conditions and substrate chemical nature [8].

A basic diagram of an SEM is shown in Fig. 2.11. The electron gun produces a beam of electrons that is attracted through the anode and condensed by the condenser lens and then focused as a very fine point on the substrate by the objective lens. A set of small coils are energized by a varying voltage produced by the scan generator and created a magnetic field that deflects the beam of electrons back and forth in a controlled pattern. When the beam of electrons strikes the substrate, a complex series of interactions occurs, resulting in the production of secondary electrons from the sample, which are collected by the detector, converted to a voltage, and amplified. The amplified voltage is then applied to the grid of the cathode-ray tube (CRT) and changes the intensity of the spot of light on the surface [52].
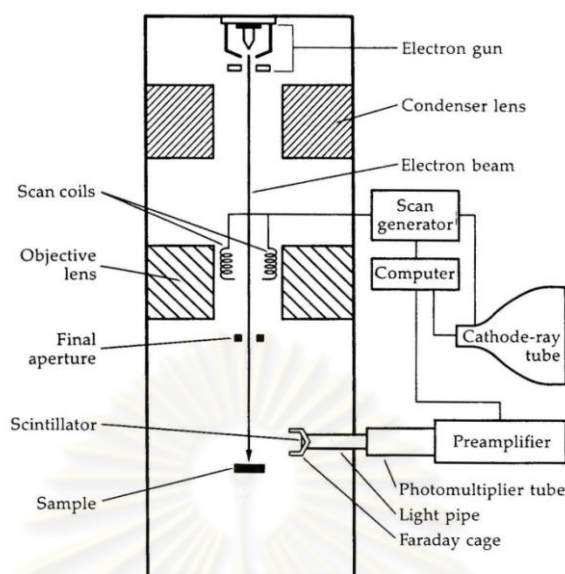
Figure 2.11 Schematic of a scanning electron microscope [52].

Based on Rujisamphan's research [53], he studied the growth of diamond thin film on silicon substrate by MW-PECVD technique. According to SEM, he found that the diameter of individual diamond nuclei was increased as deposition time increased. The film surface morphology changed from scatter well-faceted to cauliflower-like continuous film with increasing CH_4 concentration. Moreover, he observed that the surface roughness and grain size decreased with increasing in CH_4 concentration.

Askari *et al.* [43] presented that the surface morphology of growth diamond film on titanium substrate at low CH_4 concentration was well-faceted and polycrystalline morphology. The average grain size was less than 1 μm and exhibited [111] orientation. The average surface roughness of this film was approximately about 95 nm. Furthermore, the surface morphology of the grown nanocrystalline diamond film (high CH_4 concentration) showed that the film consisted of nanocrystals with average grain size of 30 nm or less. The surface roughness of nanocrystalline diamond film was approximately 35 nm.

2.8.2   Raman spectroscopy

Raman spectroscopy has been the most widely used tool for the examination of the types of bonding present in carbon films. It is a complementary technique to IR spectroscopy. A modern Raman spectrometer is designed for ultraviolet excitation. Radiation from a laser is focused on the substrate surface. The reflected and scattered radiations are collected normally to the substrate surface by a high-power microscope objective and, after reflection by a beam splitter, transferred to a grating monochromator through a Rayleigh-line rejection filter, and detected by an array detector. The filter separates the elastically scattered (Rayleigh) radiation from the inelastically scattered Raman radiation. Because the former is a general order of magnitude more intense than the latter, the development of such a notch filter constitutes a major advance of modern commercial Raman spectrophotometers. The beam splitter also directs light from an illuminator, which had been reflected by a second beam splitter, to impinge on the substrate surface. This light makes it possible to see the Raman-analyzed surface and detect inhomogeneities. Both the impinging excitation and the reflected and scattered Raman radiations are distributed over a wide solid angle. Raman spectra are plotted as frequency shifts from the exciting frequency against intensity [30, 54].

There are three types of signal in a typical Raman experiment as illustrated in Fig. 2.12. In Rayleigh scattering, a molecular is excited by the incident photon to a virtual energy level. This energy level is caused by a distortion of the electron distribution of a covalent bond. The molecular returns to the vibrational ground state by emitting the same energy. Rayleigh scattering is an elastic process. Vibration excitations can be created, and causes a decrease in the frequency of the scattered light, which causes an increase. The decrease in frequency is called Stoke scattering and the increase is called anti-Stoke scattering. Stokes scattering is the normal Raman effect and Raman spectroscopy generally uses Stokes radiation [7].
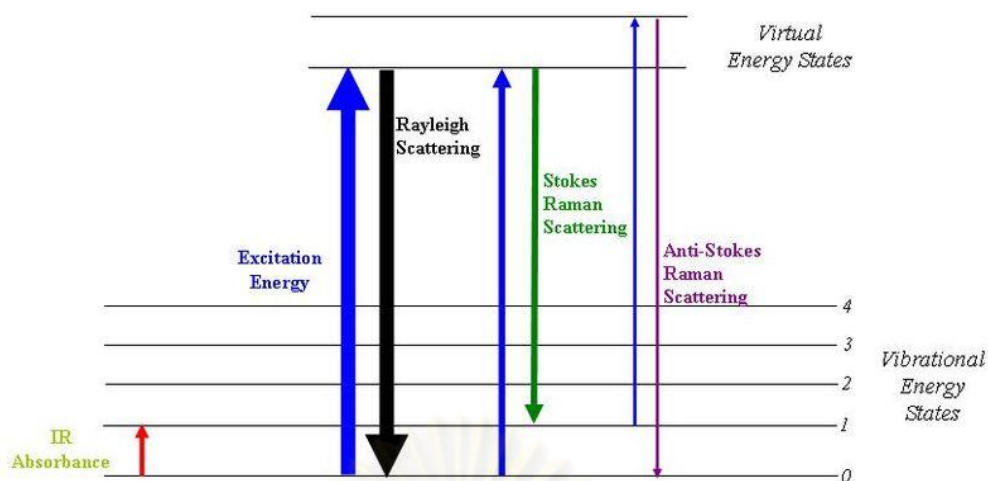
Figure 2.12 Schematic of transitions occurring in Raman spectroscopy [54].

Using the Raman spectroscopy technique with diamond, which has a phonon density of states and it has a very different form from other carbon phases. The Raman signal is very sensitive to short range disorder and subsequently it can reveal different forms of amorphous carbon and graphite. The position of various Raman bands observed in CVD diamond films, and their corresponding assignments and descriptions are given in Table 2.4.

Table 2.4 Raman bands in CVD diamond films [8].

Position (cm⁻¹)	Assignments	Descriptions
~1140	Nanocrystalline (sizes of 1-100 nm) diamond	occasionally observed in diamond films small grain sizes
1332	Cubic diamond	first order peak with FWHM of 1.9 cm⁻¹ for natural diamond
1345	Amorphous carbon	broad band
~1550	Amorphous or diamond-like carbon	broad band
~1580	Graphitic	first order peak

Askari *et al.* [43] reported that the Raman spectrum of nanocrystalline diamond film deposited on titanium substrate clearly showed the characteristic diamond and graphite phase. There was a peak at about 1334 cm^{-1}, which corresponded to the diamond peak. Raman bands around 1475-1550 cm^{-1} could be attributed to sp^2-bonded carbon. Raman peak at approximately 1130 cm^{-1} was caused by a size effect of nanoscale diamond.

Wang *et al.* [20] studied the effect of substrate temperature on the quality of diamond films, and they worked the Raman measurements on diamond films deposited on alumina substrate under 700, 780, 830 and 900 °C. They found that the films were mainly composed of the diamond phase at 1334 cm^{-1}. An obvious intensity decreased with the weak broad band around 1580 cm^{-1} (related to sp^2 bonding).

2.8.3 Nanoindentation test

Nanoindentation technique is one of the most popular applications for determination the mechanical properties of material surface. This nanoindenter can be used to characterize organic, inorganic, soft or hard materials and coatings. Examples are thin films and multilayer PVD, CVD, PECVD, and many other types of films and coatings. In the nanoindentation tests, the properties of thin films maybe measured without removing the films from the substrate as it done in other of testing. The nanoindentation tester has been designed to provide surface mechanical characterization data by indenting to depths at the nanometer-micron scales [7].

In nanoindentation tester, an indenter tip is driven into a specific site of the sample to be tested by applying an increased normal load. Indenter displacement is measured using a capacitive transducer. Using the partial-unload technique, the contact hardness of the sample can be calculated as a function of depth of penetration into the sample. The instrument applies load via calibrated electromagnetic coil and displacement of the indenter is measured using a capacitive sensor. A schematic of the instrument is shown in Fig. 2.13. A particular feature of this instrument is the use of a sapphire ring that remains in contact with the sample surface during the indentation. The ring provided a differential measurement of penetration depth and thus the load frame compliance and the thermal drift are automatically compensated [55].
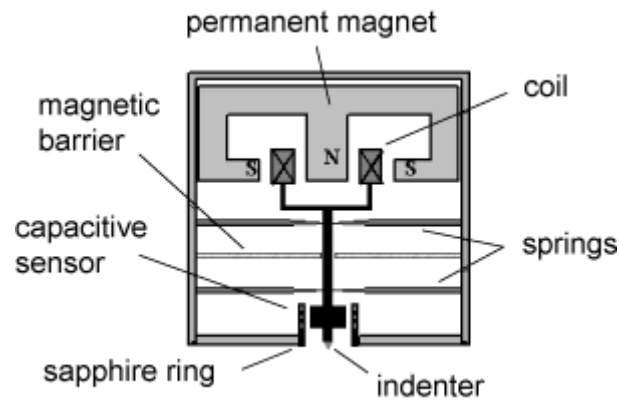
Figure 2.13 Schematic of a nanoindentation tester [56].

Based on Martinez *et al.* [57], their research studied the effects of substrate temperature on the hardness and adhesion of DLC thin films deposited on silicon substrate by radio frequency plasma CVD technique using CH_4 and H_2 gaseous mixture. In their experiment, nanoindentation system was used to evaluate the hardness of the films. The hardness and Young's modulus of the films were calculated form the load-displacement curves. These curves were obtained with a diamond Berkovich indenter and a lading and unloading rate of 0.1 mNs^{-1} up to maximum load of 5 mN, which gave contacts penetration depths lower than 20% of the films thickness. The films as a function of deposition temperatures presented hardness value in the range of 12-14 GPa. Furthermore, they found that the hardness of the films was similar in samples deposited at temperatures from 20 to 300 ℃ and decreased at higher deposition temperature to 9.5 GPa.

Regarding to Kulish *et al.* [58], their research studied the mechanical properties of nanocrystalline diamond/ amorphous carbon composite films grown on silicon substrate by microwave plasma CVD technique from CH_4 and H_2 gaseous mixture. They presented the results of the investigation of the films mechnical by nanoindentation measurements. They found that the average indentation hardness of the film at 17% CH_4 is 39.7 ± 2.2 GPa. A typical nanoindentation load-displacement curve of the film is shown in Fig. 2.14.
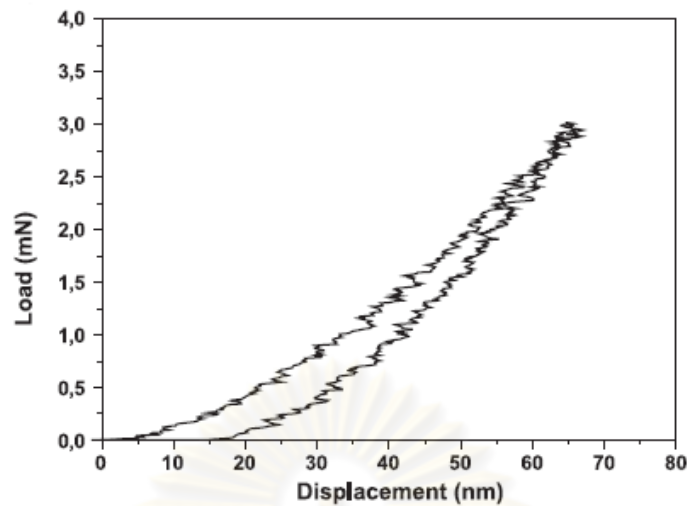
Figure 2.14 Load-displacement curve of nanocrystalline/amorphous carbon films prepared with 17% CH_4 [58].

2.8.4 Atomic force microscopy (AFM)

Atomic force microscopy (AFM) has been extensively used to investigate the surface morphology, roughness, and initial stage of nucleation [8]. AFM is an electron microscope; instead of using a beam of electrons to image the sample, a very fine mechanical probe scans the surface of sample. The instrument uses a piezoelectric device for scanning. The piezoelectric effect occurs because certain crystals increase in size when a voltage is applied. By combining crystals, movement in x, y, z directions is possible. In an AFM, the sample is mounted on the piezo device and moved. A very fine tip is mounted on a triangular piece of metal foil called the cantilever (Fig. 2.15). The piezoelectric device moves the sample under the tip. The variation in attractive forces between the electrons in the orbital shells of the tip and those of the sample causes movement of the foil. The reflected beam of the laser is detected by a photodiode. Movement of the foil causes variation in the current in the photodiode. This variation in current is then used to produce an image on cathode-ray tube (CRT). Alternatively, a feedback mechanism can be used to move the tip in order to keep the photodiode current constant, and the variation in voltage applied to the piezoelectric device can be used to produce the image. One major advantage of the AFM is that samples do not need to be conductive [52].
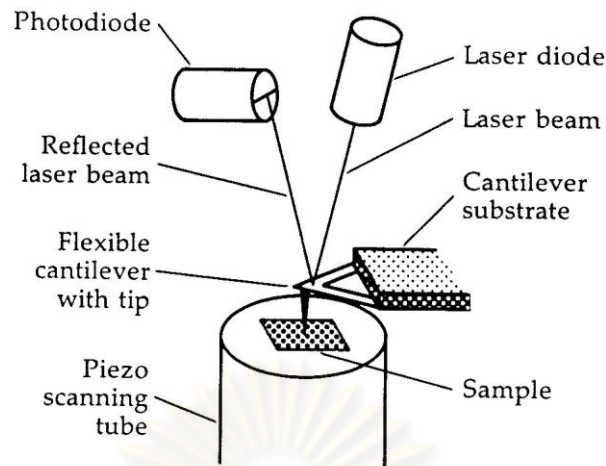
Figure 2.15 Schematic of an atomic force microscope [52].

Based on Cho *et al.* [59], their research studied the deposition of DLC films on silicon substrate by MW-PECVD technique with various DC bias voltages and by RF-PECVD technique with various RF powers. According to AFM, the surface roughness of the DLC films deposited by the MW-PECVD decreased with increasing the negative DC bias voltage due to the heat dissipation of impinging ions, which could help the surface smoothing. In case the films deposited by the RF-PECVD, the surface produced at a RF power of 25W was rough and it became smoother as the RF power increased except at a RF power of 200W.

Regarding to Liang *et al.* [14], their research studied the effect of pressure on nanocrystalline diamond films grown on silicon substrate by hot filament CVD technique from CH_4/H_2 gaseous mixture. From the results on AFM, they found that the size of most grains distribute in the range of 40-80 nm. Furthermore, the surface roughness of the films increased with decreasing the grain sizes. The root-mean-square (rms) roughness of the films was found to decrease from 16 nm to 8 nm as deposition pressure was decreased from 4 kPa to 0.125 kPa. The films deposited at pressure in between lies presented the rms roughness value in the range of 10-15 nm.

CHAPTER III

EXPERIMENTAL

In this chapter, the materials and chemicals, microwave plasma system, substrate preparation and synthesis of DLC thin films procedure will be explained. The most widely characterization techniques of DLC thin films, Scanning Electron Microscope (SEM), Raman Spectroscope, Atomic Force Microscope (AFM), and nanoindentation tester which have been used in this work will be presented.

3.1   Materials and Chemicals

The chemicals used in these experiments, carried out at the Plasma Laboratory were specified as follows:

1. Methanol (Commercial grade) was purchased from CTL.
2. Acetone (Commercial grade) was purchased from ZEN POINT.
3. De-ionized water was donated from Faculty of Science, Chulalongkorn University.
4. Sodium Hydroxide was purchased from SIGMA-ALDRICH.
5. Diamond powder (virgin diamond powder 0.1 μm type MB-1-um form EID).
6. Ultra high purity hydrogen gas was purchased from Thai Industrial Gas Co., Ltd. (TIG).
7. Methane gas was purchased from Thai Industrial Gas Co., Ltd. (TIG).

3.2   Microwave plasma system

The microwave plasma reactor was designed to be assembled as an economical home-made prototype by Rujisamphan [50], the photograph and schematic of the system are shown in Fig. 3.1 and 3.2, respectively. The system consists of vacuum chamber, microwave guiding components, and gas flowing system.

3.2.1 Vacuum chamber

The vacuum chamber was made from stainless steel. The chamber was equipped with many plates; the front plate was used for sample loading while the bottom plate was connected with three ports, leading to an Edwards Speedivalve, an air leak valve, and a substrate holder. The substrate temperature was measured by a thermocouple embedded within the substrate holder. The left plate was connected with the Edwards Penning and the Edwards Pirani vacuum gauge. The chamber was evacuated using a rotary vane pump Edwards model RV3 and the turbo molecular pump Edwards model ACX75. The top plate was connected with a doughnut-plate in which was designed for water cooling and gas inlet line.

3.2.2 Microwave guiding components

Microwave guiding components composed of cylindrical cavity, waveguide, and magnetron power supply. Traditional microwave plasma research, mostly utilized at 2.45 GHz, in which its frequency is the same as that used in conventional microwave oven. The microwave plasma system used the magnetron source that generates a microwave for forming plasma from the conventional microwave oven powered by a phase controlling power supply. A waveguide unit that guided the microwave was generated by the magnetron source toward the cylindrical cavity via an axial antenna. An antenna made of a conductive material provided a lot of microwave radiation for radiating the microwave was guided by the microwave guide unit toward the chamber. A discharge called a plasma ball was generated above the substrate.

3.2.3 Gas flowing system

The gas flowing system consists of methane (CH_4) and hydrogen (H_2) tanks, regulators, and mass flow controllers (Aalborg model GFC-17 and Dwyer model GFC-2102). These gaseous were regulated by mass flow controllers with an accurate the gas flow rate. Each of gaseous flew through a manual on-off valve and mixed in the gas inlet line. The unit of gas flow rate is the standard centimeters cubed per minute (sccm).

Figure 3.1   The photograph of MW-PECVD reactor.
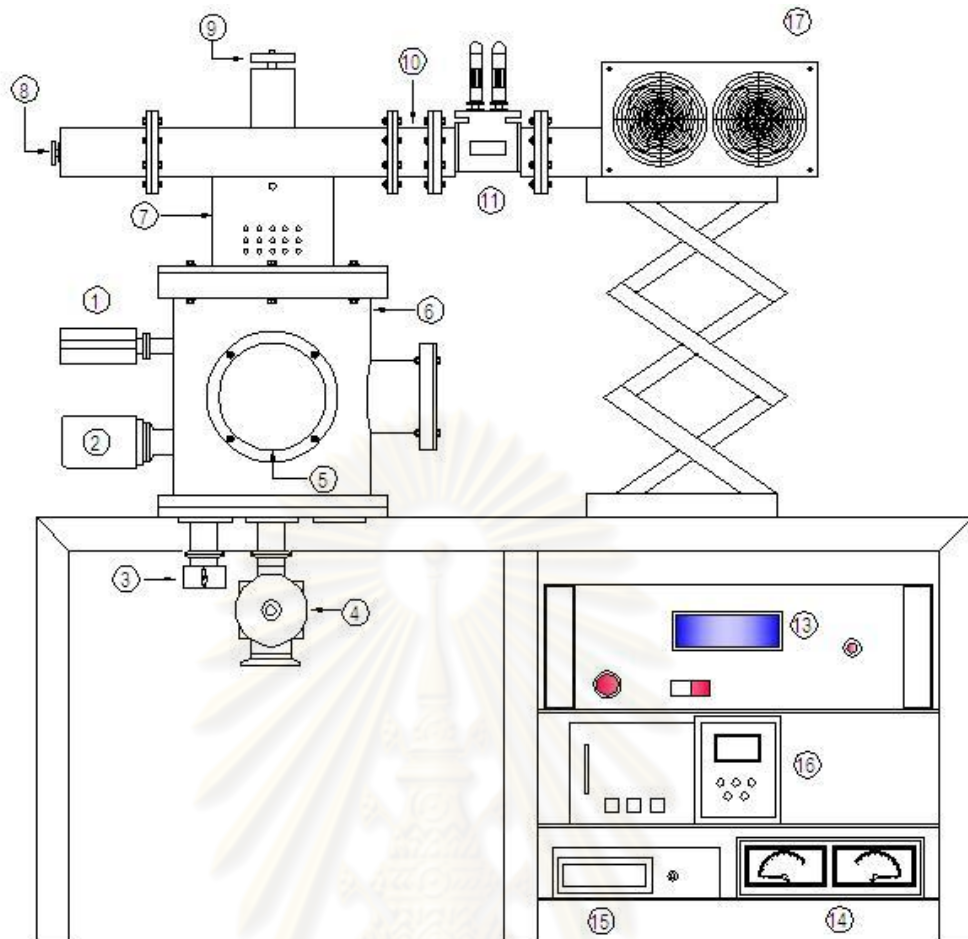
[1] Penning Gauge   [10] Waveguide

[2] Pirani Gauge   [11] Dual Power Monitor

[3] Air-leak valve   [12] Turbo controller

[4] Speedivalve   [13] Power supply

[5] Loading door   [14] Microwave power meter

[6] Chamber   [15] Temperature indicator

[7] Cylindrical cavity   [16] Gauge monitor

[8] Short-circuit plunger   [17] Magnetron source

[9] Brass antenna

Figure 3.2 The schematic diagram of MW-PECVD reactor.

3.3 Substrate preparation

In this research, prior to the deposition of diamond films, the alumina substrates were pretreated by cleaning with detergent, scratching with diamond powder (0.1 μm) by hand for 30 min, cleaning by ultrasonic for 30 min in acetone, methanol, and de-ionized water respectively. Finally, they were blown dried with nitrogen gas.

3.4 Synthesis of DLC thin films procedure

The substrates were loaded in the reactor chamber pumped by a rotary pump. This pump evacuated air in the chamber until the total gas pressure reached at about 2-2.6 x 10^{-2} torr. After the based pressure, a turbo pump evacuated air until the pressure between 1.2-1.5 x 10^{-5} torr. Then, the gaseous mixture of methane and hydrogen were fed into the chamber and deposition pressure was adjusted by the controlling valve of pump. Finally, the MW-PECVD technique was applied to deposit DLC thin films on alumina substrates. In this research, the methane (CH_4) concentration, deposition pressure and deposition time were investigated. After the growth process completed, all substrates were cooled down to room temperature within the reactor chamber under evacuating conditions. The range of growth conditions using in this study are shown below in Table 3.1.

Table 3.1 Deposition conditions for the DLC thin films.

Parameters	Range
Gas composition (%)	
$CH_4 : H_2$	0.5-5
Gas flow rate (sccm)	
H_2	100
CH_4	0.5-5
Deposition pressure (Torr)	10-50
Microwave power (W)	700
Substrate temperature (°C)	300-350
Deposition time (hr)	5-30

3.5   Characterization of DLC thin films

The obtained films were analyzed by the following methods:

3.5.1   Scanning electron microscopy (SEM)

SEM observation with a JEOL mode JSM-6480LV, at Faculty of Science, Chulalongkorn University was employed to investigate the morphology of DLC films as shown in Fig. 3.3. The samples for SEM analysis were coated with gold particles by ion sputtering device to provide electrical contact to the specimens.

Figure 3.3 Photograph of Scanning electron microscope (SEM).

3.5.2   Raman spectroscopy

Raman spectrums were measured by Renishaw invia raman microscope (Fig. 3.4) using 514.5 nm line of an argon ion laser, at The Gem and Jewelry Institute of Thailand (Public Organization) (GIT), Bangkok.

Figure 3.4 Photograph of Renishaw invia raman microscope.

3.5.3   Nanoindentation test

The hardness of CVD diamond films were determined by nanoindentaion using a CSM nano hardness tester (NHT), at Nano Shield Company Limited, Samutprakarn as shown in Fig. 3.5.   Hardness of the films was calculated from the load-displacement curves. These curves were obtained with a Berkovich diamond indenter and a loading and unloading rate of 10 mN min^{-1} up to maximum load of 5 mN. For each samples, a number of indentations have been performed at different position.

Figure 3.5 Photograph of CSM nano hardness testers (NHT).

3.5.4 Atomic force microscopy (AFM)

Atomic Force Microscope (AFM) shown in Fig. 3.6 was used to examine the surface roughness of the diamond film using Nano Scope IV with tapping mode, at Scientific Technological Research Equipment Center, Chulalongkorn University.
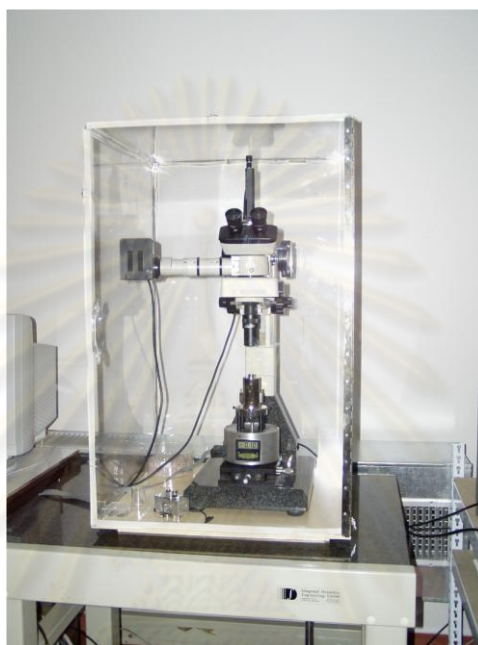

Figure 3.6 Photograph of Atomic Force Microscope (AFM).

CHAPTER IV

RESULTS AND DISCUSSION

The main purpose of this research is to investigate and characterize the effect of CVD diamond growth conditions deposited on alumina substrates including methane concentration, deposition pressure, and deposition time, which were used for the MW-PECVD system during the films formation on the films morphology, films quality, surface roughness, as well as films hardness.

4.1   Effect of methane concentration on the DLC films formation

The DLC films were deposited under various CH_4 concentrations namely 0.5%, 1%, 2%, 3%, and 5%. These samples were grown at microwave power of 700 W, deposition pressure of 30 torr, deposition time of 30 hr, and substrate temperature of 300-350 ℃ for all depositions in this section. The surface morphology, surface roughness, films quality and films hardness are presented below.

4.1.1   Film surface morphology and roughness

The investigations of surface morphology were observed with SEM and surface roughness was obtained with AFM. The SEM and AFM images deposited at different CH_4 concentrations in the range of 0.5-5% are shown in Fig. 4.1 - 4.5.
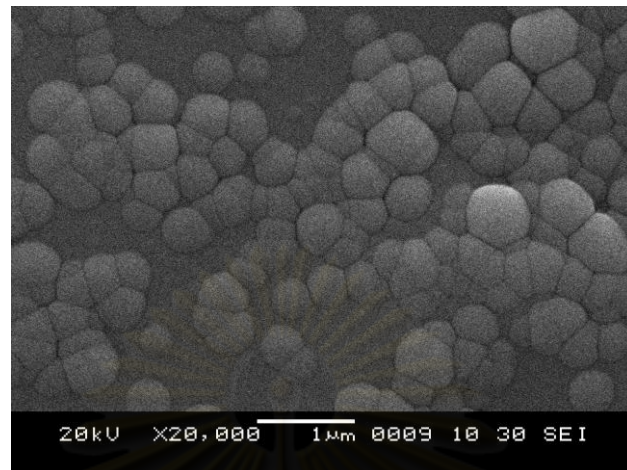
(a)
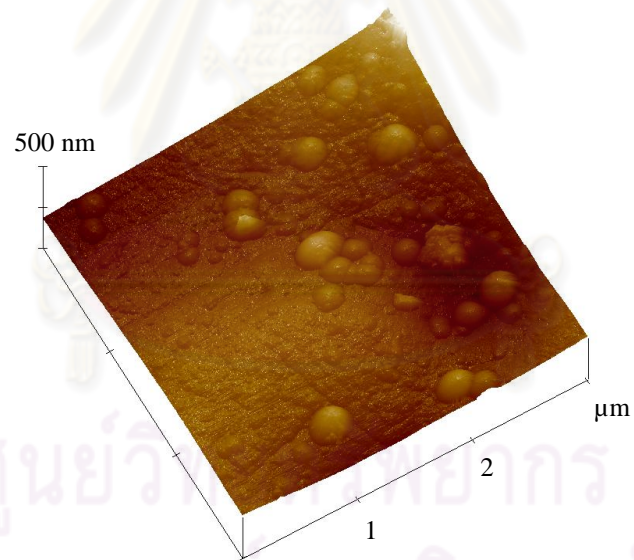
(b)

Figure 4.1 (a) SEM photograph, and (b) 2D AFM image of the film grown under CH$_4$ concentration of 0.5% and deposition pressure of 30 Torr.
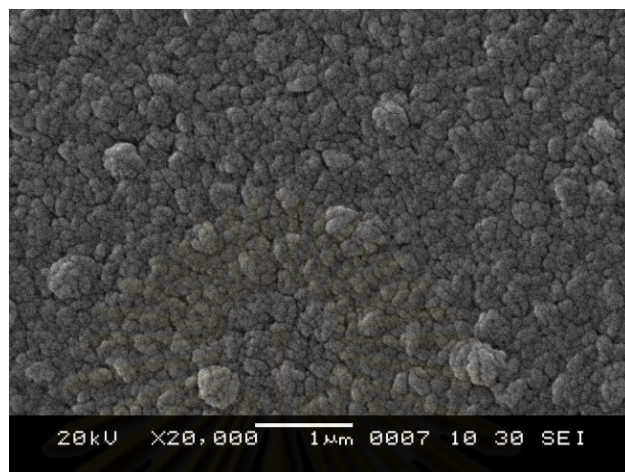
(a)
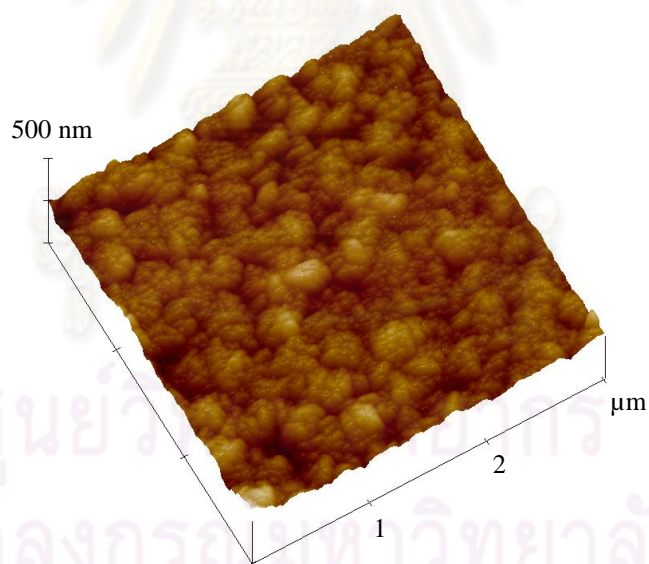
(b)

Figure 4.2 (a) SEM photograph, and (b) 2D AFM image of the film grown under the CH$_4$ concentration of 1% and deposition pressure of 30 Torr.

(a)

(b)

Figure 4.3 (a) SEM photograph, and (b) 2D AFM image of the film grown under the CH$_4$ concentration of 2% and deposition pressure of 30 Torr.

(a)

(b)

Figure 4.4 (a) SEM photograph, and (b) 2D AFM image of the film grown under the
CH_4 concentration of 3% and deposition pressure of 30 Torr.
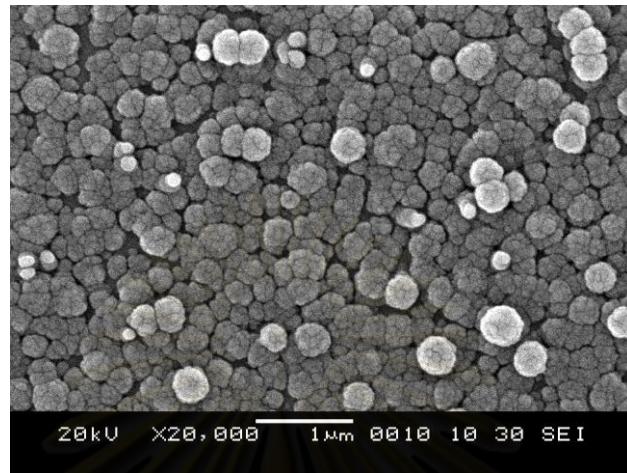
(a)
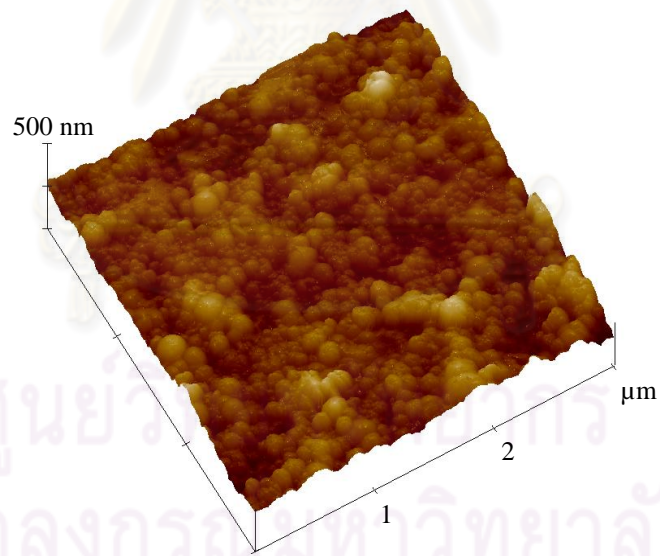
(b)

Figure 4.5 (a) SEM photograph, and (b) 2D AFM image of the film grown under the
CH$_4$ concentration of 5% and deposition pressure of 30 Torr.

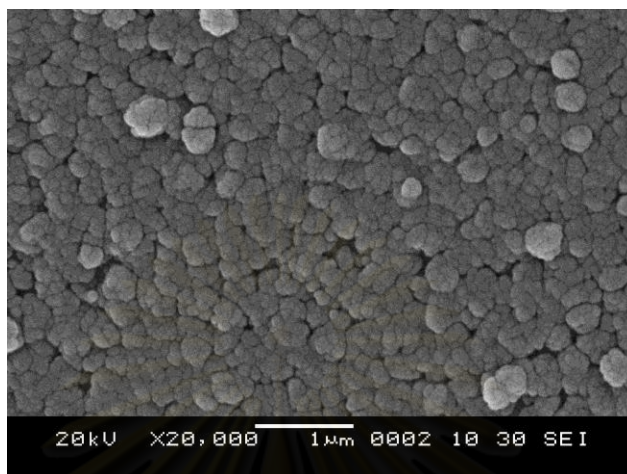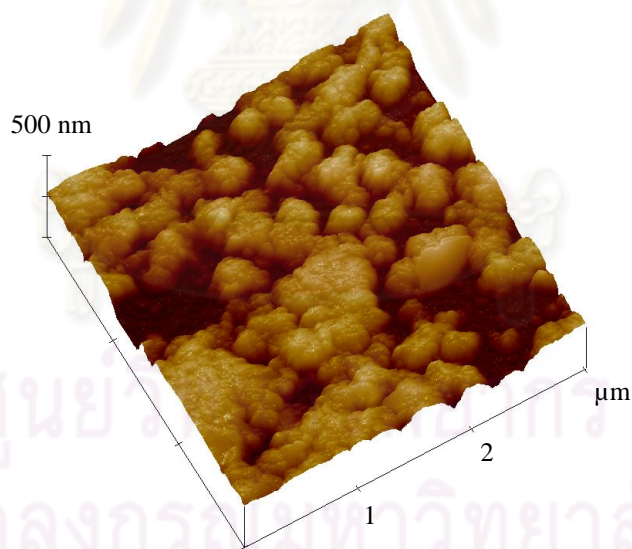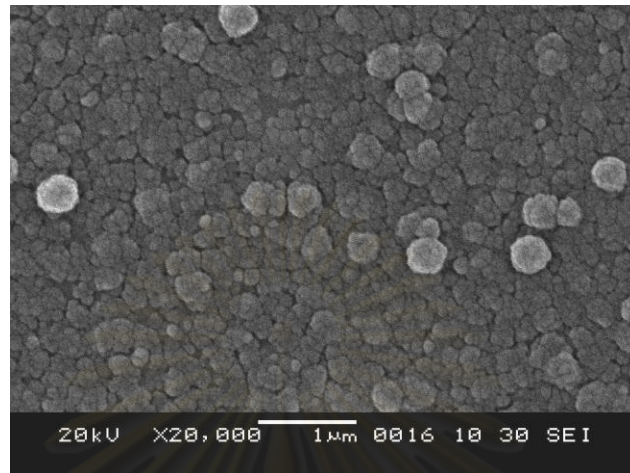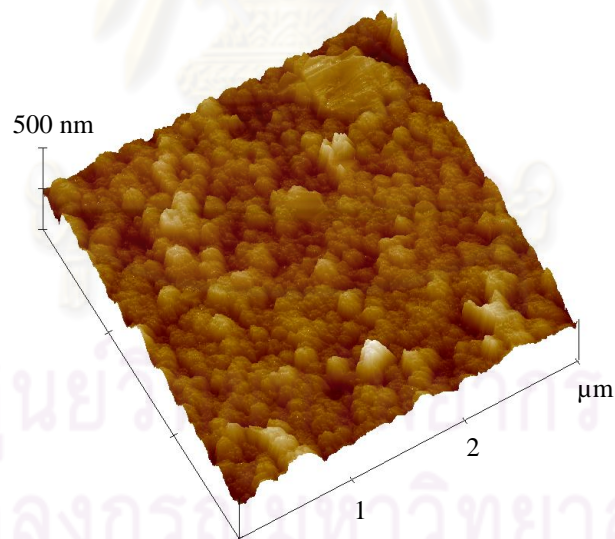The SEM image of the film in Fig. 4.1 shows the growth of DLC film at 0.5% CH_4 concentration was a ballas-like morphology and the average grain size determined by the AFM analysis was approximately about 357.1 nm. However, the surface morphology of the film investigated in this condition revealed that a continuous film was not observed on the substrate. It may cause the results from a very low flow rate of CH_4 (0.5 sccm) during the deposition process.

With increasing CH_4 concentration, a fine cauliflower-like morphology surface and continuous film of which the smaller grain size in the range of 53.6-107.1 nm was observed, as shown in Fig. 4.1-4.5. The smaller grains were formed as a consequence of the enhanced secondary nucleation effect during the deposition process. Furthermore, the surface roughness of the films decreased when the grain size reduced as shown in Fig. 4.6. The RMS surface roughness of the films was found to be decreased from 33.0 nm to 29.6 nm (shown in Table 4.1) when CH_4 concentration increased from 1% to 5%. For these experiments, it was concluded that nano-sized particles were found on the surface of the DLC films. It could also be observed that nucleation density increased with increasing CH_4 concentration, leading an indication that CH_4 concentration had a significant effect on nucleation density and grain size.
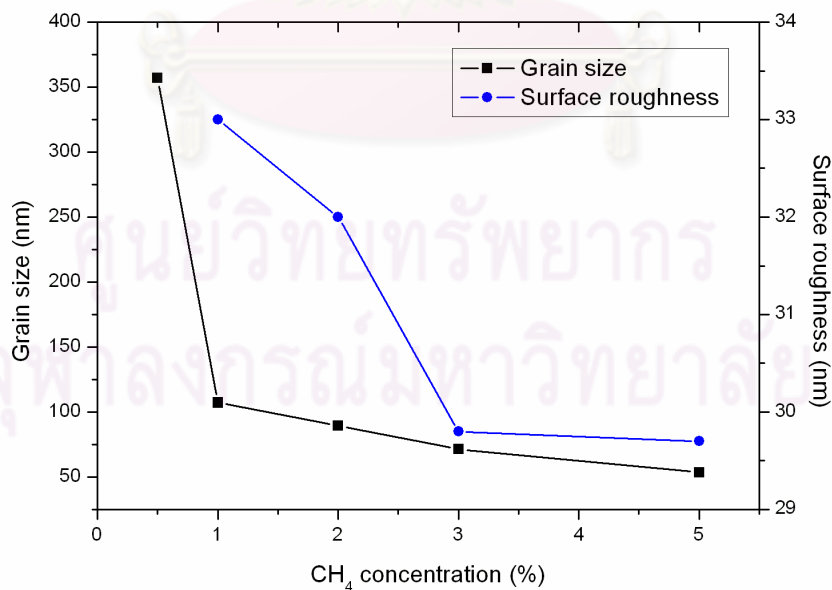
Figure 4.6 The grain size and surface roughness of the DLC films versus CH_4 concentration (%).

There are numbers of researchers who studied the influence of CH_4 concentration on the film morphology [11, 19, 43, 46]. Based on Malika *et al.* [60] research, their research demonstrated that with increasing CH_4 concentration, the grain size tended to decrease with gradual loss in quality. At 2% CH_4 concentration, the surface morphology of the diamond films on silicon nitride (Si_3N_4) was a cauliflower-type growth. They described that an increase in CH_4 concentration in the gas phase could lead to an increase in the secondary nucleation on the diamond films. This could prevent the available crystals from growing completely, leading to a decreasing of grain size. This also indicated that CH_4 concentration in the gas phase may dominate the deposition process by increasing the nucleation density

Askari *et al.* [46] described that an increase in CH_4 concentration could lead to more secondary nucleation effect. This could repress the individual crystal growth, resulting in a decreasing of grain size and surface roughness. It means that the carbon radical concentration in the gas phase may play a dominant the deposition process by increasing the nucleation density as well as reducing grain size.

4.1.2 Film quality

All Raman in this research were measured by Raman spectroscopy at a laser wavelength of 514.5 nm. The Raman spectra of diamond gives only on sharp peak, which indicate the characteristic of diamond peak located around 1332 cm^{-1} (Fig. 4.7). Fig. 4.8 shows the Raman spectra of the films at various CH_4 concentrations from 1% to 5%. The Raman spectra of these films indicated the characteristic diamond peak at 1332 cm^{-1} and the broad hump peak around 1550 cm^{-1}, corresponding to graphite or amorphous carbon phase. The difference between all of these spectra could be seen from the peak positions and intensities, which were also upon to the deposition condition.
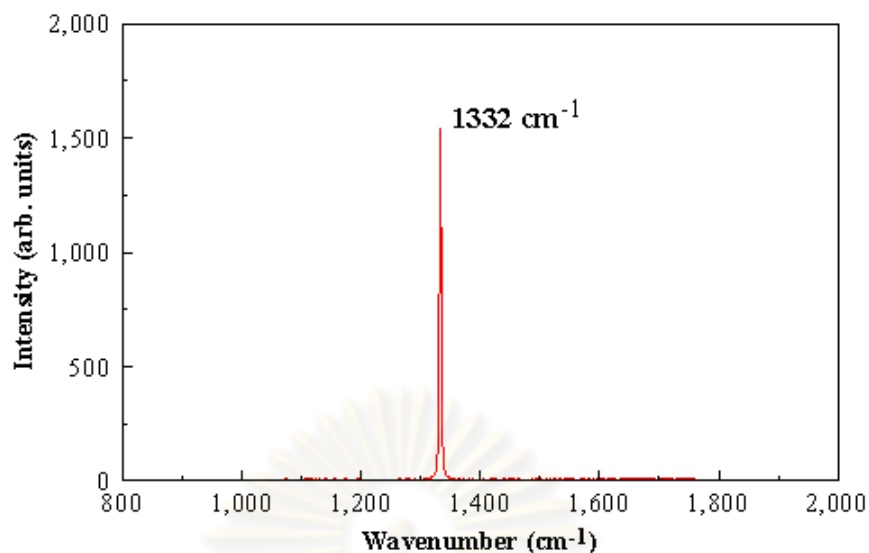
Figure 4.7 Raman spectrum of natural diamond showing the characteristic sharp peak at 1332 cm^{-1} [61].

Raman spectroscopy could be used to evaluate the film quality. For diamond films, the broad hump peak around 1550 cm^{-1} on the Raman spectra was caused by amorphous carbon and quite a sharp peak around 1332 cm^{-1} was caused by diamond phase.

The Raman spectra of the films at different CH$_4$ concentrations are illustrated in Fig. 4.8. The Raman peak was compared with the respect to the diamond and amorphous carbon phase. For the film grown at CH$_4$ concentration of 0.5% (Fig. A-1), the broad hump peak around 1550 cm^{-1} could be observed. It could also be found that the diamond peak around 1332 cm^{-1} with a full width at half maximum height (FWHM) approximately 76.5 cm^{-1}. The FWHM of the film deposited at CH$_4$ concentration of 0.5% was higher than the others spectra, which indicated that this films had relatively low purity.
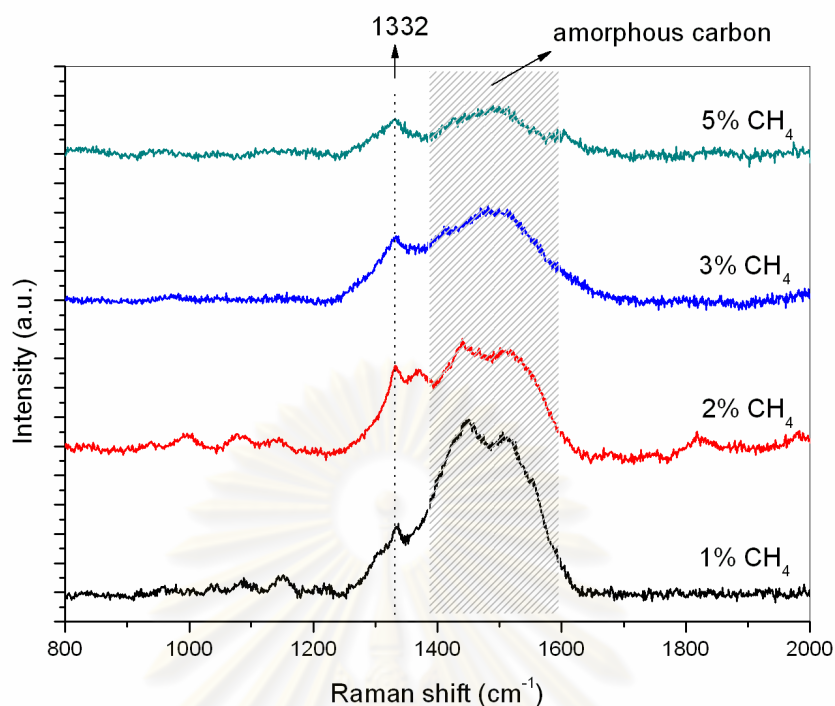
Figure 4.8 Raman spectra of the DLC films grown at deposition pressure of 30 torr under various CH_4 concentrations.

The diamond band around 1332 cm^{-1} was significant broaden that by increasing CH_4 concentration from 1% to 5%, a full width at half maximum height (FWHM) around 1332 cm^{-1} increased from 61.2 cm^{-1} to 74.8 cm^{-1} respectively. The FWHM in this section are shown in Table 4.1. The broad band around 1500-1600 cm^{-1} represented sp^2-bonded carbon or amorphous carbon phase. It indicated that the films had a lower sp^3-bonded carbon and higher sp^2-bonded carbon with increasing CH_4 concentration, which means that the films have low diamond phase purity [51]. The FWHM normally reflected the amount of defect assembled in the films. Thus, an increase in the FWHM of 1332 cm^{-1} with increasing CH_4 concentration was significant. An increase in the FWHM could be attributed to an increase in the defects and the non-diamond contents with increasing CH_4 concentration as described by Mallika et al. [60]. The results are in good agreement with the variation of hardness shown in Fig. 4.11.

In the characterization, all the Raman spectra of the DLC films were fitted using Gaussian peak with variable parameters for peak width at half maximum and position. In order to obtain a good fit, different numbers of peaks were used for different samples, which reflect the change in the films, depending on the deposition conditions. After the curve fitting, the Raman spectra were found that two main peaks occur (Fig. 4.9), quite a broad diamond peak around 1332 cm^{-1} and broad hump peak around 1550 cm^{-1}, corresponding to graphite-like sp^2 structure. However, some Raman spectra were fitted with three Gaussian line shape peak. The third peak in Fig. 4.10 was found at around 1470 cm^{-1}, which was speculatively due to carbon-hydrogen bonds in the grain boundaries [17]. Some researchers attributed this band to the diamond nanocrystals [62], others assigned this band to trans-polyacetylene situated at the grain boundaries of the diamond nanocrystallites [63]. An example curves fit of the DLC films Raman spectra are shown in Fig.4.9-4.10. For the others Raman spectra are shown in Appendix A.
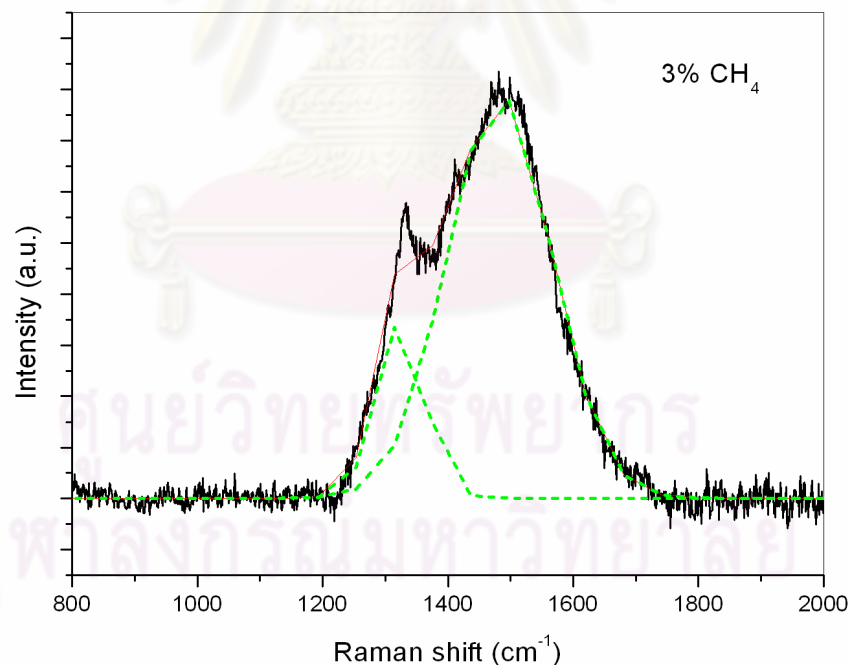
Figure 4.9 Example of Raman spectra of DLC film with two Gaussians peak.
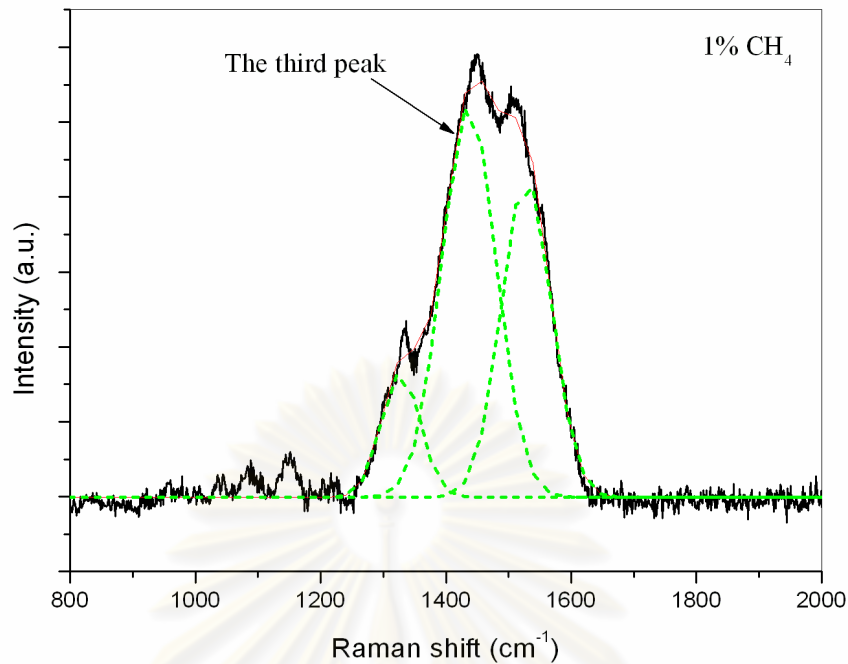
Figure 4.10 Example of Raman spectra of DLC film with three Gaussians peak.

4.1.3 Film hardness

The hardness of the DLC films was evaluated by the Nano-indentation test. The composition of DLC films (hydrogen, sp^3, and sp^2 contents) determined the hardness values of the films. Hardness values of uncoated alumina and after coated with the DLC films as a function of CH_4 concentration are plotted in Fig. 4.11. The hardness of alumina found to increase from 7.3±2.0 GPa in uncoated to 39.4±10.0 – 52.2±2.1 GPa after coated with DLC. It was found that the film hardness increase with increasing CH_4 concentrations reached at maximum at a CH_4 concentration of 1% and then started decreasing with an increasing in CH_4 concentration of 2%. As a result, the maximum value hardness was 52.2±2.1 GPa at CH_4 concentration of 1%. The hardness values were even higher when the films were grown under optimized parameters, in which the structure will be mostly sp^3-bonded carbon with a trace amount of sp^2 fractions [64]. The surface roughness, FWHM values, and hardness of the films at different CH_4 concentration are summarized in Table 4.1.
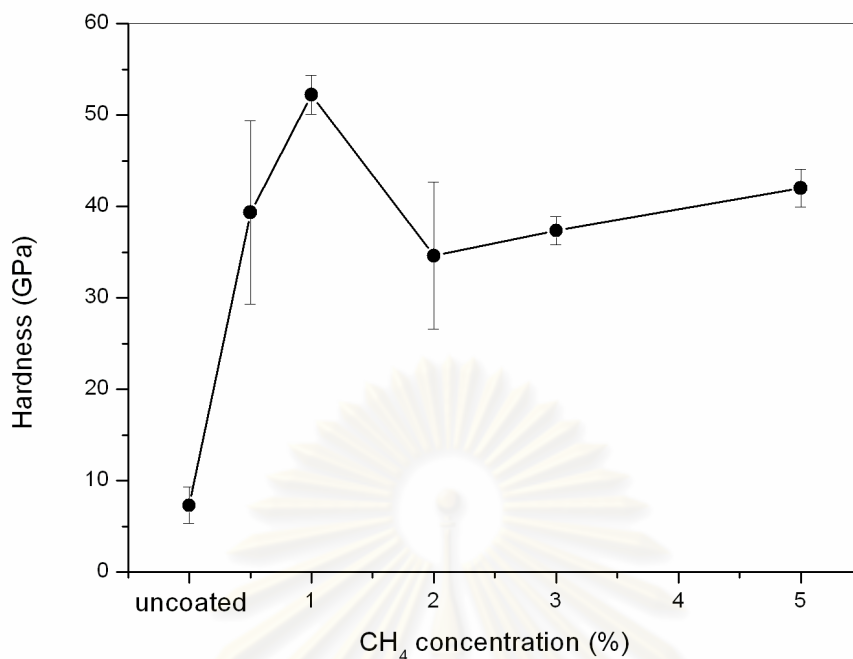
Figure 4.11 Hardness of DLC films deposited at deposition pressure 30 torr under various CH_4 concentrations.

Table 4.1 The grain size, surface roughness, FWHM (1332 cm^{-1}) and hardness of the DLC films at different CH_4 concentration.

CH_4 concentration (%)	Grain size (nm)	Surface roughness (nm)	FWHM (cm^{-1})	Hardness (GPa)
0.5	357.1	32.4	87.6	39.4±10.0
1	107.1	33.0	42.9	52.2±2.1
2	89.3	32.0	53.0	34.6±8.1
3	71.4	29.8	60.7	37.4±1.5
5	53.6	29.7	61.1	42.1±2.1

4.2 Effect of deposition pressure on the DLC films formation

The DLC films were deposited at different deposition pressure of 10 torr, 20 torr, 30 torr, and 50 torr. These samples were grown at microwave power of 700 W, CH_4 concentration of 1%, deposition time of 30 hr, and substrate temperature of 300-350 ℃ for all depositions in this section. Details of the films characteristics *e.g.* surface morphology, surface roughness, films quality, and films hardness were described in the following sections.
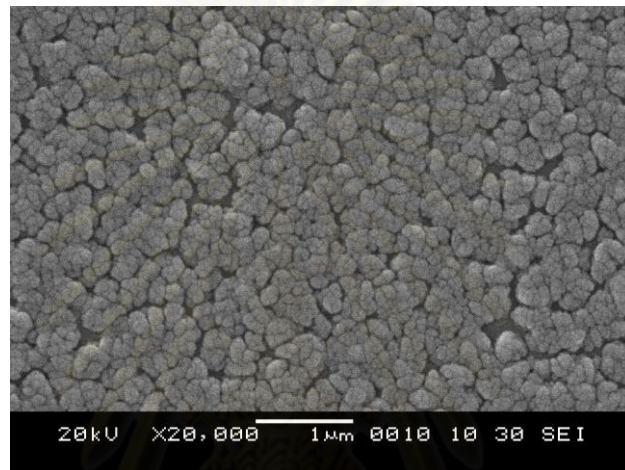
(a)
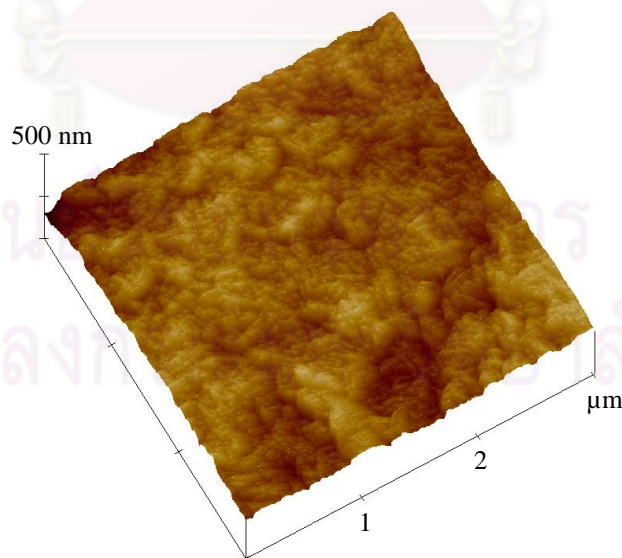
(b)

Figure 4.12 (a) SEM photograph, and (b) 3D AFM image of the film grown under the CH_4 concentration of 1% and deposition pressure of 10 Torr.
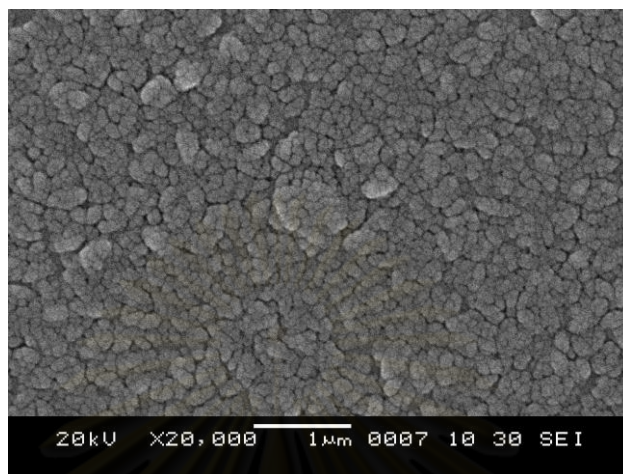
(a)
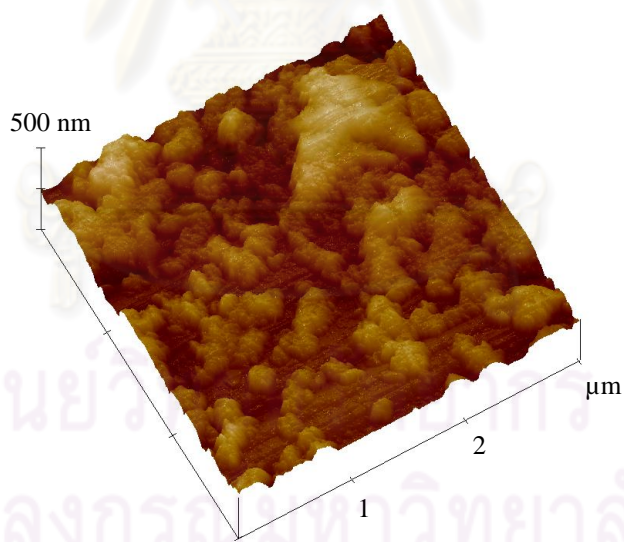
(b)

Figure 4.13 (a) SEM photograph, and (b) 3D AFM image of the film grown under the CH$_4$ concentration of 1% and deposition pressure of 20 Torr.
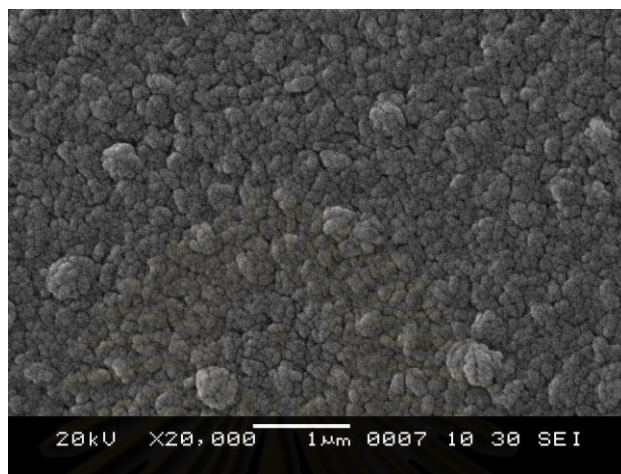
(a)
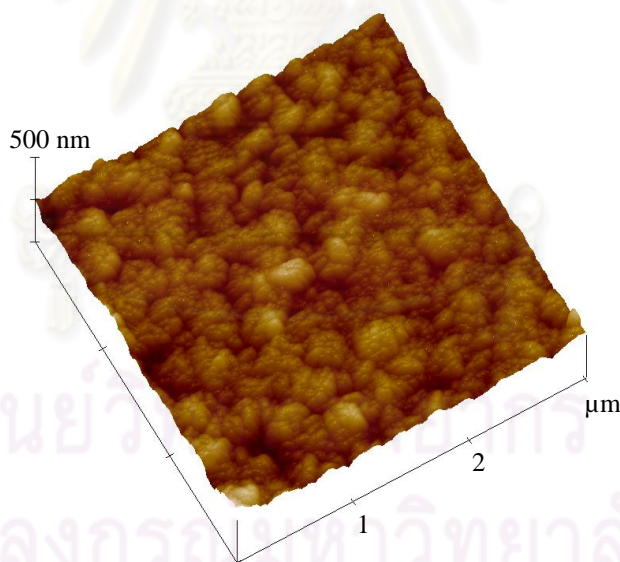
(b)

Figure 4.14 (a) SEM photograph, and (b) 3D AFM image of the film grown under the CH$_4$ concentration of 1% and deposition pressure of 30 Torr.

(a)

(b)

Figure 4.15   (a) SEM photograph, and (b) 3D AFM image of the film grown under the CH$_4$ concentration of 1% and deposition pressure of 50 Torr.

4.2.1 Film morphology and roughness

The investigations of surface morphology were observed with SEM and surface roughness was obtained using AFM. Fig. 4.12-4.15 show SEM and AFM images of the deposited DLC films under various deposition pressures in the range of 10-50 torr.

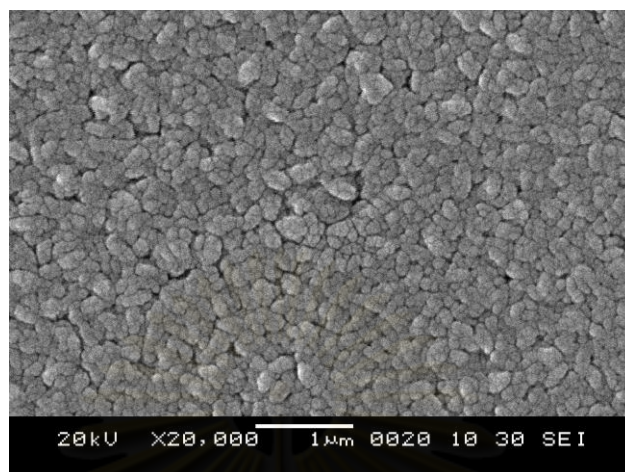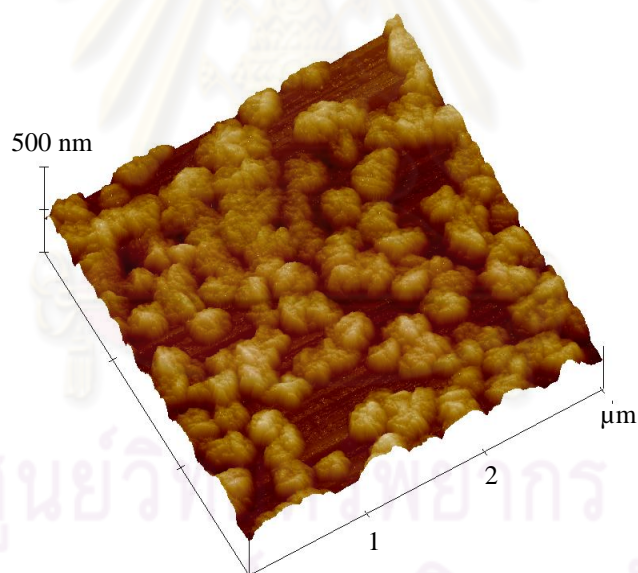As seen in Fig. 4.12, SEM image shows a cauliflower-like morphology and continuous film on alumina substrate. When the deposition pressure increased from 10 to 50 torr, the grain sizes increased gradually from 53.6 to 125 nm, and the dense continuous film could be observed. The diamond crystals started to grow uniformly with increasing deposition pressure, as shown in Fig. 4.13-4.15. This indicates an extremely high nucleation density and growth rate. The smaller grains were formed at low deposition pressure, which were considered as the result of enhanced secondary nucleation.

A comparison of the surface roughness of the films grown at various pressures was carried out by AFM. The surface roughness of the films at 10 torr (Fig. 4.12) was about 23.1 nm, which was lower than that of the others. From AFM images in Fig. 4.13-4.14, the surface roughness evaluated at 33.0 nm and 42.0 nm for the films grown at deposition pressure of 20 and 30 torr respectively. At higher deposition pressure of up to 50 torr (Fig. 4.15), the surface roughness of the film was about 45.0 nm, indicating the amount of secondary nucleation decreased. This showed that the surface roughness of the films increased significantly with increasing deposition pressure. The variations of grain size and surface roughness of the DLC films as a function of deposition pressure are plotted in Fig. 4.16.

These results correspond to the earlier observation by Liang *et al.* [14]. They investigated the influence of deposition pressure on the diamond films from CH_4/H_2 gas mixture in the HF-CVD system. They reported that with reducing deposition pressure, the diamond grain sizes decreasing gradually to nanometer scale. Furthermore, the surface roughness of the films decreased with the reduction of grain sizes. They described that according to kinetic theory of gaseous, the mean free path between electrons and molecules increases with decreasing pressure and leads to an increase in the amount of H atoms etching onto the substrate. Thus, there are few or no collisions of H atom on the substrate, so the kinetic energy remains high. The high

kinetic energy caused enhanced surface mobility of these active species, which leads to high rate of secondary nucleation.
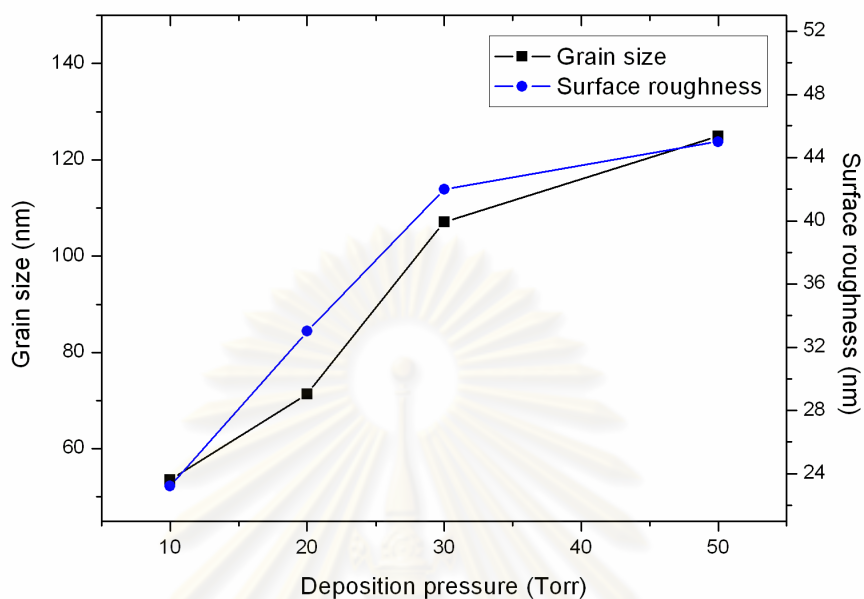
Figure 4.16 The grain size and surface roughness of the DLC films versus deposition pressure (Torr).

4.2.2 Film quality

As seen in Fig. 4.17, at a fixed CH_4 concentration of 1%, the DLC films quality increased with increasing deposition pressure, as indicated by FWHM values of the diamond peak at around 1332 cm^{-1} in Raman spectra. According to the spectra, a Raman peak around 1332 cm^{-1}, indicated the occurrence of diamond phase. The broad hump peak around 1550 cm^{-1} corresponds with the graphite-like sp^2 bonded structure. The FWHM of the 1332 cm^{-1} absorption characteristic of diamond was quite broad. With increasing deposition pressure from 10 torr to 30 torr, the FWHM of the diamond peak decreased from 79.4 cm^{-1} to 56.9 cm^{-1}, resulting in higher purity of the diamond phase. Johnson et al. [65] reported that the broadening effect can be caused by the large mismatch in thermal expansion coefficients between alumina and diamond, which could introduce residual stress on the films.
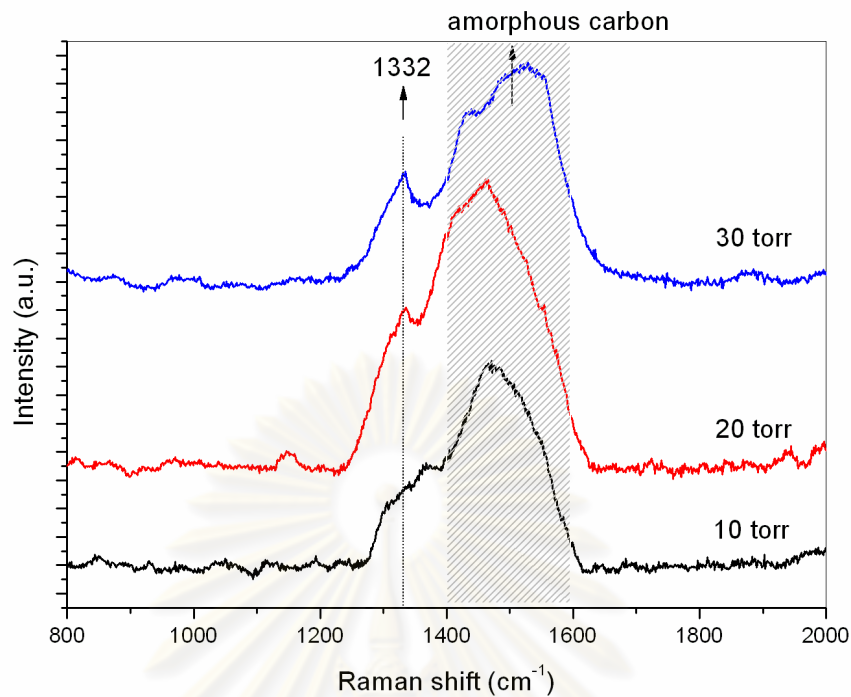
Figure 4.17 Raman spectra of the DLC films deposited at 1% CH_4 concentration under different deposition pressure.

Liang *et al.* [14] reported that the FWHM of the diamond peak increased when deposition pressure decreased. The FWHM of the diamond peak was quite broad. They believed that the FWHM broadening was primarily due to crystallite size effect. In addition, it may be caused by the average crystallite size decreased as deposition pressure decreased.

4.2.3 Film hardness

The variations of hardness values of uncoated alumina and after coating with the DLC films as a function of deposition pressure are plotted in Fig. 4.18. The hardness of alumina found to increase from 7.3±2.0 GPa in uncoated to 13.9±1.3 – 52.2±2.1 GPa after coated with DLC. The hardness value of the film grown at deposition pressure of 10 torr was 13.9±1.3 GPa. With increasing deposition pressure, the films hardness increased first, reaching a maximum at 52.2±2.1 GPa, then decreased to a lower value at 40.8±8.8 GPa. The results were corresponding with the

results from FWHM values. The summaries of surface roughness, FWHM values, and hardness of the films under various deposition pressures are showed in Table 4.2.

Generally, the hardness of CVD diamond is known to be varied over a wide range of sp^3 and sp^2 bonding ratios, depending on the kinetic energy of the active species and amount of H atom [66]. The hardness of DLC films increased dramatically with decreasing amount of H content. However, such increase increased more than to offset the decreased in hardness due to decreasing sp^3 content, could explain the substantial increase in the hardness of the film as described by Ravi *et al.* [67]. Basically, diamond structure formed by sp^3-bonded carbon or small non-diamond carbon gives high hardness.

Figure 4.18 Hardness of uncoated alumina and after coated with DLC film deposited at 1% CH_4 concentration under various deposition pressures.

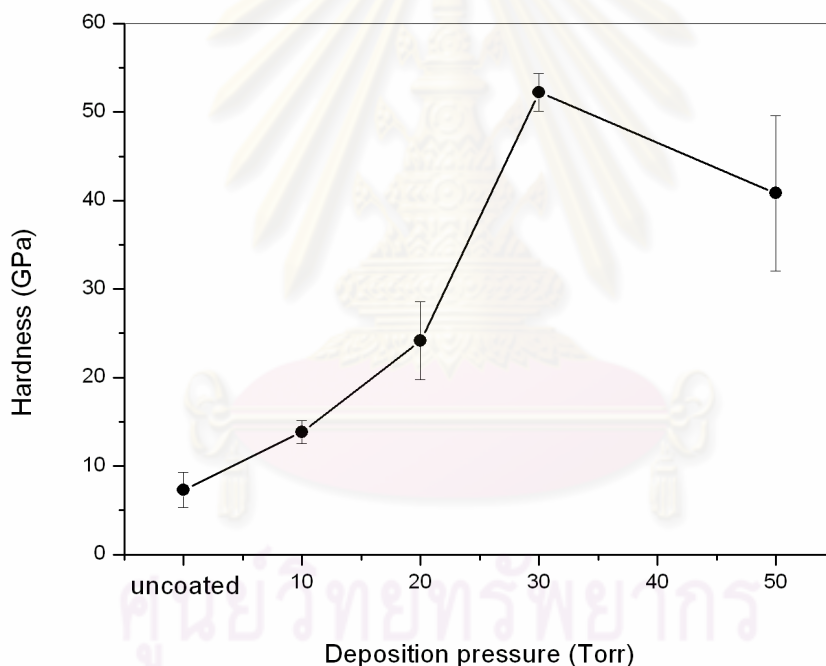**Table 4.2** The grain size, surface roughness, FWHM (1332 cm^{-1}) and hardness of the DLC films under various deposition pressures.

Deposition pressure (Torr)	Grain size (nm)	Surface roughness (nm)	FWHM (cm^{-1})	Hardness (GPa)
10	53.6	23.2	79.4	13.9±1.3
20	71.4	33.0	59.7	24.2±4.4
30	107.1	42.0	56.9	52.2±2.1
50	125.0	45.0	70.6	40.8±8.8

4.3 Effect of deposition time on the DLC films formation

The DLC films were deposited at various deposition times, namely 5 hr, 10 hr, 20 hr, and 30 hr. These samples were grown at microwave power of 700 W and substrate temperature of 300-350 ºC. Deposition pressure was kept at 30 torr and CH$_4$ concentration was held constant of 1%. The various contributions of the surface morphology, surface roughness, quality, and hardness within these films were discussed as below.

4.3.1 Film surface morphology and roughness

The SEM images of the DLC films are prepared at different deposition time in the range of 5-30 hr, as shown in Fig. 4.20-4.22. Obviously, it could be found that the nucleation density was a function of deposition time. For the film deposited at deposition time of 5 hr (Fig. 4.20), the film contained very small individual diamond nuclei. With increasing deposition time to 10 and 20 hr, the grain sizes of individual diamond nuclei increased, as shown in Fig. 4.21 and 4.22 respectively. When deposition time reached at 30 hr (Fig. 4.23), the film became a dense continuous DLC coating all over the alumina substrate. Furthermore, a minimum surface roughness of the films after 5 hr was obtained at about 8.2 nm. With increasing deposition time from 10 hr to 30 hr, not only grain size increased from 87.7 to 107.1 nm but also

surface roughness increased from 22.9 nm to 33.0 nm, respectively. Surface roughness and grain size of the DLC films as a function of deposition time are plotted in Fig. 4.19. The variation of the DLC films formation with deposition time was similar to the observations of earlier researchers [13, 68].
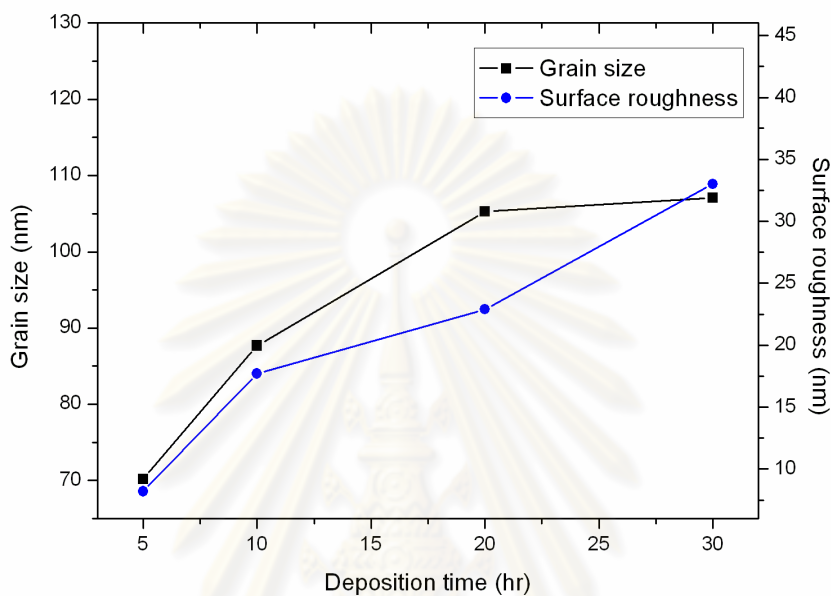
Figure 4.19 The grain size and surface roughness of the DLC films as a function of deposition time (hr).

ศูนย์วิทยทรัพยากร

จุฬาลงกรณ์มหาวิทยาลัย
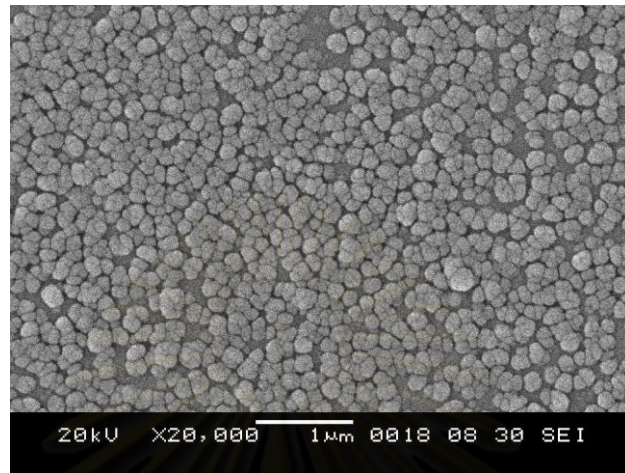
(a)
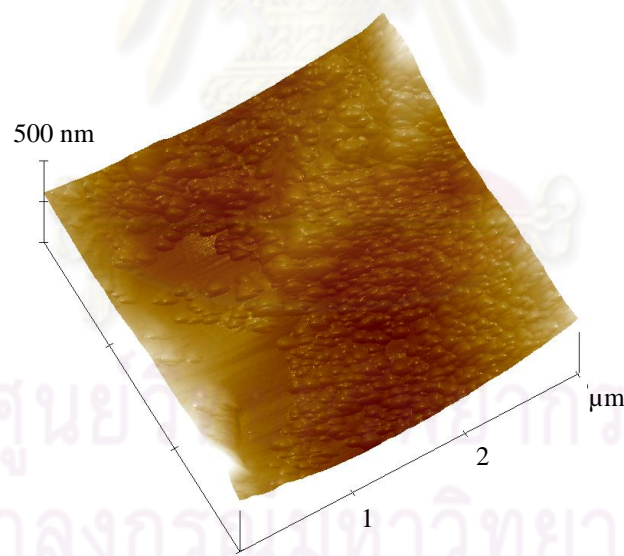
(b)

Figure 4.20   (a) SEM photograph, and (b) 2D AFM image of the film grown under the CH$_4$ of 1% and deposition pressure of 30 Torr at deposition time of 5 hr.
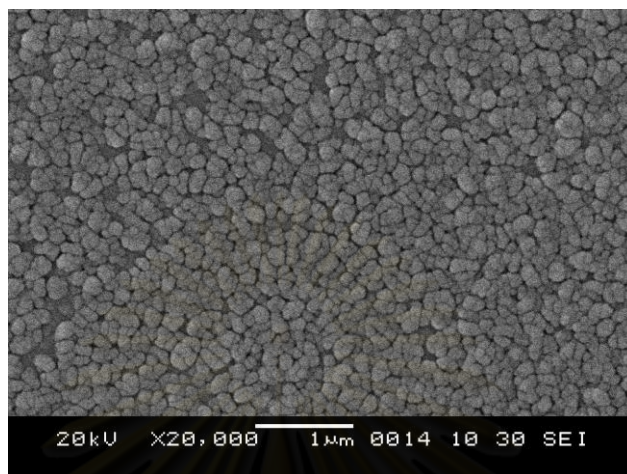
(a)
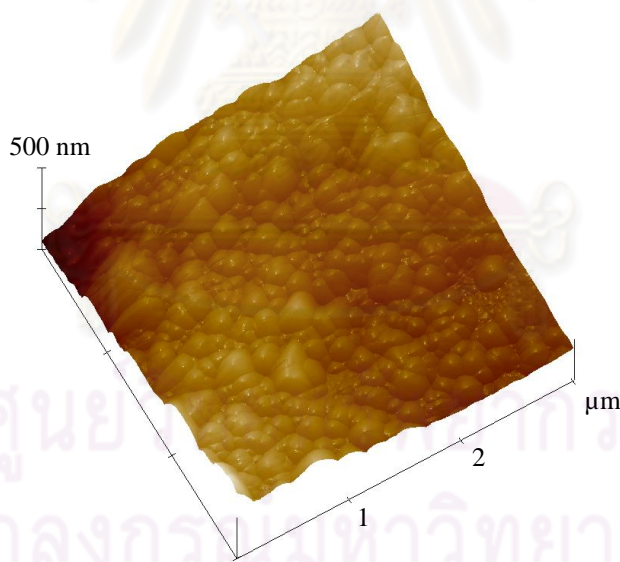
(b)

Figure 4.21 (a) SEM photograph, and (b) 2D AFM image of the film grown under the CH$_4$ of 1% and deposition pressure of 30 Torr at deposition time of 10 hr.
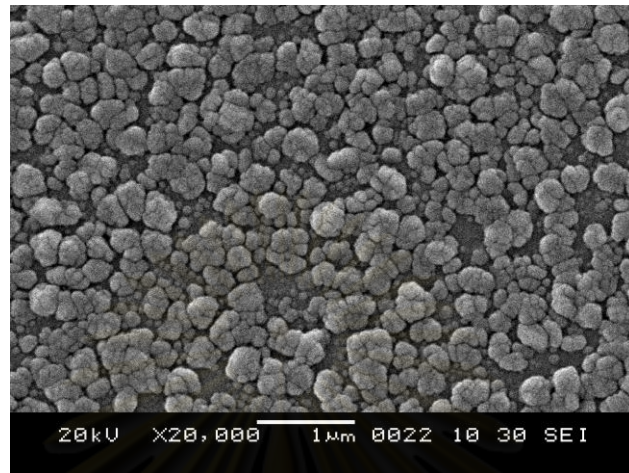
(a)
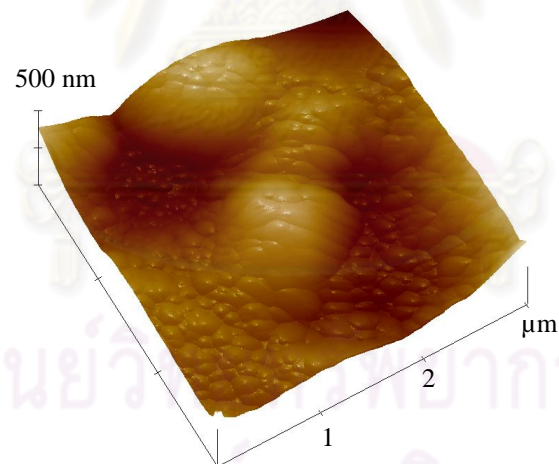
(b)

Figure 4.22 (a) SEM photograph and (b) 2D AFM image of the film grown under the CH_4 of 1% and deposition pressure of 30 Torr at deposition time of 20 hr.
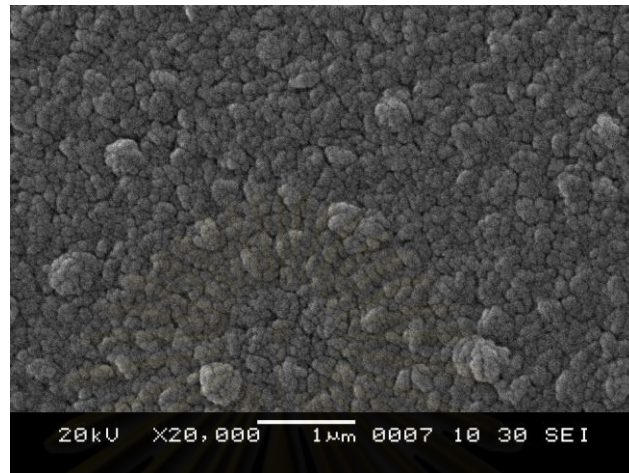
(a)
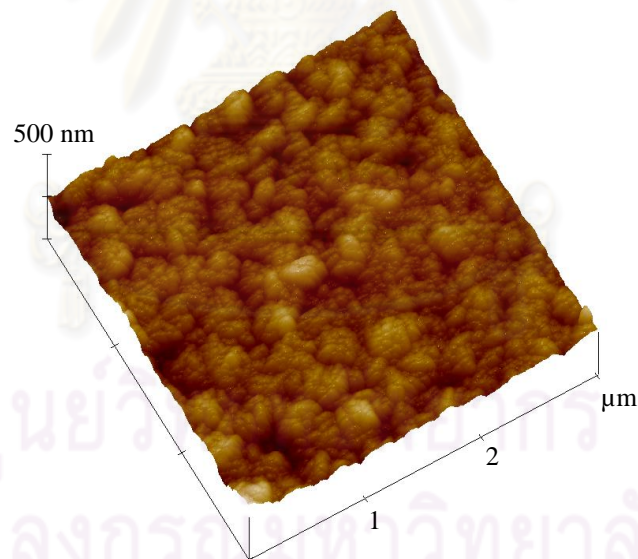
(b)

Figure 4.23 (a) SEM photograph, and (b) 2D AFM image of the film grown under the CH$_4$ of 1% and deposition pressure of 30 Torr at deposition time of 30 hr.

4.3.2 Film quality

The Raman spectra of the DLC films grown at various deposition times from 10 hr to 30 hr were measured by employing the 514.5 nm excitation. The deconvolutions of the Raman spectra with three and four Gaussians in these films are shown in Fig. 4.24. Two of which are situated around 1332 and 1550 cm^{-1}, could be assigned to the typical Raman spectrum of diamond and graphite-like sp^2 bonded structure, respectively. The Raman spectra in Fig. 4.24(b) and (c) were fitted with four peaks. The forth peak in Fig. 4.24(a) was situated at around 1230 cm^{-1}, which attributed to the polycrystalline structure of diamond [43]. While the third peak in Fig. 4.24(b) and (c) were found at around 1470 cm^{-1}, which was speculatively due to carbon-hydrogen bonds in the grain boundaries [17] or the diamond nanocrystals [62-63]. The FWHM of the diamond peak decreased from 64.2 cm^{-1} to 56.9 cm^{-1} with increasing deposition time from 20 hr to 30 hr. It indicated that higher purity of the diamond phase was significant. Besides, the Raman shift from the standard diamond peak to 1335-1345 cm^{-1} resulting from residual stress, due to the large mismatch in thermal expansion coefficient between the alumina substrate and diamond films with increasing thickness of the films, as described by Ye *et al.* [68].
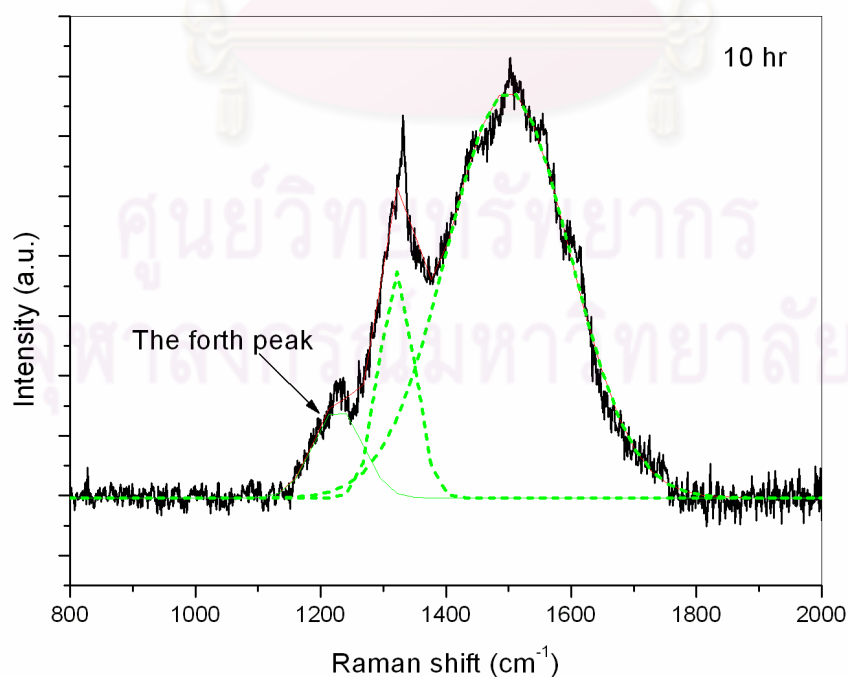
(a)
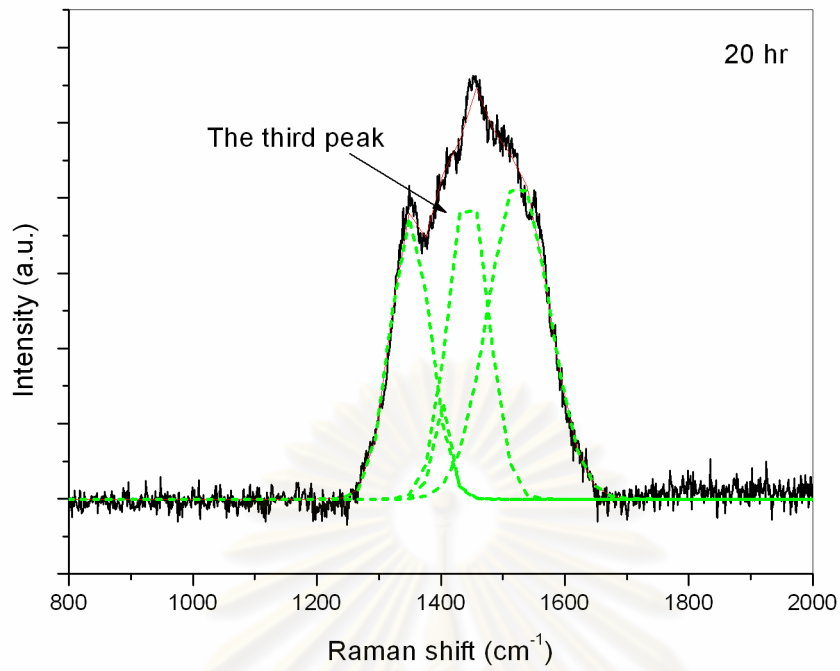
(b)
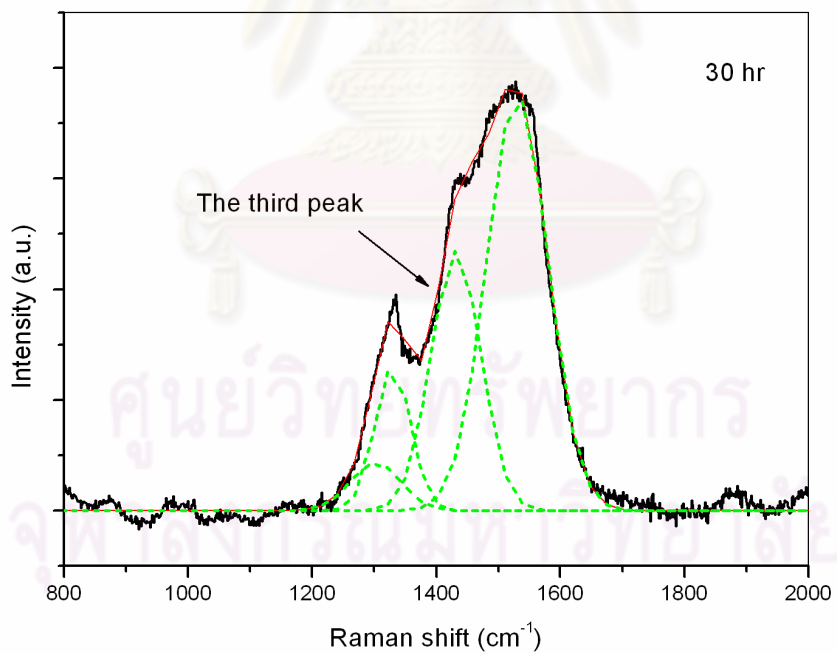
(c)

Figure 4.24 Deconvolution of the Raman spectrum with two and three Gaussians in the DLC film grown under various deposition times, (a) 10 hr, (b) 20 hr, and (c) 30 hr.

4.3.3 Film hardness

Hardness values of uncoated alumina and after coating with the DLC films as a function of deposition time are plotted in Fig. 4.25. The hardness of alumina was found to be increased from 7.3±2.0 GPa in uncoated to 15.8±4.5 – 52.2±2.1 GPa after coated with DLC. At a deposition time of 5 hr, the film hardness value was 15.8±4.5 GPa. With increasing deposition time from 10 hr to 20 and 30 hr, the films hardness values increased from 30.7±3.2 GPa to 37.3±1.0 and 52.2±2.1 GPa, respectively. This result indicates that higher hardness values of the films with increasing deposition time were significant, corresponds with the FWHM values of the Raman spectra in these films under the same conditions. The summaries of surface roughness, FWHM values, and hardness of the films at different deposition time are showed in Table 4.3.
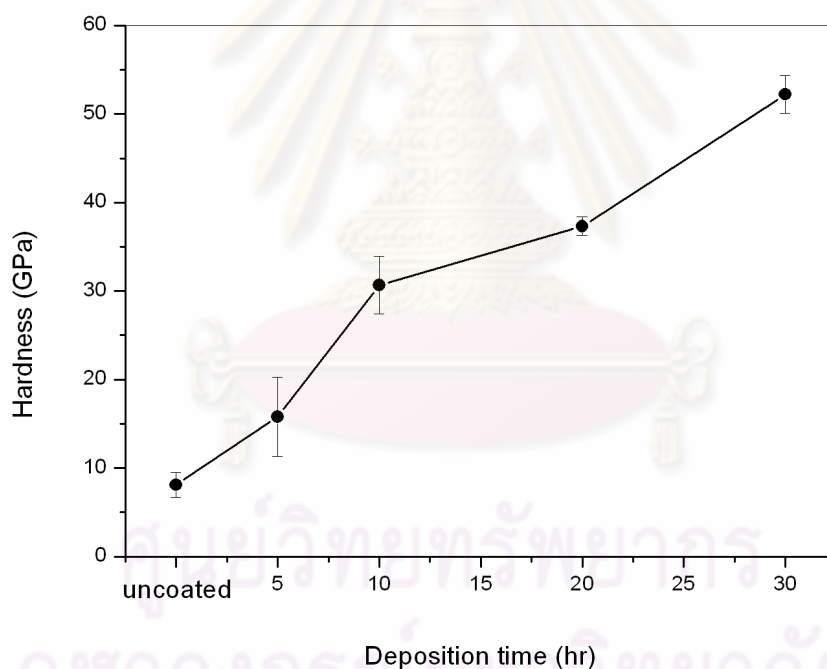
Figure 4.25 Hardness of uncoated alumina and after coated with DLC film grown at 1% CH_4 concentration and deposition of 30 torr under various deposition times.

Table 4.3 The grain size, surface roughness, FWHM (1332 cm^{-1}) and hardness of the DLC films under various deposition times.

Deposition time (hr)	Grain size (nm)	Surface roughness (nm)	FWHM (cm^{-1})	Hardness (GPa)
5	70.2	8.2	-	15.8±4.5
10	87.7	17.7	55.7	30.7±3.2
20	105.3	22.9	64.2	37.3±1.1
30	107.1	33.0	56.9	52.2±2.1

CHAPTER V

CONCLUSION

5.1 Conclusions

This research was focused on the properties improvement of alumina surface coated with synthesize DLC films using MW-PECVD technique. The influences of CH_4 concentrations, deposition pressure, and deposition time were studied in order to obtain the optimum conditions which can lead to an increase in hardness of the films and examined the effects of the conditions to the surface morphology, surface roughness, quality, and hardness on the DLC films.

For the films deposited under a low CH_4 concentration of 0.5%, the ballas-like shape particle could be seen in the film. With CH_4 concentration increasing, a fine grained surface similar to cauliflower-like morphology was observed. The surface roughness decreased from 33.0 to 29.7 nm as well as the grain size decreased from 107.1 to 53.6 nm when increasing CH_4 concentration from 1 to 5%, respectively. It is believe that an increase in CH_4 concentration can lead to a more secondary nucleation effect, resulting to an increase in the nucleation density, as well as the reduction of the grain size. The Raman spectra is found to have two main peaks; quite a broad diamond peak around 1332 cm^{-1} and broad hump peak around 1550 cm^{-1}, corresponding to graphite-like sp^2 structure or amorphous carbon phase. However the diamond peak was quite broad, which broadens effect can be caused by the large mismatch in thermal expansion coefficient between alumina and diamond. The FWHM of 1332 cm^{-1} increased from 61.2 to 74.8 cm^{-1} with increasing CH_4 concentration from 1 to 5%, respectively. It indicated that the films had a lower sp^3-bonded carbon and higher sp^2-bonded carbon with increasing CH_4 concentration, which means that the films have low diamond phase purity. This result was in good agreement with the variation of hardness. The hardness of alumina found to increase from 7.3±2.0 GPa in uncoated to 39.4±10.0 − 52.2±2.1 GPa after coated with DLC under various CH_4 concentrations. As a result, the maximum value hardness was 52.2±2.1 GPa at CH_4 concentration of 1%.

The DLC films were deposited at different deposition pressure, SEM images indicates a cauliflower-like morphology and continuous DLC films coating over the alumina substrate. With increasing deposition pressure from 10 to 50 torr, the grain size increased gradually from 53.6 to 125 nm and the dense continuous films were obtained. The smaller grain sizes were formed at low deposition pressure, which were considered as the result of enhanced secondary nucleation. The surface roughness of the films increased significantly from 23.1 to 45.0 nm, while the FWHM of the Raman spectra of 1332 cm^{-1} decreased from 79.4 to 56.9 cm^{-1}, with increasing deposition pressure from 10 to 30 torr respectively. The hardness of these films was in the range of 13.9±1.3 to 52.2±2.1 GPa. The maximum hardness of the film was deposited at deposition pressure of 30 torr.

For the DLC films grown at different deposition time, it could be found that the nucleation density was a function of deposition time. With increasing deposition time, the particle diameter of individual diamond nuclei was increased. When deposition time reached at 30 hr, a dense continuous DLC films coating all over the alumina substrate could be obtained. A minimum surface roughness for the films after 5 hr was obtained at about 8.2 nm. With increasing deposition time from 10 to 30 hr, not only the grain sizes increased but also the surface roughness increased from 22.9 to 33.0 nm. In contrast, the FWHM of diamond peak decreased from 64.2 to 56.9 nm, with increasing deposition time from 20 to 30 hr. It indicated that higher purity of the diamond phase in the films deposited at higher deposition time was significant, corresponds with the hardness of the films. These films presented the hardness values in the range of 37.3±1.0 to 52.2±2.1 GPa. With deposition time increasing, the hardness of these films increased.

For these experiments, it could be concluded that DLC films have been successfully deposited on alumina substrate using MW-PECVD technique. The main process parameters extremely affected the characteristics of DLC films and optimum conditions at CH$_4$ concentration of 1%, deposition pressure of 30 torr, and deposition time of 30 hr, which were able to achieve superior quality of the films. The maximum film hardness was 52.2±2.1 GPa, indicating the films deposited under the optimum conditions could be very hard. It demonstrated that the improvement on the hardness of the coated alumina was significant.

5.2   Recommendations

In CVD process, the optimization of deposition conditions space is very large and complex. The properties of diamond growth films are upon to deposition conditions such as methane gas concentration, deposition pressure, substrate temperature, and also the substrate materials. CVD process enables to synthesize diamond films on several materials with different shapes and sizes that can be used to differentiate technological and industrial applications. This research demonstrated that DLC films have been successfully deposited on alumina substrate that can increase in hardness of the coated alumina. It is therefore very interesting to explore the possibility of coating of DLC films on other substrate materials. Furthermore, the additional heating of the substrate beneath the substrate holder can produce more efficient plasma, resulting in an increase in growth rate. However, there may be alternative methods for future work.

REFERENCES

[1]   May, P. W. Diamond thin films: a 21-st century material. *Phicosophical Transactions of the Royal Society A* **358** (2000): 473-495.

[2]   Esteve, J., Polo, M.C., and Sanchez, G. Diamond and diamond-like carbon films. *Vacuum* 52 (1999) 133-139.

[3]   Settineri, L., Bucciotti, F., Cesano, F., and Faga M.G. Surface Properties of Diamond Coatings for Cutting Tools. *Annals of the CIRP* **56** (2007): 573-576.

[4]   Roger J. Narayan. Nanostructured diamond-like carbon thin films for medical applications. *Materials Science and Engineering* C **25** (2005) 405 – 416.

[5]   Olszyna, A., and Smolik, J. Nanocrystalline diamond-like carbon coatings produced on the Si_3N_4–TiC composites intended for the edges of cutting tools. *Thin Solid Films* **459** (2004) 224–227.

[6]   Silva, S., Mammana, V.P., Salvadori, M.C., Monteiro, O.R., and Brown, I.G. WC-Co cutting tool inserts with diamond coatings. *Diamond and Related Materials* **8** (1999) 1913–1918.

[7]   Carter, C. B., and Norton, M. G. *Ceramic Materials Science and Engineering*. USA: Springer Science and Business Media, LLC., 2007.

[8]   Hari Singh Nalwa. *Handbook of Thin Film materials*. Vol. 2: Characterization and Spectroscopy of Thin Films. USA: Academic Press, 2002.

[9]   Dandy, D.S., and Coltrin, M.E. *Diamond Thin Films Handbook*. New York: Marcel Dekker, 2002.

[10]   Huang, W. S., Tran, D. T., Asmussen, J., Grotjohn, T. A., and Reinhard, D. Synthesis of thick, uniform, smooth ultrananocrystalline diamond films by microwave plasma-assisted chemical vapor deposition. *Diamond and Related Materials* **15** (2006) 341-344.

[11]   Hiramatsu, M., Lau, C. H., Bennett, A., and Foord, J. S. Formation of diamond and nanocrystalline diamond films by microwave plasma CVD. *Thin Solid Films* **407** (2002) 18-25.

[12] Nagatsu, M., Miyake, M., and Maeda, J. Plasma CVD reactor with two-microwave oscillator for diamond films synthesis. *Thin Solid Films* **506-507** (2006) 617-621.

[13] Ternyak, O, Akhvlediani, R., and Hoffman, A. Evolution and properties of adherent diamond films with ultra high nucleation density deposited onto alumina. *Diamond and Related Materials* **14** (2005) 144-154.

[14] Liang, X., Wang, L., Zhu, H., and Yang, D. Effect of pressure on nanocrystalline diamond films deposition by hot filament CVD technique from CH_4/H_2 gas mixture. *Surface and Coating Technology* **202** (2007) 261-267.

[15] Yu, S. J., Ding, Z. F., Xu., J., Zhang, J. L., and Ma, T. C. CVD of hard DLC films in a radio frequency inductively coupled plasma source. *Thin Solid Films* **390** (2001) 98-103.

[16] Gomes, J. R., Camargo Jr., S. S., Simao, R. A., Carrapichano, J. M. Achete, C. A., Silva, R. F. Trobological properties of silicon nitride ceramics coated with DLC and DLC-Si against 316L stainless steel. *Vacuum* **81** (2007) 1448-1452.

[17] Meng, X. M., Tang, W. Z., Hei, L. F., Askari, S. J., Chen, G. C., and Lu, F. X. Application of CVD nanocrystalline diamond films to cemented carbide drill. *International Journal of Refractory Metals and Hard Materials* **26** (2008) 485-490.

[18] Li, D., Zuo, D., Lu, W., Chen, R., Xiang, B., and Wang, M. Effects of methane concentration on diamond spherial shell films prepared by DC-plasma jet CVD. *Solid State Ionics* **179** (2008) 1263-1267.

[19] Quan-yan, Q., Wan-qi, Q., De-chang, Z., Zhong-wu, L, Ming-jiang, D., and Ke-song, Z. Effects of deposition parameters on microstructure and thermal conductivity of diamond films deposited by DC arc plasma jet chemical vapor deposition. Trans. *Nonferrous Met. Soc. China* **19** (2009) 131-137.

[20] Wang, L., Lu, J., Su, Q., Wu, N., Liu, J., Shi, W., and Xia, Y. [100]-textured growth of polycrystalline diamond films on alumina substrates by microwave plasma chemical vapor deposition. *Materials Letters* **60** (2006) 2390–2394.

[21] Mo, Y., Xia Y., and Wu, W. A nucleation mechanism for diamond film deposited on alumina substrates by microwave plasma CVD. *Journal of Crystal Growth* **191** (1998) 459-465.

[22] Wikipedia. The free encyclopedia of aluminum oxide [online]. 2009. Available from: http://en.wikipedia.org/wiki/Alumina [2010, March 19]

[23] Terpstra, R.A. Ceramic Processing. New Delhi: Chapman & Hall, 1995.

[24] Othmer, K. *Encyclopedia of Chemical Technology*. 3rd ed. Vol. 5. USA: John Wiley and Sons, 1978.

[25] Accuratus. Aluminium Oxide [online]. 2002. Available from: http://www.accuratus.com/alumox.html [2010, March 19]

[26] Xia, Y., Mo., Y., Wang, Y., Huang, X., Chen, D., and Wang, H. Nucleation mechanism of polycrystalline diamond film deposited on ceramic alumina by microwave plasma chemical vapor deposition. *Chinese Physics Letters* **13** (1996) 557-560.

[27] Othmer, K. *Encyclopedia of Chemical Technology*. 3rd ed. Vol. 4. USA: John Wiley and Sons, 1978.

[28] The A to Z nanotechnology [online]. 2010. Available from: http://www.azonano.com/details.asp [2010, March 9]

[29] Spear, K. E., and Dismukes, J. P. *Synthetic diamond: Emerging CVD science and technology*. USA: John Wiley and Sons, 1994.

[30] Lewis, I. R., and Edwards, G. M. *Handbook of Raman Spectroscopy from the Research Laboratory to the Process Line* (*Practical Spectroscopy Series*). Volume 28. USA: Marcel Dekker Inc, 2001.

[31] Diameter Advanced Material Applications. Diamond-like Carbon [online]. 2007. Available from: http://www.diameterltd.co.uk/images/dlc-structure.gif [2010, March 9]

[32] Goldston, R. J., and Rutherford, P. H. *Introduction to Plasma Physics*. UK: IOP Publishing Ltd., 1995.

[33] Sugawara, M. *Plasma Etching Fundamentals and Applications*. USA: Oxford Science Publications by Oxford University Press Inc, 1998.

[34] Plasma Technology. <u>Korea Plasma Civil Engineering Co. Ltd.</u> [online]. 2007. Available from: http://koreaplasma.net/english/koreap2_1.htm [2010, March 9]

[35] Satas, D., and Tracton, A. A. *Coating Technology Handbook*. 2nd ed. USA: Marcel Dekker Inc, 2001.

[36] Field, J.E. *The Properties of Natural and Synthetic Diamond.* USA: Academic Press, 1992.

[37] Ohring, M. *Materials Science of Thin Films Deposition and Structure*. 2nd ed. USA: Academic Press, 2002.

[38] Pohang University of Science and Technology All Rights Reserved, <u>Chemical Vapor Deposition (CVD)</u> [online]. 2007. Available from: http://www.postech.ac.kr/ce/lamp/research/cvd/cvd-1.jpg [2010, March 9]

[39] Roth, J. R. *Industrial Plasma Engineering*. Vol. 2 (Application to Nonthermal Plasma Processing). UK: Institute of Physics Publishing Bristol and Philadelphia, 2001.

[40] Smirnov, B. M. *Physics of Ionized Gaseous*. USA: John Wiley and Sons, 2001.

[41] Eliezer, S. and Eliezer, Y. *The Fourth State of Matter an Introduction to Plasma Science*. 2nd ed. UK: IOP Publishing Ltd., 2001.

[42] Kulisch, W., Popov, C., Boycheva, S., Jelinek, M., Gibson, P.N., and Vorlicek, V. Influence of the substrate temperature on the properties of nanocrystalline diamond/amorphous carbon composite films. *Surface and Coating Technology* **200** (2006) 4731-4736.

[43] Askari, S.J., Chen, G.C., and Lu, F.X. Growth of polycrystalline and nanocrystalline diamond films on pure titanium by microwave plasma assisted CVD process. *Materials Research Bulletin* **43** (2008) 1086–1092.

[44] Buhlmann, S., Blank, E., Haubner, R., and Lux, B. Characterization of ballas diamond depositions. *Diamond and Related Materials* **8** (1999): 194-201.

[45] Wang, W.L., Liao, K.J., Fang, L., Esteve, J., and Polo, M.C. Analysis of diamond nucleation on molybdenum by biased hot filament chemical vapor deposition. *Diamond and Related Materials* **10** (2001) 383-387.

[46] Askari, S.J., Akhtar, F., Islam, S.H., Qi, H., Tang, W.Z., and Lu, F.X. Two-step growth of high-quality nano-diamond films using CH_4/H_2 gas mixture. *Vacuum* **81** (2007) 713-717.

[47] Yagyul, H., Deguchi, M., Won, J. H., Mori, Y., Hatta, A., Kitabatake, M., Ito, T., Hirao, T., and Hiraki, A. Ion implantation in CVD diamond and plasma treatment effect. *Diamond and Related Materials* **4** (1995) 575-579.

[48] Baba, K., and Hatada, R. Deposition of diamond-like carbon films on polymers by plasma source ion implantation. *Thin Solid Films* **506– 507** (2006) 55 – 58.

[49] Chattopadhyay, A., Sarangi, S.K., and Chattopadhyay, A.K. Effect of negative dc substrate bias on morphology and adhesion of diamond coating synthesised on carbide turning tools by modified HFCVD method. *Applied Surface Science* **255** (2008) 1661–1671.

[50] Ristic, G.C., Bogdanov, Z.D., Zec, S., Romcevic, N., Mitrovic, Z.D., and Miljanic, S.S. Effect of the substrate material on diamond CVD coating properties. *Materials Chemistry and Physics* **80** (2003) 529-536.

[51] Tyagi, P.K., Misra, A., Narayanan Unni, K.N., Rai, P., Singh, M.K., Palnitkar, U., Misra, D.S., Normand, F.L., Roy, M., and Kulshreshtha, S.K. Step growth in single crystal diamond grown by microwave plasma chemical vapor deposition. *Diamond and Related Materials* **15** (2006) 304 – 308.

[52] Flegler, S. L., Heckman, J. W., and Klomparens, K. L. *Scanning and Transmission Electron Microscopy an Introduction*. USA: Oxford University Press Inc, 1993.

[53] Rujisamphan, N. *Design and construction of microwave-PECVD and preliminary characterizations of synthesized polycrystalline diamond film*. Thesis of master degree, Department of Physics Faculty of Science, Chulalongkorn University, 2006.

[54] Smith, E., and Dent, G. Modern Raman Spectroscopy (A Practical Approach). UK: John Wiley and Sons, 2005.

[55] Fischer-Cripps, A. C. *Nanoindentation*. 2nd ed. USA: Springer-Verlag New York LLC, 2004.

[56] Nanoindentation [online]. 2003. Available from:
http://www.nanoindentation.cornell.edu/Machine/commercial_macine.htm
[2010, March 19]

[57] Martinez, E., Polo, M. C., Pascual, E., and Esteve, J. Substrate temperature effects on the microhardness and adhesion of diamond-like thin films. *Diamond and Related Materials* **8** (1999) 563-566.

[58] Kulich, W., Popov, C., Boycheva, S., Buforn, L., Favaro, G., and Conte, N. Mechanical properties of nanocrystlline diamond/amorphous carbon composite films prepared by microwave plasma chemical vapor deposition. *Diamond and Related Materials* **13** (2004) 1997-2002.

[59] Cho, C. W., Hong, B., and Lee, Y. Z. Wear life evaluation of diamond-like carbon films deposited by microwave plasma-enhanced CVD and RF plasma-enhanced CVD method. *Wear* **259** (2005) 789-794.

[60] Mallika, K., and Komanduri, R. Low pressure microwave plasma assisted chemical vapor deposition (MPCVD) of diamond coating on silicon nitride cutting tools. *Thin Solid Films* **396** (2001) 145-165.

[61] Analytical Techniques lectures at University of Bristol [online]. 2009. Available from: http://www.chm.bris.ac.uk/pt/diamond/rolythesis/chapter2.htm [2010, March 14].

[62] Kulisch, W., Popov, C., Vorlicek, V., Gibson, P.N., and Favaro, G. Nanocrystalline diamond growth on different substrates. *Thin Solid Films* **515** (2006) 1005-1010.

[63] Popov, C., Novotny, M., Jelinek, M., Boycheva, S., Vorlicek, V., Trchova, M., and Kulisch, W. Chemical bonding study of nanocrystalline diamond films prepared by plasma techniques. *Thin Solid Films* **506-507** (2006) 297-302.

[64] Sahoo, S., Pradhan, S.S., Bhavanasi, V., and Pradhan, S.K. Structural and mechanical characterization of diamond like carbon films grown by microwave plasma CVD. *Surface and Coating Technology* **204** (2010) 2817-2821.

[65] Johnson, C., Crossley, A., Jones, A.M., Chalker, P.R., Cullen, F.L., and Buckley-Golden, I.M. High temperature stress measurement in CVD diamond films. *Journal De Physique II* **1** (1991) 931-937.

[66] Chowdhury, S., Barra, E.D., and Laugier, M.T. Study of mechanical properties of CVD diamond on SiC substrates. *Diamond and Related Materials* **13** (2004) 1625-1631.

[67] Ravi, N., Bukhovets, V.L., Vashavskaya, I.G., and Sundararajan, G. Deposition of diamond-like carbon films on alumina substrates by RF-PECVD technique: Influence of process parameters. *Diamond and Related Materials* 16 (2007) 90-97.

[68] Ye, H., Sun, C.Q., Hing, P., Xie, H., Zhang, S., and Wei, J. Nucleation and growth dynamics of diamond films by microwave plasma-enhanced chemical vapor deposition (MPECVD). *Surface and Coatings Technology* **123** (2000) 129.

APPENDICES
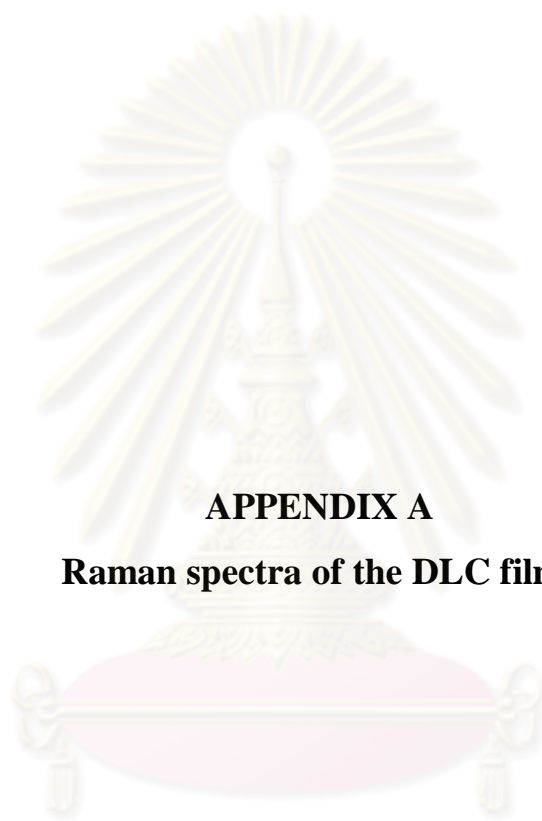
APPENDIX A

Raman spectra of the DLC films

A-1 Raman spectra of the DLC films grown under various CH_4 concentrations, deposition pressure of 30 torr, and deposition time of 30 hr.

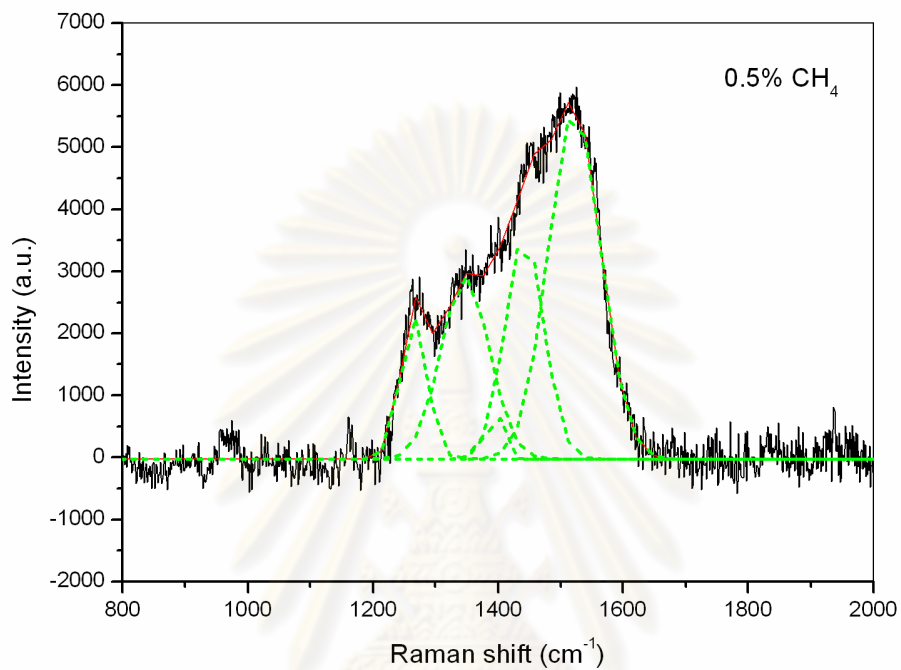**A-1.1** Raman spectra of the films deposited at 0.5% CH_4 concentration.

Figure A-1 Raman spectra of DLC film deposited at 0.5% CH_4 concentration with three Gaussians peak.

A-1.2 Raman spectra of the films deposited at 2% CH$_4$ concentration.

Figure A-2 Raman spectra of DLC film deposited at 2% CH$_4$ concentration with three Gaussians peak.
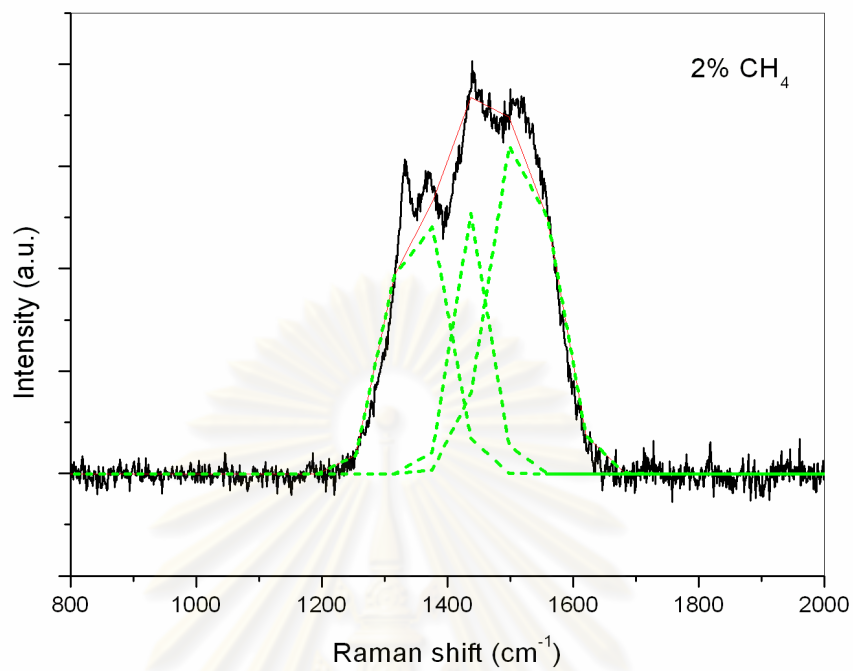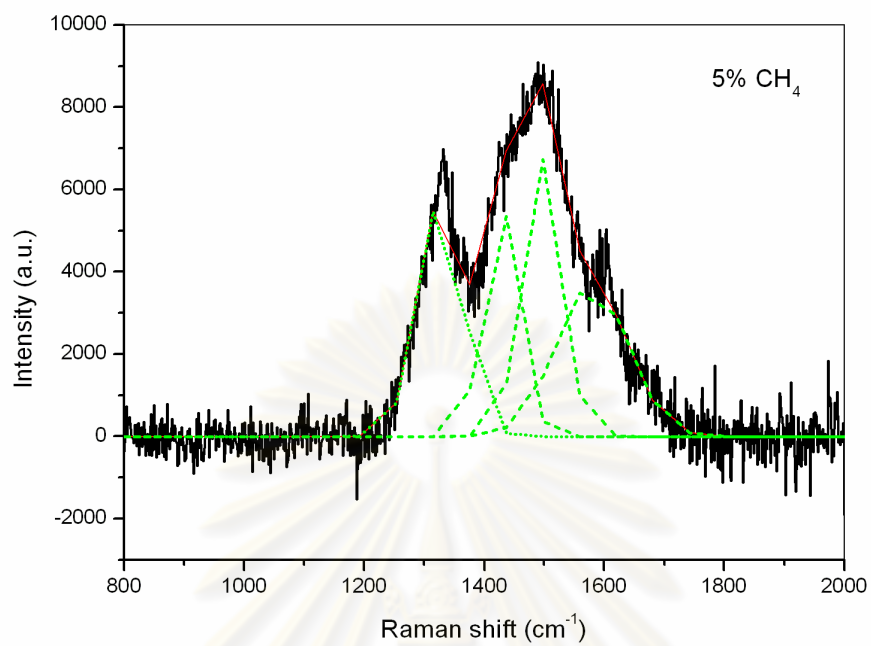
A-1.3 Raman spectra of the films deposited at 2% CH$_4$ concentration.

Figure A-3 Raman spectra of DLC film deposited at 5% CH$_4$ concentration with three Gaussians peak.

A-2 Raman spectra of the DLC films grown under different deposition pressure, CH_4 concentration of 1%, and deposition time of 30 hr.

A-2.1 Raman spectra of the films deposited at deposition pressure of 10 torr.

Figure A-4 Raman spectra of DLC film deposited at deposition pressure of 10 torr with two Gaussians peak.

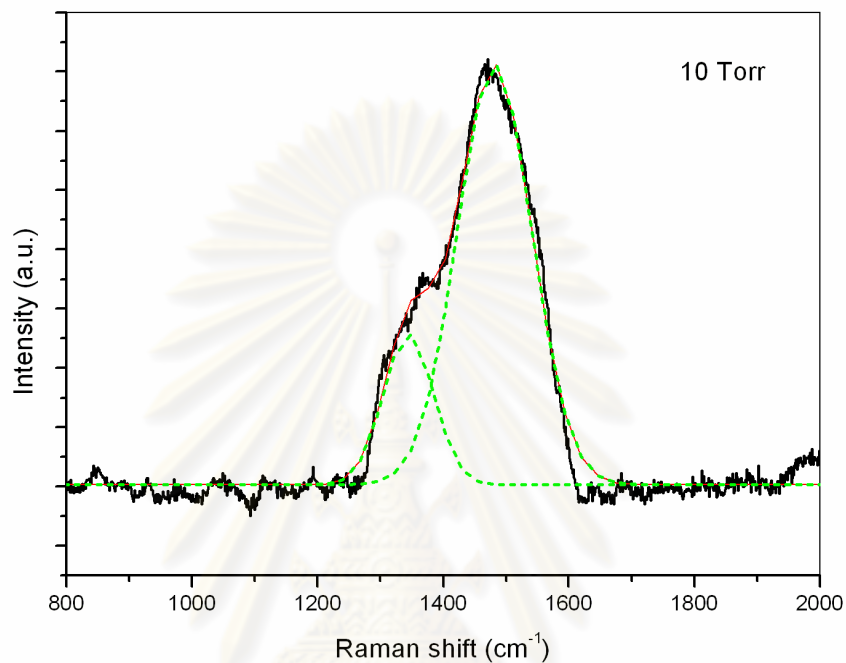**A-2.2** Raman spectra of the films deposited at deposition pressure of 20 torr.

Figure A-5 Raman spectra of DLC film deposited at deposition pressure of 20 torr with two Gaussians peak.
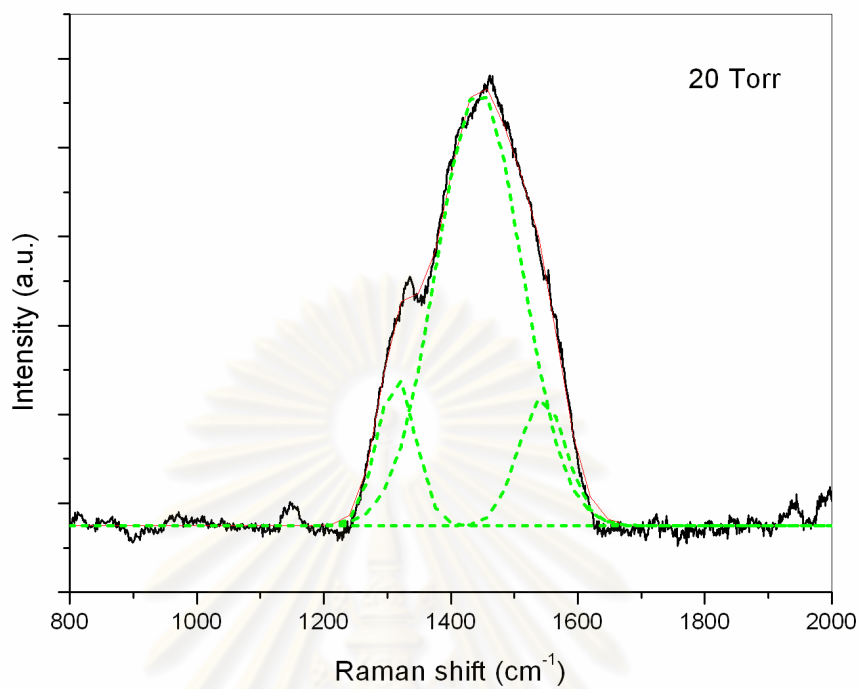
ศูนย์วิทยทรัพยากร

จุฬาลงกรณ์มหาวิทยาลัย

A-2.3 Raman spectra of the films deposited at deposition pressure of 30 torr.

Figure A-6 Raman spectra of DLC film deposited at deposition pressure of 30 torr with three Gaussians peak.
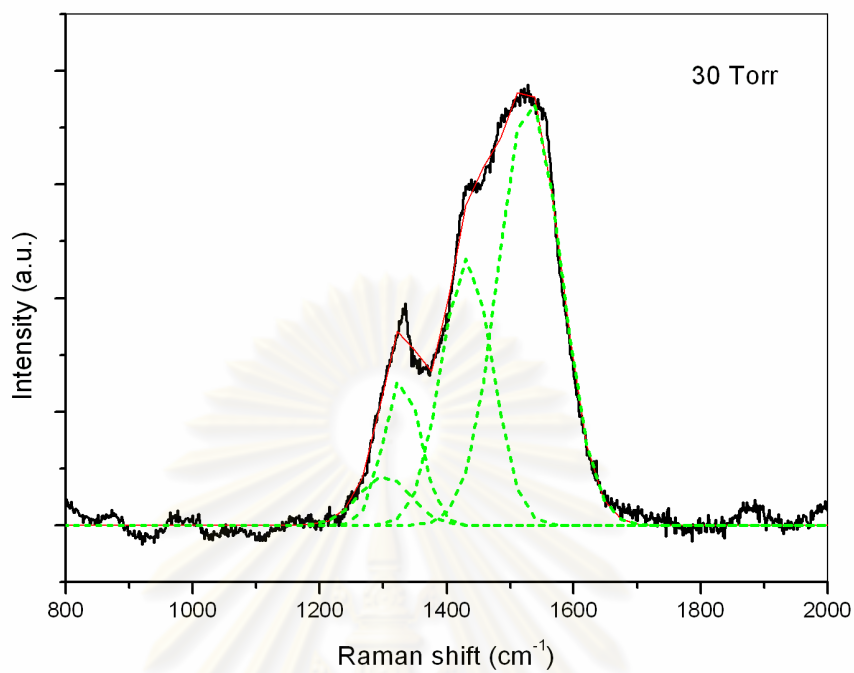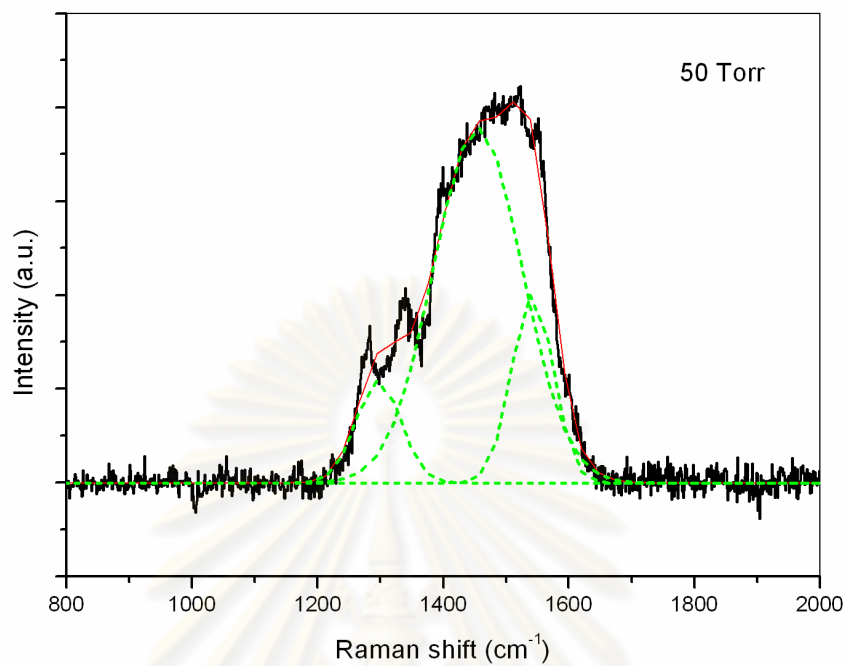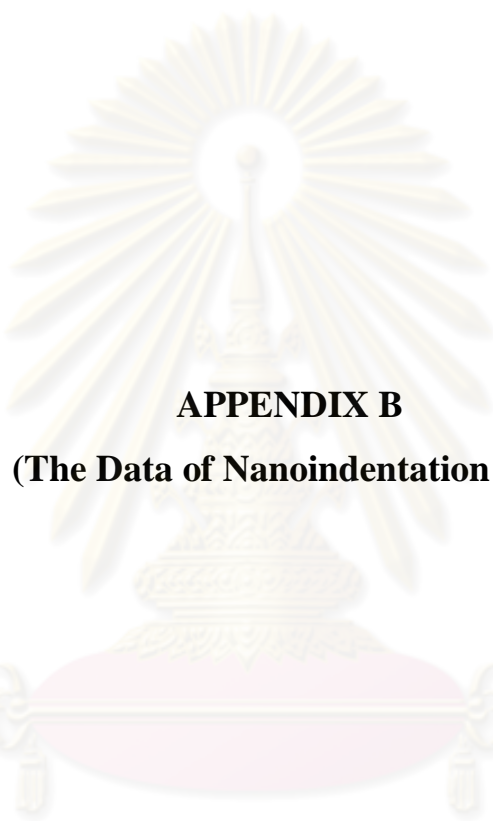
A-2.4 Raman spectra of the films deposited at deposition pressure of 50 torr.

Figure A-7 Raman spectra of DLC film deposited at deposition pressure of 50 torr with three Gaussians peak.

APPENDIX B
(The Data of Nanoindentation test)

B-1 The experimental data and graph information.

Table B-1 The indentation parameters of Nanoindentation tester for all samples.

Indentation parameters

Standard

Standard

+ Instrument : TTX-NHT S/N: 00-00003

+ Hardware settings

  Approach speed : 8000 nm/min

  Dz sensor in fine range

  Delta Slope contact : 20 %

+Measurement

  Acquisition Rate : 10.0 [Hz]

  Linear Loading

  Max load : 5 mN

  Loading rate : 10.00 mN/min

  Unloading rate : 10 mN/min

  Pause : 15.0 s

Indentors

  Type : Berkovich

  Serial number : BJ-07 (08_10_2009)

  Material :Diamond

B-1.1 The Nanoindentation test data of the DLC films grown under various CH$_4$ concentrations, deposition pressure of 30 torr, and deposition time of 30 hr.

Table B-2 The hardness of the DLC films grown at 0.5% CH$_4$ concentration.

		DLC_CVD
Hit (O&P)	Data : 1	27871.936
[MPa]	Data : 2	43647.578
	Data : 5	46539.113
	Mean	39352.875
	Std Dev	10047.350
	Min	27871.936
	Max	46539.113
	N	3.000

DLC -1 -Fn [mN]
DLC -2 -Fn [mN]
DLC -5 -Fn [mN]

Figure B-1 Load-displacement curve of the DLC films deposited at 0.5% CH$_4$ concentration.

Table B-3 The hardness of the DLC films grown at 1% CH$_4$ concentration.

		DLC
Hit (O&P)	Data : 4	49967.059
[MPa]	Data : 7	54165.820
	Data : 8	52553.164
	Mean	52228.676
	Std Dev	2118.104
	Min	49967.059
	Max	54165.820
	N	3.000

DLC -4 -Fn [mN]
DLC -7 -Fn [mN]
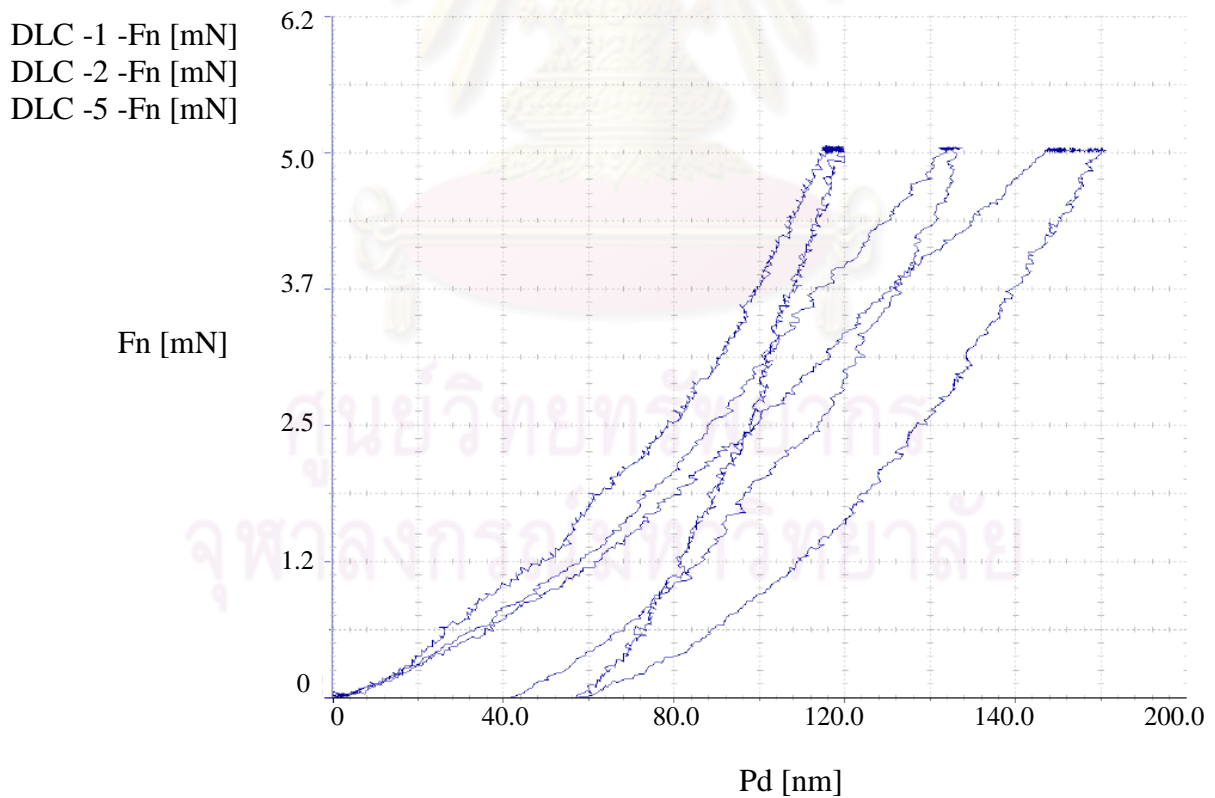DLC -8 -Fn [mN]

Fn [mN]

Pd [nm]

Figure B-2 Load-displacement curve of the DLC films deposited at 1% CH$_4$ concentration.

Table B-4 The hardness of the DLC films grown at 2% CH$_4$ concentration.

		DLC
Hit (O&P)	Data : 2	*34069.043*
[MPa]	Data : 3	*42916.535*
	Data : 5	*26838.486*
	Mean	34608.020
	Std Dev	8052.564
	Min	26838.486
	Max	42916.535
	N	3.000

DLC -2 -Fn [mN]
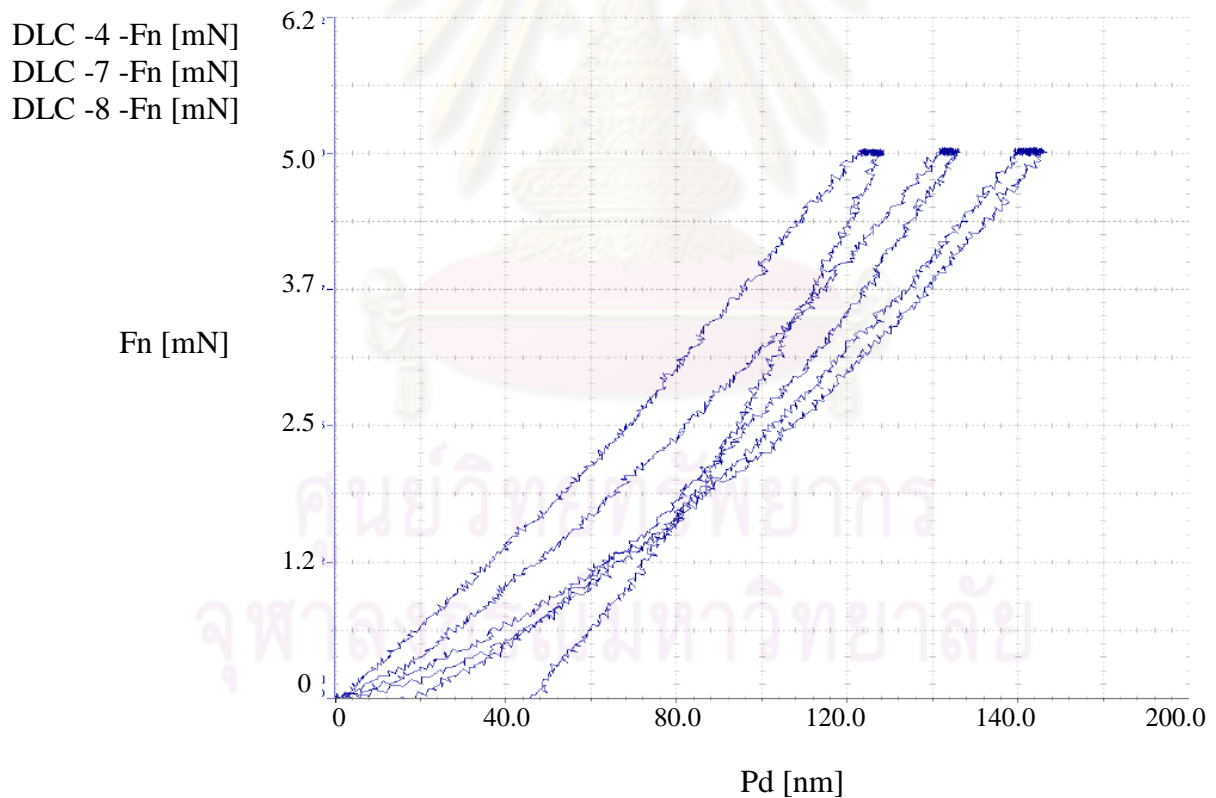DLC -3 -Fn [mN]
DLC -5 -Fn [mN]

Figure B-3 Load-displacement curve of the DLC films deposited at 2% CH$_4$ concentration.

Table B-5 The hardness of the DLC films grown at 3% CH_4 concentration.

		DLC
Hit (O&P)	Data : 1	37597.535
[MPa]	Data : 2	38739.555
	Data : 3	35724.324
	Mean	37353.809
	Std Dev	1522.320
	Min	35724.324
	Max	38739.555
	N	3.000

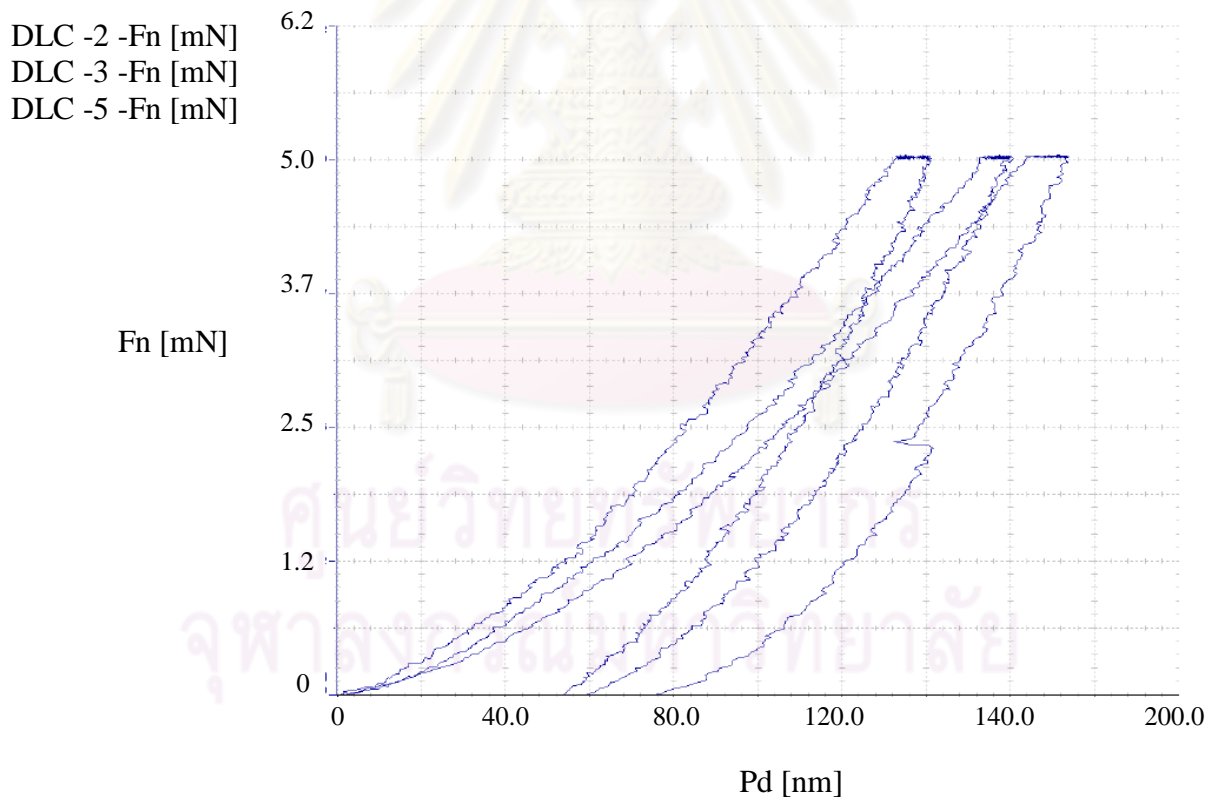DLC -1 -Fn [mN]
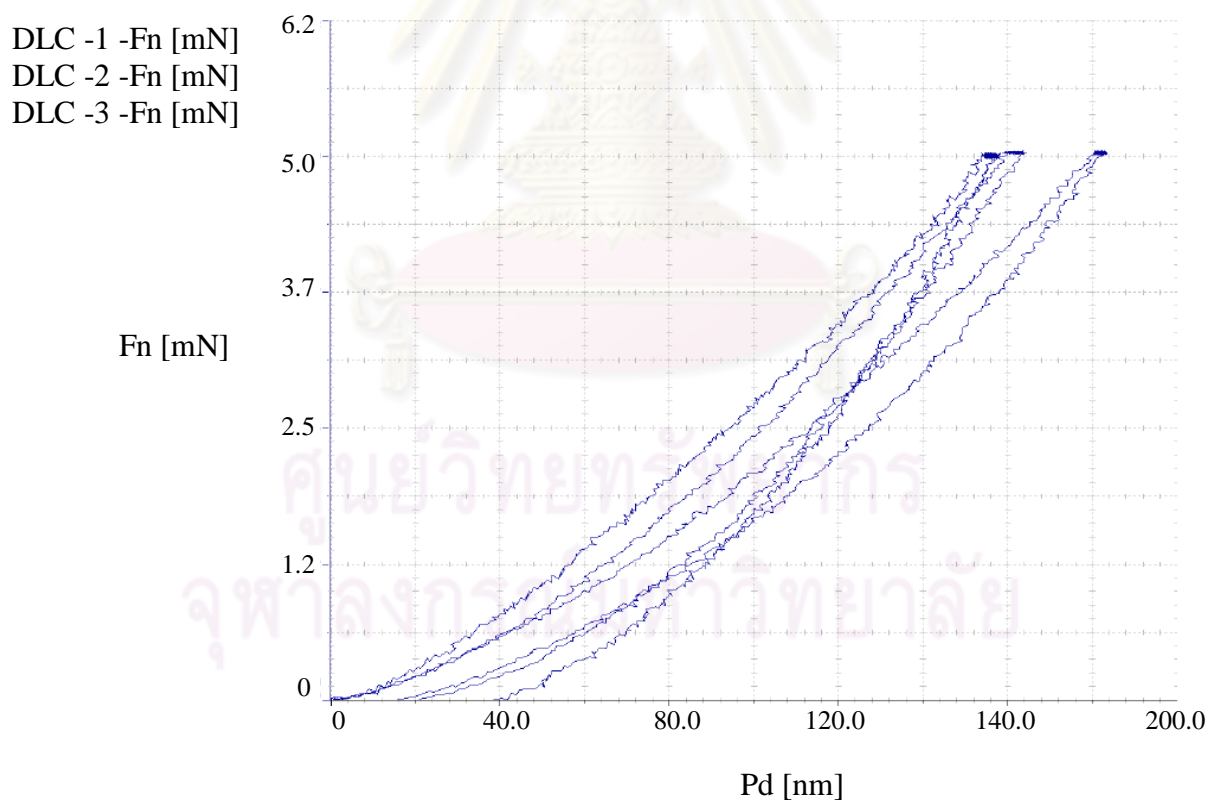DLC -2 -Fn [mN]
DLC -3 -Fn [mN]

Figure B-4 Load-displacement curve of the DLC films deposited at 3% CH_4 concentration.

Table B-6 The hardness of the DLC films grown at 5% CH_4 concentration.

.

		DLC
Hit (O&P)	Data : 3	43251.676
[MPa]	Data : 4	39622.559
	Data : 5	43180.512
	Mean	42018.250
	Std Dev	2075.034
	Min	39622.559
	Max	43251.676
	N	3.000

DLC -3 -Fn [mN]
DLC -4 -Fn [mN]
DLC -5 -Fn [mN]
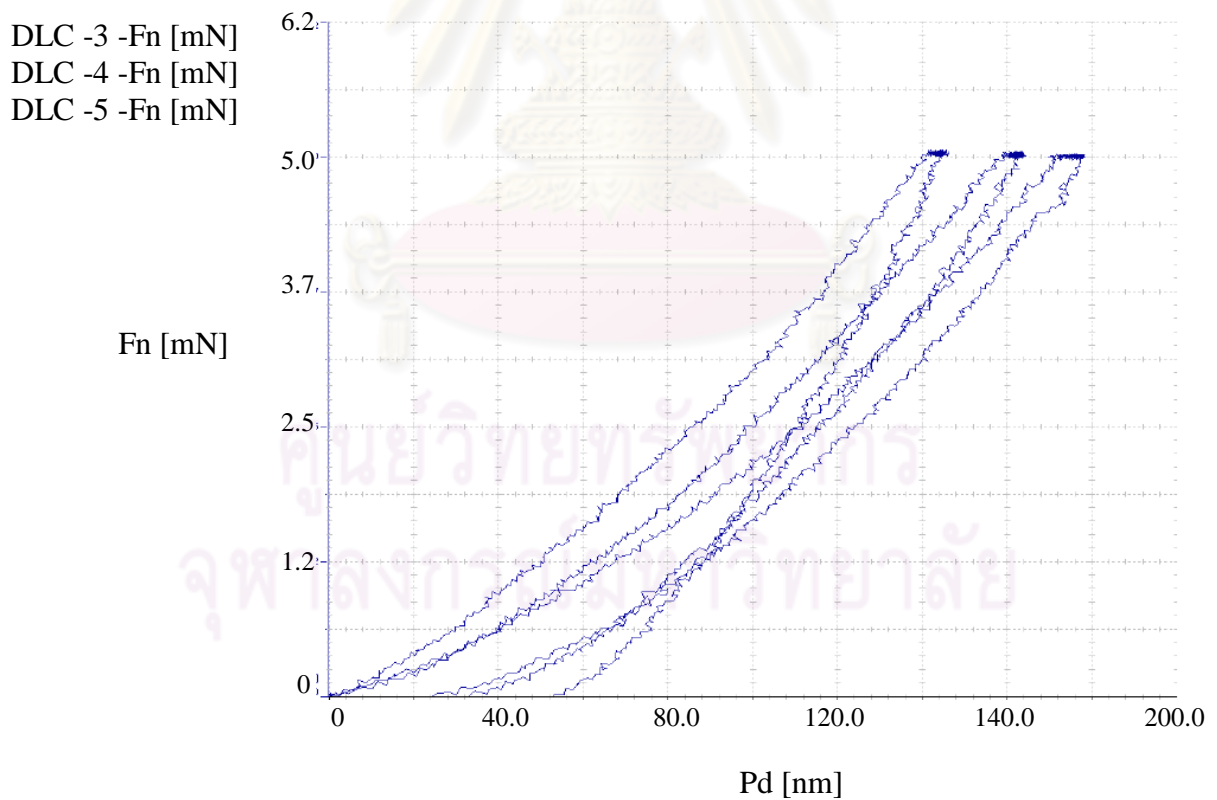
Figure B-5 Load-displacement curve of the DLC films deposited at 5% CH_4 concentration.

B-1.2 The Nanoindentation test data of the DLC films grown under different deposition pressure, CH_4 concentration of 1%, and deposition time of 30 hr.

Table B-7 The hardness of the DLC films grown at deposition pressure of 10 torr.

		DLC
Hit (O&P)	Data : 1	12972.665
[MPa]	Data : 2	15365.926
	Data : 3	13201.118
	Mean	13846.569
	Std Dev	1320.750
	Min	12972.665
	Max	15365.926
	N	3.000

DLC -1 -Fn [mN]
DLC -2 -Fn [mN]
DLC -3 -Fn [mN]

Figure B-6 Load-displacement curve of the DLC films deposited at deposition pressure of 10 torr.

Table B-8 The hardness of the DLC films grown at deposition pressure of 20 torr.

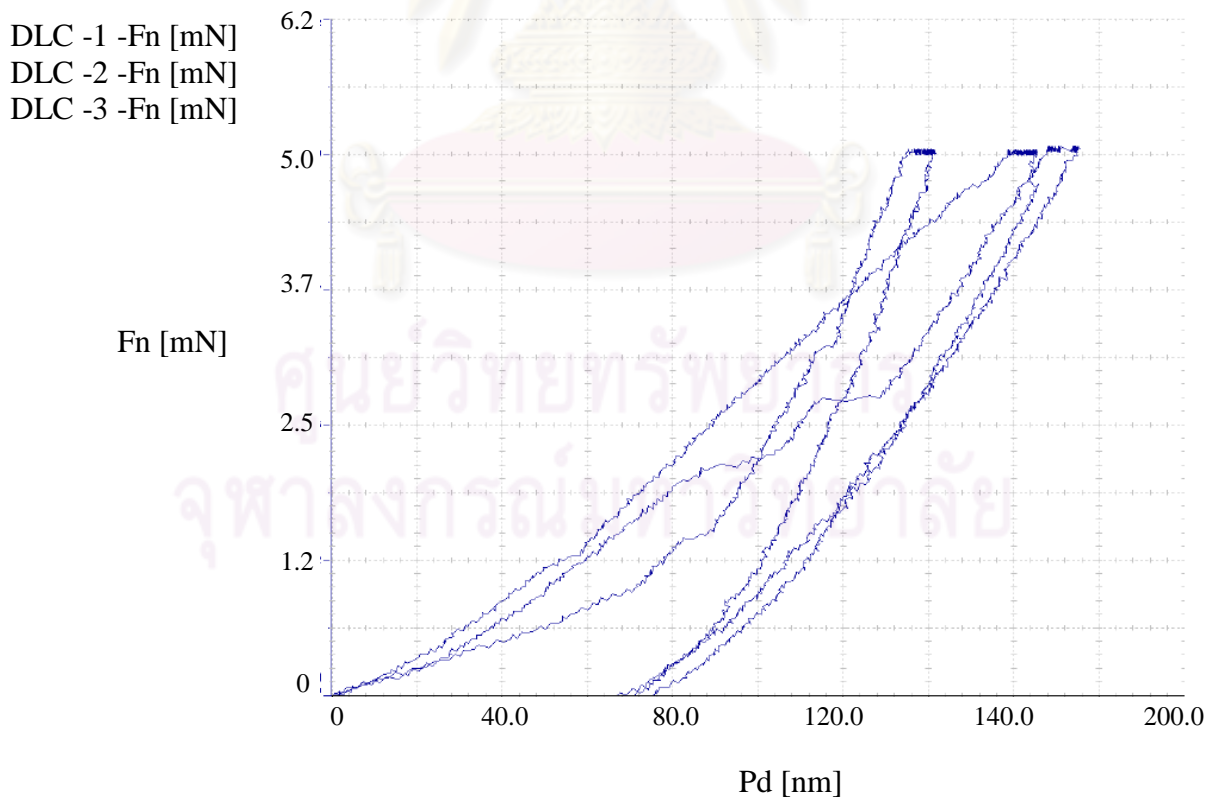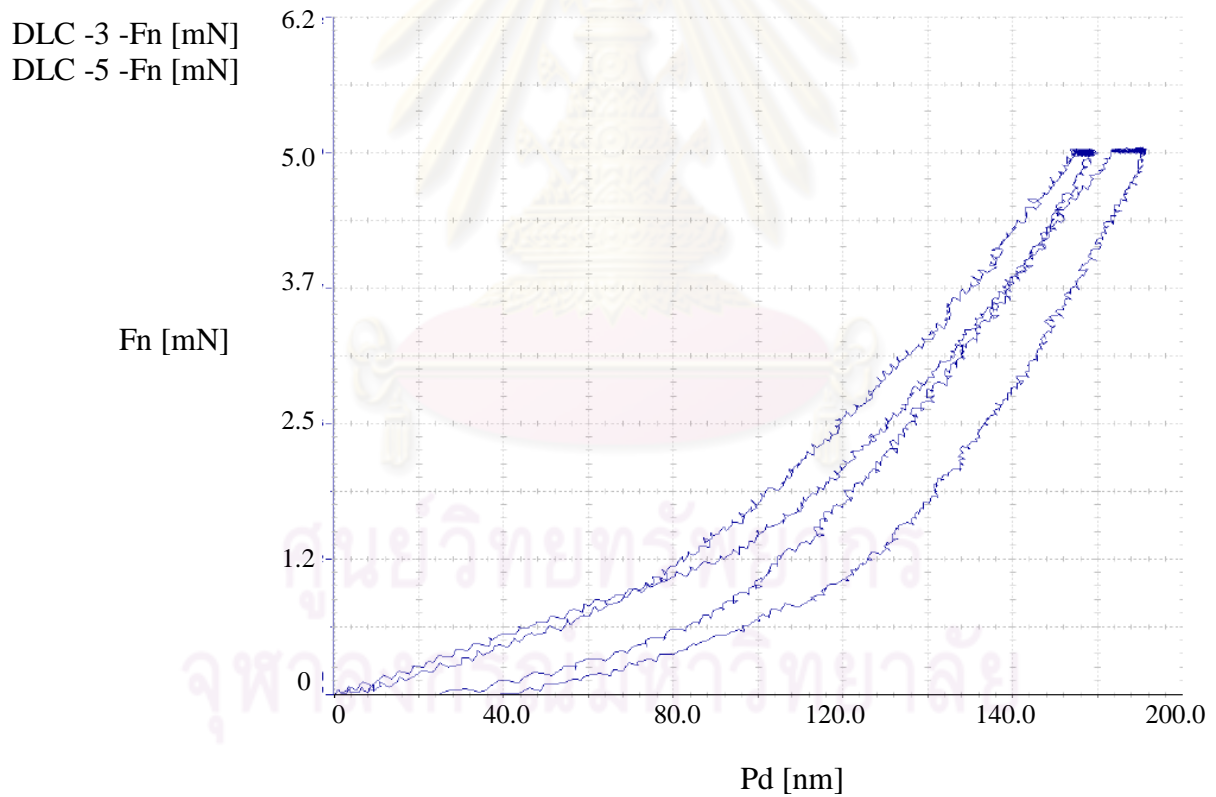|		DLC
Hit (O&P)	Data : 3	27294.301
[MPa]	Data : 5	21069.807
	Mean	24182.055
	Std Dev	4401.382
	Min	21069.807
	Max	27294.301
	N	2.000

DLC -3 -Fn [mN]
DLC -5 -Fn [mN]

Figure B-7 Load-displacement curve of the DLC films deposited at deposition pressure of 20 torr.

Table B-9 The hardness of the DLC films grown at deposition pressure of 50 torr.

		DLC
Hit (O&P)	Data : 1	*34623.613*
[MPa]	Data : 4	*46998.160*
	Mean	40810.887
	Std Dev	8750.126
	Min	34623.613
	Max	46998.160
	N	2.000

DLC -1 -Fn [mN]
DLC -4 -Fn [mN]

Fn [mN]

Pd [nm]
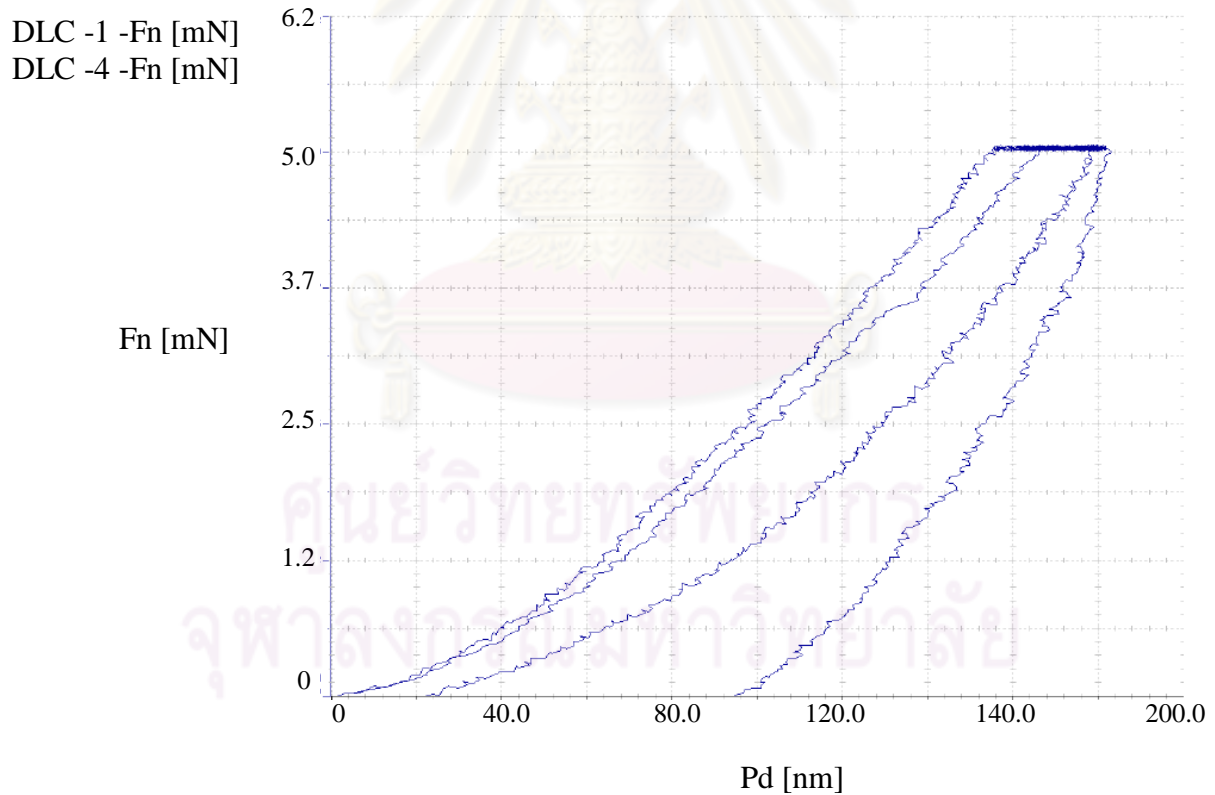
Figure B-8 Load-displacement curve of the DLC films deposited at deposition pressure of 50 torr.

B-1.3 The Nanoindenatation test data of the DLC films grown under various deposition times, CH_4 concentration of 1%, and deposition pressure of 30 torr.

Table B-10 The hardness of the DLC films grown at deposition time of 5 hr.

		DLC
Hit (O&P)	Data : 1	*12629.441*
[MPa]	Data : 2	*18952.854*
	Mean	15791.147
	Std Dev	4471.328
	Min	12629.441
	Max	18952.854
	N	2.000

Figure B-9 Load-displacement curve of the DLC films deposited at deposition time of 5 hr.

Table B-11 The hardness of the DLC films grown at deposition time of 10 hr.

		DLC
Hit (O&P)	Data : 2	29383.254
[MPa]	Data : 3	34358.152
	Data : 4	28263.406
	Mean	30668.271
	Std Dev	3244.216
	Min	28263.406
	Max	34358.152
	N	3.000

DLC -2 -Fn [mN]
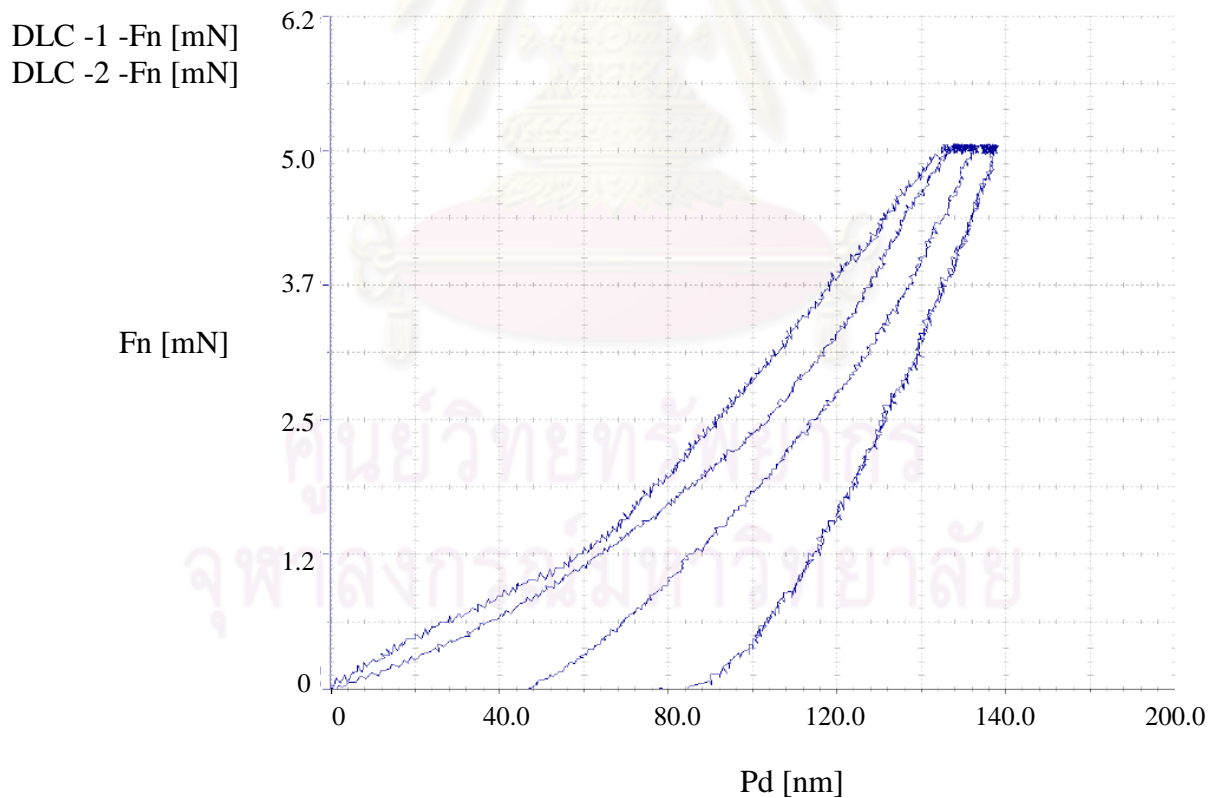DLC -3 -Fn [mN]
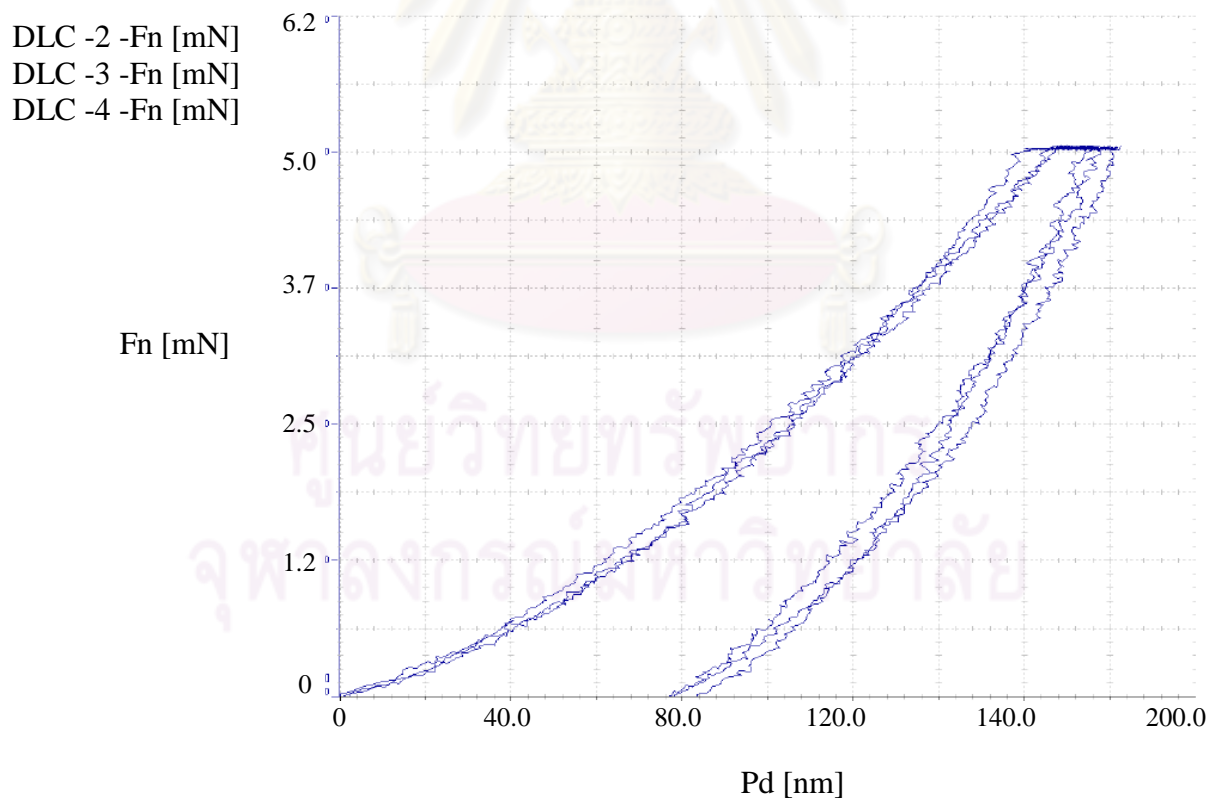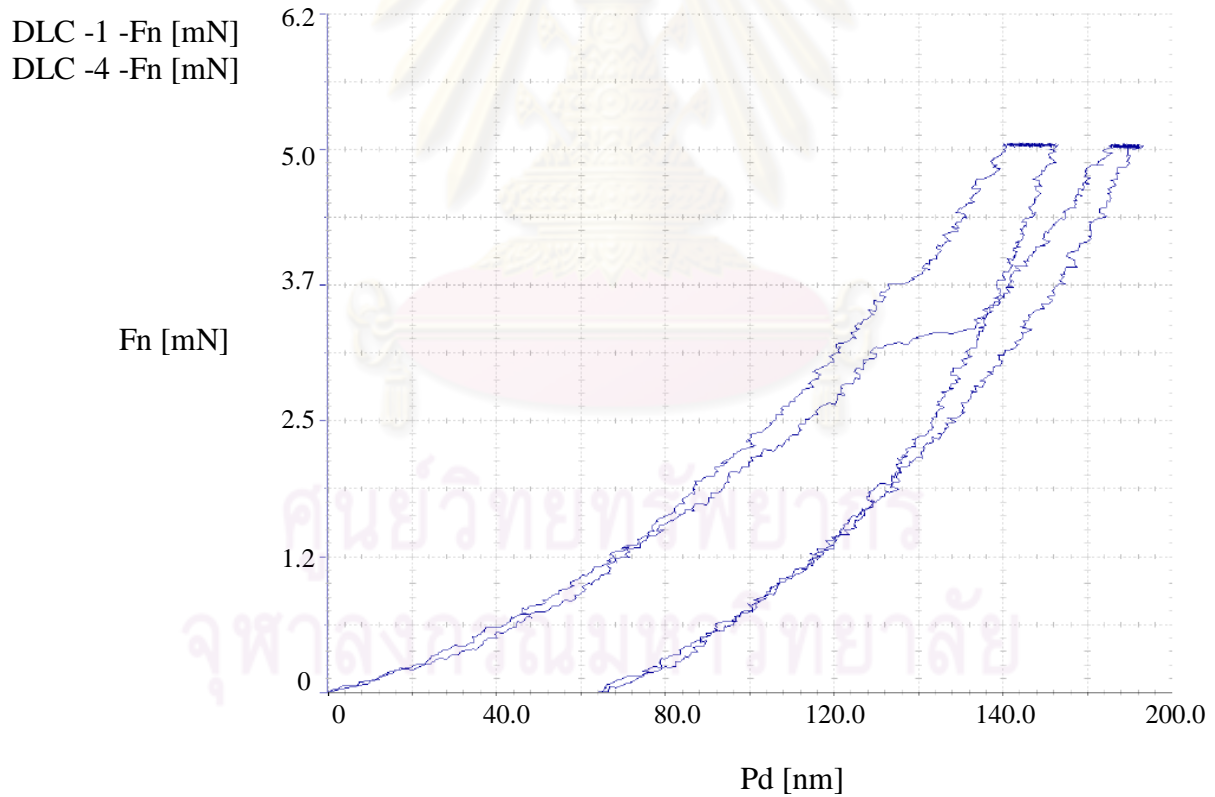DLC -4 -Fn [mN]

Fn [mN]

Pd [nm]

Figure B-10 Load-displacement curve of the DLC films deposited at deposition time of 10 hr.

Table B-12 The hardness of the DLC films grown at deposition time of 20 hr.

		DLC
Hit (O&P)	Data : 1	36564.621
[MPa]	Data : 4	38050.203
	Mean	37307.414
	Std Dev	1050.465
	Min	36564.621
	Max	38050.203
	N	2.000

DLC -1 -Fn [mN]
DLC -4 -Fn [mN]

Fn [mN]

Pd [nm]

Figure B-11 Load-displacement curve of the DLC films deposited at deposition time of 20 hr.

VITAE

Miss Chotiwan Rattanasatien was born on December 17, 1985 in Ratchaburi, Thailand. She received the bachelor's degree from the Department of Industrial Chemistry, Faculty of Science, King Mongkut's Institute of Technology Ladkrabang in 2007. She was admitted to the Master Degree Program of Chemical Engineering, Faculty of Engineering, Chulalongkorn University and completed the program in 2010.

Conferences:

C. Rattanasatien, N. Tonanon and B. Paosawatyanyong. Synthesis of diamond-like carbon thin film on alumina by microwave plasma enhanced chemical vapor deposition technique. 35th Congress on Science and Technology of Thailand, Thailand (October 15-17, 2009).

C. Rattanasatien, N. Tonanon and B. Paosawatyanyong. Growth of diamond-like carbon film on alumina by MW-PECVD technique. Pure and Applied Chemistry International Conference 2010, Thailand (January 21-23, 2010)

C. Rattanasatien, N. Tonanon and B. Paosawatyanyong. DLC coating on alumina by MW-PECVD technique. 2nd International Symposium on Advanced Plasma Science and its Applications for Nitrides and Nanomaterials, Meijo University, Nagoya, Japan (March 7-10, 2010)

C. Rattanasatien, N. Tonanon and B. Paosawatyanyong. DLC growth on alumina by microwave plasma enhanced chemical vapor deposition technique. Siam Physics Congress 2010, Thailand (March 25-27, 2010)

C. Rattanasatien, N. Tonanon and B. Paosawatyanyong. Coating of DLC nanofilm on alumina by MW-PECVD technique. Asian Conference on Nanoscience & Nanotechnology (AsiaNANO 2010), Tokyo, Japan (November 1-3, 2010)